A bootstrap study of minimal model deformations

António Antunes[1,2], Edoardo Lauria[3,4], and Balt C. van Rees[4]

[1] Deutsches Elektronen-Synchrotron DESY,
Notkestr. 85, 22607 Hamburg, Germany

[2] Centro de Física do Porto, Departamento de Física e Astronomia,
Faculdade de Ciências da Universidade do Porto,
Rua do Campo Alegre 687, 4169-007 Porto, Portugal

[3] LPENS, Département de physique, École Normale Supérieure - PSL
Centre Automatique et Systèmes (CAS), Mines Paris - PSL
Université PSL, Sorbonne Université, CNRS, Inria, 75005 Paris

[4] CPHT, CNRS, École polytechnique, Institut Polytechnique de Paris,
91120 Palaiseau, France

antonio.antunes@desy.de, edoardo.lauria@minesparis.psl.eu
balt.van-rees@polytechnique.edu

Abstract

For QFTs in AdS the boundary correlation functions remain conformal even if the bulk theory has a scale. This allows one to constrain RG flows with numerical conformal bootstrap methods. We apply this idea to flows between two-dimensional CFTs, focusing on deformations of the tricritical and ordinary Ising models. We provide non-perturbative constraints for the boundary correlation functions for these flows and compare them with conformal perturbation theory in the vicinity of the fixed points. We also reproduce a completely general constraint for the $T\bar{T}$ deformation in two dimensions.

Contents

1 Introduction

The aim of this work is to constrain the physics of quantum field theories that undergo an RG flow between two non-trivial fixed points.

We largely focus on flows around the two lowest-lying diagonal minimal models in two space-time dimensions: the tricritical Ising model with $m = 4$ and $c = 7/10$ and the Ising model with $m = 3$ and $c = 1/2$. Of particular interest is the flow *between* these theories, which is triggered by the relevant $\phi_{(1,3)}$ deformation of the tricritical Ising model [1, 2]. More generally, the $\phi_{(1,3)}$ deformation of the m'th minimal model triggers a flow to the $m-1$'th minimal model. This is (a limit of) the integrable 'staircase' flow of [3] which we will also briefly investigate.

Our method is to apply numerical conformal bootstrap techniques to the boundary correlation functions of the QFT in a hyperbolic background. For an RG flow parametrized by a scale μ in a hyperbolic space with curvature radius R this setup leads to a one-parameter family of solutions of the boundary conformal crossing equations where the OPE data depends on the dimensionless combination μR. We will aim to numerically constrain these families of consistent OPE data. A similar analysis was done earlier for deformations of the free massless scalar and the Sine-Gordon RG flow in AdS [4].

We get our most interesting results when the boundary correlation functions of the fixed point saturate (extrapolated) numerical bounds. This is because first-order corrections to the OPE data, which for specific deformations can be computed in conformal pertubation theory, can sometimes point *into* the disallowed region. In such a case there is an inconsistency: the first-order correction to the OPE data may look totally innocuous, but in actuality the deformation cannot be consistently exponentiated in that direction.

Our most relevant example of this scenario is the $T\bar{T}$ deformation [5–7] of a general two-dimensional CFT in AdS. From a first-order analysis we find that an irrelevant deformation of the form

$$\delta S = \lambda \int_{\mathrm{AdS}_2} T\bar{T} + (\text{more irrelevant deformations}) \tag{1.1}$$

can only be consistent if

$$\lambda \geq 0\,. \tag{1.2}$$

We note that in flat space a similar condition was found in [8, 9], but the derivation from conformal bootstrap methods is new. Furthermore, our bound applies in an AdS space of arbitrary radius and sheds some light on the $T\bar{T}$ deformation in curved space which can be of interest by itself [10, 11].

We stress that constraints of the form (1.2) are independent of subleading irrelevant deformations in equation (1.1). Instead we merely need to compute the first-order correction to the

boundary OPE data to disallow certain signs. In that sense the constraint (1.2) is more general than the (equivalent) sign constraint obtained from integrability for a pure $T\bar{T}$ deformation [8, 9].

We finally note that sign constraints for irrelevant couplings are reminiscent of the older causality constraints of [12]. The simplest of these, a bound on the $(\partial\phi)^4$ coupling for a massless shift-invariant scalar, was reproduced in two dimensions from QFT in AdS in [4]. These bounds have also been vastly generalized with numerical methods [13, 14] and they were 'uplifted' to AdS in [15] using the techniques of analytic functionals and conformal dispersion relations [16–18]. In those cases the IR theory however always consisted of a free massless field. Our QFT in AdS approach, on the other hand, allows one to constrain the irrelevant couplings around a general IR CFT.

The universality of our bootstrap bounds implies the following caveat. Consider a CFT deformed by two operators $\mathcal{O}_1$ and $\mathcal{O}_2$ with dimensionful couplings λ_1 and λ_2, so the dimensionless boundary OPE data becomes a function of

$$g_1 := \lambda_1 R^{d-\Delta_1} \qquad \text{and} \qquad g_2 := \lambda_2 R^{d-\Delta_2}\,. \tag{1.3}$$

With our numerical methods we can hope to carve out the embedding of the (allowed region in the) (g_1, g_2) plane in the space of all boundary OPE data. On this plane there are however distinguished curves which correspond to the actual RG flows. For example, if both couplings are relevant then the fixed point is approached along specific curves which are most easily described by saying that they become straight lines in the plane spanned by $(g_1^{1/(d-\Delta_1)}, g_2^{1/(d-\Delta_2)})$. Without further assumptions these RG flow lines will however remain invisible in the bootstrap analysis. As an example we will find below a bound that is saturated to first order by a straight line in the (g_1, g_2) plane instead of an actual RG flow.

In the next section we discuss some general properties of QFTs in AdS. We will compute some pertinent results to first order in conformal perturbation theory in section 3, and compare these with the numerical results in section 4. Section 5 lists some possible future directions.

2 Setting the stage

In this section we discuss conformal boundary conditions (b.c.) for 2d CFTs on the upper half-plane, or 2d BCFTs. Our goal is to recall the basic concepts that will be important for our subsequent study, as well as setting up the conventions. A more detailed discussion and references to the original literature can be found for example in the books [19–22]. Note that what we discuss here also applies to BCFTs on AdS_2, since the two backgrounds are related by a Weyl rescaling.

2.1 CFTs on the upper half-plane

Consider placing a generic unitary 2d CFT with central charge c on the upper half-plane

$$\mathbb{H}^+ = \{z \in \mathbb{C} \mid \text{Im } z \geq 0\} \ .$$

In Cartesian coordinates we write $z = x + iy$, so that the real axis is the boundary of the domain and $y > 0$ is a transverse coordinate. The boundary geometry is preserved by local conformal transformations that are real-analytic functions of the coordinates. The latter are generated by a single copy of the Virasoro algebra, with central charge c

$$[L_n \, , L_m] = (n-m)L_{n+m} + \frac{c}{12} n(n^2-1)\delta_{n+m,0} \ , \quad m, n \in \mathbb{Z} \ . \tag{2.1}$$

The vacuum of any (euclidean) 2d BCFT is therefore invariant under $SO(2,1) \simeq SL(2,\mathbb{R})$.

As usual in CFTs with boundaries (or defects), we shall distinguish between 'bulk' and 'boundary' (or 'defect') local operators, respectively denoted as:

$$\phi(x+iy, x-iy) \ , \quad \psi(x) \ .$$

Occasionally, we will use the complex notation and write $\phi(z, \bar{z})$ for bulk local operators. Here we are further allowed to distinguish between 'Virasoro' and 'global' primaries, the latter being Virasoro descendants that are primaries with respect to the conformal group.

2.1.1 Universal boundary operators and bulk one-point functions

An important feature of any local 2d BCFT is that its spectrum generically features a displacement operator. The latter is a boundary global primary defined as the restriction of $T = T(z)$ (the holomorpic component of the stress-energy tensor) to the boundary, i.e.

$$\mathrm{D}(x) = T(x+iy)|_{y=0} \ . \tag{2.2}$$

The displacement belongs to the boundary identity module, and in particular it is a level-two Virasoro descendant of the boundary identity $\hat{\mathbb{1}}$. The restriction of the anti-holomorphic component $\bar{T}(\bar{z})$ of the stress-energy tensor to the boundary defines the same displacement, since by the absence of momentum flow across the boundary

$$T(z) = \bar{T}(\bar{z}) \ , \quad \text{Im } z = 0 \ . \tag{2.3}$$

This is known as Cardy's condition [23–25]. It follows from these considerations that correlation functions with the displacement can be obtained from correlation functions with the stress-energy

tensor T on the upper half-plane, by restricting all T-insertions to the real axis, so for instance we have

$$\langle \mathrm{D}(x_1)\mathrm{D}(x_2)\rangle_{\mathbb{H}^+} = \frac{c/2}{x_{12}^4} \ , \quad \langle \mathrm{D}(x_1)\mathrm{D}(x_2)\mathrm{D}(x_3)\rangle_{\mathbb{H}^+} = \frac{c}{(x_{12})^2(x_{23})^2(x_{31})^2} \ ,$$
$$\langle \mathrm{D}(x_1)\mathrm{D}(x_2)\mathrm{D}(x_3)\mathrm{D}(x_4)\rangle_{\mathbb{H}^+} = \frac{c^2/4}{(x_{12})^4(x_{34})^4}\left[1+\eta^4+\left(\frac{\eta}{\eta-1}\right)^4+\frac{8\eta^2((\eta-1)\eta+1)}{c(\eta-1)^2}\right] \ , \quad (2.4)$$

with the four-point cross-ratio given by

$$\eta = \frac{x_{12}x_{34}}{x_{13}x_{24}} \ , \quad 0<\eta<1 \ . \quad (2.5)$$

More examples are discussed in appendix A.3 of [26].

Beside the displacement, the boundary identity module $[\hat{\mathbb{1}}]$ provides us with as many global boundary primaries as there are in the bulk identity module, when restricted to the holomorphic part. In particular, $[\hat{\mathbb{1}}]$ contains only one boundary global primary at level four, as it follows from considering the restriction of the $T\times T$ OPE to the boundary, i.e.

$$\mathrm{D}(x)\mathrm{D}(0) = \frac{c/2}{x^4}\hat{\mathbb{1}} + \frac{2}{x^2}\mathrm{D}(0) + \frac{1}{x}\mathrm{D}'(0) + \frac{3}{10}\mathrm{D}''(0) + \mathrm{D}^2(0) + O(x^2) \ , \quad (2.6)$$

where $'$ indicates derivatives along the boundary and we omitted higher-order contributions. The displacement D and its closest cousin D^2 will play a central role in our analysis.

One-point functions of bulk local operators provide an important set of observables in any BCFT. By $SL(2,\mathbb{R})$ symmetry these can be non-trivial only for scalar bulk (global) primaries [27–29], so for an operator with scaling dimension Δ we have

$$\langle \phi(x+iy, x-iy)\rangle_{\mathbb{H}^+} = \frac{B_\phi}{(2y)^\Delta} \ , \qquad (y>0) \ . \quad (2.7)$$

2.1.2 Minimal model conformal boundary conditions

An important set of exactly solvable examples is provided by the minimal models. We will focus on unitary and diagonal minimal models $\mathcal{M}_{m+1,m}$ with central charge

$$c = 1 - \frac{6}{m(m+1)} \, , \qquad m = 3,\, 4,\, 5, \ldots \quad (2.8)$$

Allowed bulk Virasoro primaries are labelled by a pair of positive integers (r,s) as follows

$$(r,s) \ , \quad 1\le r\le m-1 \ , \quad 1\le s\le m \ , \quad (r,s)\cong(m-r, m+1-s) \ . \quad (2.9)$$

Their scaling dimensions and spins are

$$\phi_{(r,s)}(z,\bar z): \qquad \Delta_{r,s} = h_{r,s} + \bar h_{r,s} \ , \quad \ell_{r,s} = h_{r,s} - \bar h_{r,s} = 0 \ , \quad (2.10)$$

with holomorphic scaling dimensions

$$h_{r,s} = \frac{\big((m+1)r - ms\big)^2 - 1}{4m(m+1)} \ . \tag{2.11}$$

The m'th diagonal minimal model enjoys a $\mathbb{Z}_2$ symmetry under which the charge of a Virasoro primary with labels (r,s) is [30–32]

$$\epsilon^{(m)}_{(r,s)} = (-1)^{(m+1)r+ms+1} \ . \tag{2.12}$$

We will sometimes refer to 'holomorphic' Virasoro primaries to indicate primaries with $\Delta_{r,s} = \ell_{r,s} = h_{r,s}$, and therefore to 'holomorphic' fusion rules, correlators, etc. These turn out to be useful gadgets, because boundary Virasoro primaries

$$\psi_{(r,s)}(x): \qquad \hat{\Delta}_{r,s} = h_{r,s} \ , \tag{2.13}$$

where (r,s) satisfy eq. (2.9) behave as holomorphic Virasoro primaries, as far as the Ward identities are concerned, see e.g. the discussion in [26].

The (holomorphic) fusion rules read

$$\phi_{(r,s)} \times \phi_{(r',s')} = \sum_{\substack{r''=|r-r'|+1 \\ r+r'+r'' \text{ odd}}}^{r_{\max}} \ \sum_{\substack{s''=|s-s'|+1 \\ s+s'+s'' \text{ odd}}}^{s_{\max}} \phi_{(r'',s'')} \ , \tag{2.14}$$

where $r_{\max} = \min(r+r'-1,\ 2m-r-r'-1)$ and $s_{\max} = \min(s+s'-1,\ 2m-s-s'+1)$.

The space of possible conformal boundary conditions for $\mathcal{M}_{m+1,m}$ is highly constrained by modular invariance. Allowed 'elementary' conformal boundary conditions (which have a unique identity operator) are in one-to-one correspondence with the Cardy states [24], which in turn are in one-to-one correspondence with the scalar Virasoro primaries of the bulk CFT [23–25]. So, yet again, we label the elementary conformal boundary conditions with a pair of positive integers a_1, a_2 that satisfy

$$\mathbf{a} = (a_1,a_2)_m \ , \quad 1 \le a_1 \le m-1 \ , \quad 1 \le a_2 \le m \ , \quad (a_1,a_2) \cong (m-a_1, m+1-a_2) \ . \tag{2.15}$$

We recall two useful properties that such elementary conformal boundary conditions enjoy:

(i) In a given b.c. $\mathbf{a}$, the allowed boundary Virasoro primaries are those that can appear in the 'holomorphic' fusion $\phi_{\mathbf{a}} \times \phi_{\mathbf{a}}$. The annulus partition function with b.c. $\mathbf{a}$ reads:

$$Z_{\mathbf{aa}}(\delta) = \sum_{(r,s)} N^{(r,s)}_{\mathbf{aa}} \chi_{(r,s)}(e^{-\pi\delta}) \ , \tag{2.16}$$

where $\chi_{(r,s)}$ is the (holomorpic) Virasoro character of the (r,s) primary, δ is the width of the annulus, and N is the fusion coefficient of $\phi_{\mathbf{a}} \times \phi_{\mathbf{a}}$ into $\phi_{(r,s)}$ – see eq. (2.14). A list of elementary conformal b.c. for diagonal minimal models with $m \le 5$ can be found in Table 12 on page 43.

(ii) In a given b.c. **a**, the allowed boundary Virasoro primaries in the bulk-boundary fusion of a bulk Virasoro primary $\phi_{(r,s)}$ are those that can appear in the 'holomorphic' fusion $\phi_{(r,s)} \times \phi_{(r,s)}$.

(iii) The one-point function coefficients in eq. (2.7) are completely determined by the Cardy state [33, 34]. The explicit formula is:

$$B^{\mathbf{a}}_{(r,s)} = \frac{S^{(r,s)}_{(a_1,a_2)}\sqrt{S^{(1,1)}_{(1,1)}}}{S^{(1,1)}_{(a_1,a_2)}\sqrt{S^{(r,s)}_{(1,1)}}} \ ,$$

$$S^{(r,s)}_{(a_1,a_2)} = \sqrt{\frac{8}{m(m+1)}}(-1)^{1+a_1 s+a_2 r} \sin\left(\tfrac{m+1}{m}\pi a_1 r\right)\sin\left(\tfrac{m}{m+1}\pi a_2 s\right) \ . \tag{2.17}$$

In this paper we shall mostly focus on elementary conformal boundary conditions **a** for the unitary and diagonal minimal models. However we should keep in mind that the most generic conformal boundary condition is a superposition of the elementary conformal boundary conditions defined above.

2.2 From BCFTs to AdS

Correlation functions in BCFT are related to correlation functions in AdS by a simple Weyl rescaling. We will work in Poincaré coordinates of AdS_2 with radius R

$$ds^2 = g_{\mu\nu}dx^\mu dx^\nu = \frac{R^2}{y^2}(dy^2+dx^2) \ , \quad (x,y)\in\mathbb{R}^2 \mid y\geq 0 \tag{2.18}$$

For bulk (global) primary operators with scaling dimension Δ the Weyl rescaling rule is

$$\langle\phi(x+iy,x-iy)\ldots\rangle_{\mathrm{AdS}} = (y/R)^\Delta\langle\phi(x+iy,x-iy)\ldots\rangle_{\mathrm{BCFT}} \ . \tag{2.19}$$

Boundary operators remain untouched. Notice that under such Weyl rescaling from the upper half-plane the anomalous contribution to the stress-energy tensor T vanishes, hence $T_{\mathrm{BCFT}} = T_{\mathrm{AdS}}$, see e.g. the discussion in section 5.1 of ref. [35].

3 Perturbative results

Suppose we switch on a deformation of a 2d BCFT in AdS_2 by a local operator $\phi(x)$. The correlation functions in the deformed theory can be computed perturbatively by expanding

$$\langle\ldots\exp\left(-g_\phi R^{\Delta_\phi-2}\int d^2x\sqrt{g}\,\phi(x)+\text{counterterms}\right)\rangle \ , \tag{3.1}$$

in the dimensionless coupling g_ϕ. This deformation generically induces both UV and IR divergences. The UV divergences are essentially the same as in flat space, even though new counterterms involving the AdS curvature may be needed. The IR divergences can be cured by including bulk counterterms evaluated at a cut-off surface near the boundary. As discussed for example in [26], as long as there are no marginal operators in the bulk-boundary OPE of ϕ, these counterterms preserve boundary conformal invariance and the 'boundary follows the bulk'. This is generically not the case for generic BCFTs in flat space, see for instance refs. [36–38].

In sections 3.1 and 3.2 we take the undeformed theory to be a generic local 2d BCFTs with bulk central charge c. In sections 3.4 and 3.3 we will specifically focus on the first two diagonal minimal models.

3.1 $T\bar{T}$ deformed CFTs to first order

We switch on the $T\bar{T}$ deformation of a CFT in AdS_2. In Poincaré coordinates:

$$\delta S = g_{T\bar{T}} R^2 \int d^2x \sqrt{g}\; T\bar{T}(x+iy, x-iy) + \text{counterterms} \; . \tag{3.2}$$

In this expression, x runs along the conformal boundary of AdS_2 and y is the transverse direction. At the level of correlation functions, the $T\bar{T}$ insertion on AdS_2 is a Weyl rescaling away from the $T\bar{T}$ insertion on the upper half-plane, where the latter is obtained from an insertion of $T(z)T(z')$ on the complex plane, with $z' = z^*$, i.e.[1]

$$\begin{aligned} \langle \dots T\bar{T}(z) \rangle_{\mathbb{H}^+} &\equiv \lim_{z' \to z} \langle \dots T(z')\bar{T}(z) \rangle_{\mathbb{H}^+} \\ &= \lim_{z' \to z} \langle \dots T(z')T(z^*) \rangle_{\mathbb{H}^+} = \langle \dots T(z)T(z^*) \rangle_{\mathbb{H}^+} \; . \end{aligned} \tag{3.3}$$

As we turn on the interaction operators will generically pick up anomalous dimensions. Starting from correlation functions with $T\bar{T}$ insertions computed in ref. [26], in appendix E we compute the anomalous dimensions of D and D^2 under the deformation of eq. (3.2), at the first order in the coupling. We show that

$$\begin{aligned} \Delta_{\text{D}}(g_{T\bar{T}}) &= 2 + g_{T\bar{T}}\, \delta\hat{\Delta}_{\text{D}} + O(g_{T\bar{T}}^2) \; , \quad \delta\hat{\Delta}_{\text{D}} = \pi \; , \\ \Delta_{\text{D}^2}(g_{T\bar{T}}) &= 4 + g_{T\bar{T}}\, \delta\hat{\Delta}_{\text{D}^2} + O(g_{T\bar{T}}^2) \; , \quad \delta\hat{\Delta}_{\text{D}^2} = 6\pi \; . \end{aligned} \tag{3.4}$$

The spectrum of our undeformed BCFT_2 might feature a boundary Virasoro primary ψ with tree-level dimension $\hat{\Delta}$. The $T\bar{T}$ deformation of such BCFT then results in the following anomalous dimension for ψ, as shown in appendix E

$$\hat{\Delta}_\psi(g_{T\bar{T}}) = \hat{\Delta} + g_{T\bar{T}}\, \delta\hat{\Delta}_\psi + O(g_{T\bar{T}}^2) \; , \quad \delta\hat{\Delta}_\psi = \frac{\pi}{2}\hat{\Delta}(\hat{\Delta}-1) \; . \tag{3.5}$$

[1] Note that the $T \times \bar{T}$ OPE is regular, as dictated by holomorphy.

We note that $\delta\hat{\Delta}_\psi = \hat{\Delta}^2$ at large $\hat{\Delta}$, generalizing the expectation from AdS effective field theory [39, 40]. In appendix E we also compute the following boundary correlation functions

$$\begin{aligned}\langle \mathrm{D}(1)\mathrm{D}(x)\mathrm{D}(0)\rangle &\propto \hat{\lambda}_{\mathrm{DDD}}(g_{T\bar{T}}) \ , \quad \langle \psi(1)\psi(x)\mathrm{D}(0)\rangle \propto \hat{\lambda}_{\psi\psi\mathrm{D}}(g_{T\bar{T}}) \ , \\ \langle \mathrm{D}(1)\mathrm{D}(x)\mathrm{D}^2(0)\rangle &\propto \hat{\lambda}_{\mathrm{DDD}^2}(g_{T\bar{T}}) \ , \quad \langle \psi(1)\psi(x)\mathrm{D}^2(0)\rangle \propto \hat{\lambda}_{\psi\psi\mathrm{D}^2}(g_{T\bar{T}}) \ ,\end{aligned} \tag{3.6}$$

at one-loop in the $T\bar{T}$ deformation. As we show in the appendix, these correlators remain conformal along the full RG, and for unit-normalized boundary operators we find:

$$\begin{aligned}\hat{\lambda}_{\mathrm{DDD}}(g_{T\bar{T}}) &= \frac{2\sqrt{2}}{c}\left(1 - \frac{\pi(c-24)}{8} g_{T\bar{T}} + O(g_{T\bar{T}}^2)\right) \ , \\ \hat{\lambda}_{\psi\psi\mathrm{D}}(g_{T\bar{T}}) &= \frac{\sqrt{2}\hat{\Delta}}{\sqrt{c}}\left(1 - \pi\left(1 + \frac{c}{24} - 2\hat{\Delta}\right) g_{T\bar{T}} + O(g_{T\bar{T}}^2)\right) \ , \\ \hat{\lambda}_{\psi\psi\mathrm{D}^2}(g_{T\bar{T}}) &= \frac{\sqrt{\frac{2}{5}}\hat{\Delta}(5\hat{\Delta}+1)}{\sqrt{c(5c+22)}}\left(1 - \frac{\pi}{60}(5c - 240\hat{\Delta} + 262) g_{T\bar{T}} + O(g_{T\bar{T}}^2)\right) \ , \\ \hat{\lambda}_{\mathrm{DDD}^2}(g_{T\bar{T}}) &= \frac{1}{c}\sqrt{\frac{2}{5}}\sqrt{c(5c+22)}\left(1 + \frac{109\pi}{30} g_{T\bar{T}} + O(g_{T\bar{T}}^2)\right) \ .\end{aligned} \tag{3.7}$$

3.2 Deformations by a bulk Virasoro primary

Consider a 2d CFT in AdS_2 with a generic conformal boundary condition and central charge c. If this theory supports a scalar bulk Virasoro primary with scaling dimension Δ_ϕ, we can turn on the following deformation in the bulk of AdS

$$\delta S = g_\phi R^{\Delta_\phi - 2} \int d^2x \sqrt{g}\, \phi(x+iy, x-iy) + \text{counterterms} \ . \tag{3.8}$$

We assume that ϕ does not contain any marginal boundary global primary in its bulk-boundary OPE.[2] The undeformed theory features again both D and D^2. The anomalous dimensions of these operators under the deformation of eq. (3.8) at the first order in the coupling read

$$\begin{aligned}\Delta_{\mathrm{D}}(g_\phi) &= 2 + g_\phi\, \delta\hat{\Delta}_{\mathrm{D}} + O(g_\phi^2) \ , \\ \Delta_{\mathrm{D}^2}(g_\phi) &= 4 + g_\phi\, \delta\hat{\Delta}_{\mathrm{D}^2} + O(g_\phi^2) \ ,\end{aligned} \tag{3.9}$$

with [26] (see also appendix F for a derivation)

$$\begin{aligned}\delta\hat{\Delta}_{\mathrm{D}} &= \frac{B_\phi}{2^{\Delta_\phi}} \frac{4\pi}{c}(\Delta_\phi - 2)\Delta_\phi \ , \\ \delta\hat{\Delta}_{\mathrm{D}^2} &= \frac{B_\phi}{2^{\Delta_\phi}} \frac{2\pi\Delta_\phi(\Delta_\phi - 2)(20c + 25(\Delta_\phi - 2)\Delta_\phi + 64)}{c(5c+22)} \ .\end{aligned} \tag{3.10}$$

[2] If it does, then the bulk RG will induce a boundary RG flow and potentially destabilize the boundary condition, see e.g. the discussion in [26, 35].

In the equations above, B_ϕ is the tree-level one-point function coefficient for the operator ϕ with a generic conformal boundary condition, see eq. (2.7). In appendix F we also compute the following boundary correlation functions

$$\langle \mathrm{D}(1)\mathrm{D}(x)\mathrm{D}(0)\rangle \propto \hat{\lambda}_{\mathrm{DDD}}(g_\phi)\ , \quad \langle \mathrm{D}(1)\mathrm{D}(x)\mathrm{D}^2(0)\rangle \propto \hat{\lambda}_{\mathrm{DDD}^2}(g_\phi) \tag{3.11}$$

at one-loop in the Virasoro deformation above. As we show in the appendix, these correlators remain conformal along the full RG, and for unit-normalized boundary operators we find

$$\begin{aligned}
\hat{\lambda}_{\mathrm{DDD}}(g_\phi) &= \frac{2\sqrt{2}}{c}\left(1+\frac{B_\phi}{2^{\Delta_\phi}}\frac{3\pi}{c}(\Delta_\phi-2)\Delta_\phi^2\, g_\phi + O(g_\phi^2)\right)\ , \\
\hat{\lambda}_{\mathrm{DDD}^2}(g_\phi) &= \frac{1}{c}\sqrt{\frac{2}{5}}\sqrt{c(5c+22)}\left(1+\frac{B_\phi}{2^{\Delta_\phi}}\frac{\pi(\Delta_\phi-2)\Delta_\phi(5\Delta_\phi+2)(25\Delta_\phi+336)}{30c(5c+22)}g_\phi + O(g_\phi^2)\right)\ .
\end{aligned} \tag{3.12}$$

3.3 Ising model and its deformations

Bulk theory. The Ising model is the $m=3$ diagonal minimal model. It has $c=1/2$ and it is characterized by the following set of scalar Virasoro primaries

Δ	Symbol	(r,s)
0	$\mathbb{1}$	$(1,1)$ or $(2,3)$
$1/8$	σ	$(1,2)$ or $(2,2)$
1	ϵ	$(1,3)$ or $(2,1)$

The non-trivial fusion rules are

$$\epsilon\times\epsilon=\mathbb{1}\ , \quad \sigma\times\epsilon=\sigma\ , \quad \sigma\times\sigma=\mathbb{1}+\epsilon\ . \tag{3.13}$$

The bulk theory is invariant under a $\mathbb{Z}_2$ global symmetry. Such $\mathbb{Z}_2$ flips the sign of σ, and leaves invariant $\mathbb{1}$ and ϵ, see e.g. [30, 31].

The $\mathbb{Z}_2$-invariant conformal boundary conditions. There are three elementary conformal boundary conditions. The ones labelled by $(1,1)_3$ and $(1,3)_3$ are $\mathbb{Z}_2$-breaking while the one labelled by $(1,2)_3$ is $\mathbb{Z}_2$-preserving.[3] We will focus on the latter, for which the spectrum of allowed boundary Virasoro primaries, as well as non-vanishing bulk one-point functions are reported in Table 1.

[3] A conformal boundary condition is $\mathbb{Z}_2$-invariant when the corresponding Cardy state is. Equivalently, all bulk one-point functions of $\mathbb{Z}_2$-odd operators vanish.

$(a_1, a_2)_m$	Boundary spectrum	$\mathbb{Z}_2$	$\hat{\Delta}$
$(1,2)_3$	$\hat{\mathbb{1}}$	$+1$	0
	$\psi_{(1,3)} \simeq \psi_{(2,1)}$	-1	$1/2$

Bulk primary	Δ	$(1,2)_3$ b.c.
$(1,1)$	0	1
$(1,3)$ or $(2,1)$	1	-1

Table 1: $\mathbb{Z}_2$-preserving conformal boundary conditions for the Ising model. In the first table: spectrum of boundary Virasoro primaries. In the second table, non-vanishing one-point functions $B^{\mathbf{a}}_{\phi}$ (see eq. (2.7)) of bulk Virasoro primaries.

Let us now discuss the $\mathbb{Z}_2$ charges in Table 1. In a given $\mathbb{Z}_2$-preserving conformal boundary condition, a boundary global primary that appears in the bulk-boundary OPE of a $\mathbb{Z}_2$-even (odd) operator, is $\mathbb{Z}_2$-even (odd). For example, in any $\mathbb{Z}_2$-invariant boundary condition, the boundary identity $\hat{\mathbb{1}}$ must appear in the bulk-boundary OPE of the bulk identity. Since the displacement operator D is a level-two Virasoro descendant of $\hat{\mathbb{1}}$, it must be $\mathbb{Z}_2$-even. For 'less universal' boundary primaries, understanding their $\mathbb{Z}_2$ charges requires in general to study correlation function with both bulk and boundary operators insertions.

For instance, in order to determine the $\mathbb{Z}_2$ charge for the $\psi_{(1,3)}$ boundary operator in the $(1,2)_3$ conformal boundary condition, the relevant bulk-boundary OPE is

$$\sigma(x+iy, x-iy) = \frac{B^{\mathbf{a}}_{\sigma}}{(2y)^{\Delta_\sigma}}\hat{\mathbb{1}} + \frac{B^{\mathbf{a}\,(1,3)}_{\sigma}}{(2y)^{\Delta_\sigma - \hat{\Delta}_{1,3}}}\psi_{(1,3)}(x) + \text{desc.} \tag{3.14}$$

After deriving the bulk two-point function of σ one finds that [34, 41, 29]

$$(B^{\mathbf{a}\,(1,3)}_{\sigma})^2 = \frac{1}{\sqrt{2}} \ , \tag{3.15}$$

(see also our appendix D.1 for an independent derivation of this result). Hence, $\psi_{(1,3)}$ is $\mathbb{Z}_2$-odd, and so the following boundary fusion rule must hold

$$\psi_{(1,3)} \times \psi_{(1,3)} = \hat{\mathbb{1}} \ . \tag{3.16}$$

We have reconstructed the holomorphic counterpart of the fusion rules in eq. (3.13). This is not surprising: as already emphasized earlier, boundary Virasoro primaries behave as holomorphic Virasoro primaries as far as Ward identities are concerned.

Bulk perturbations. We will consider both relevant and (leading) irrelevant, $\mathbb{Z}_2$-preserving, bulk perturbations of the Ising model in AdS with $(1,2)_3$ boundary conditions,

$$\delta S_{\rm rel} = g_{(1,3)} R^{\Delta_{1,3}-2} \int d^2x \sqrt{g}\, \phi_{(1,3)}(x+iy, x-iy) + \text{counterterms} \ ,$$
$$\delta S_{\rm irrel} = g_{T\bar{T}} R^2 \int d^2x \sqrt{g}\, T\bar{T}(x+iy, x-iy) + \text{counterterms} \ . \tag{3.17}$$

For each allowed global boundary primary with tree-level dimension $\hat{\Delta}$ we will compute, at the leading order in the deformation

$$\hat{\Delta}_\psi(g_{(i)}) = \hat{\Delta} + \sum_i g_{(i)} \delta\hat{\Delta}^{(i)}_\psi + \dots, \quad g_{(i)} = \{g_{(1,3)},\ g_{T\bar{T}}\} \ . \tag{3.18}$$

For the contributions of the $\phi_{(1,3)}$ deformation to the anomalous dimensions of $\psi_{(r,s)}$ we can use the result of ref. [26]. For the one-loop anomalous dimensions under the $T\bar{T}$ deformation we use eq. (3.5) while for that of D, D^2 under a generic bulk Virasoro primary we use eq. (3.10).

3.3.1 The $(1,2)_3$ conformal b.c. and its deformations

Tree-level analysis. Beside the boundary identity $\hat{\mathbb{1}}$, the only allowed boundary Virasoro primary is $\psi_{(1,3)} \simeq \psi_{(2,1)}$ and is $\mathbb{Z}_2$-odd, see Table 1. We will study the $\mathbb{Z}_2$-invariant four-point correlation functions between $\psi_{(1,3)}$ and D along the RG. At tree-level, the leading OPEs are (schematically)

$$\begin{aligned} \psi_{(1,3)} \times \psi_{(1,3)} &\sim \hat{\mathbb{1}} + \mathrm{D} + \dots \ , \\ \psi_{(1,3)} \times \mathrm{D} &\sim \psi_{(1,3)} + \psi^{(4)}_{(1,3)} + \psi^{(7)}_{(1,3)} + \dots \ , \\ \mathrm{D} \times \mathrm{D} &\sim \hat{\mathbb{1}} + \mathrm{D} + \mathrm{D}^2 + \dots \ , \end{aligned} \tag{3.19}$$

The superscript (n) denotes level-n Virasoro descendants which are global primaries. The quantum numbers of the operators that appear in eq. (3.19) are reported in Table 2 (the analysis of the parity-odd channel in correlation functions with the displacement is worked out in appendix C).

	$\hat{\Delta}$	$\mathbb{Z}_2$	P
$\psi_{(1,3)}$	$\frac{1}{2}$	-1	$+1$
D	2	$+1$	$+1$
$\psi^{(4)}_{(1,3)}$	$4+\frac{1}{2}$	-1	$+1$
D^2	4	$+1$	$+1$
$\psi^{(7)}_{(1,3)}$	$7+\frac{1}{2}$	-1	-1

Table 2: Ising model with $(1,2)_3$ conformal boundary condition. Quantum numbers of the leading global boundary primaries appearing in the OPEs (3.19).

One-loop results. The one-loop anomalous dimensions for the boundary operators $\psi_{(r,s)}$, D and D^2 under the bulk deformations of eq. (3.17) can be found in Table 3.

	$g_{(1,3)}\phi_{(1,3)}$	$g_{T\bar{T}}T\bar{T}$
$\delta\hat{\Delta}^{(i)}_{(1,3)}$	2π	$-\frac{\pi}{8}$
$\delta\hat{\Delta}^{(i)}_{\mathrm{D}}$	4π	π
$\delta\hat{\Delta}^{(i)}_{\mathrm{D}^2}$	4π	6π

Table 3: Anomalous dimensions of the leading boundary primaries in the $(1,2)_3$ conformal boundary condition under the deformation of eq. (3.17).

3.4 Tricritical Ising model and its deformations

Bulk theory. The tricritical Ising model is the $m = 4$ diagonal minimal model. It has $c = 7/10$ and it is characterized by the following set of scalar Virasoro primaries

Δ	Symbol	(r,s)
0	$\mathbb{1}$	$(1,1)$ or $(3,4)$
$1/5$	ϵ	$(1,2)$ or $(3,3)$
$6/5$	ϵ'	$(1,3)$ or $(3,2)$
3	ϵ''	$(1,4)$ or $(3,1)$
$3/40$	σ	$(2,2)$ or $(2,3)$
$7/8$	σ'	$(2,4)$ or $(2,1)$

The non-trivial fusion rules are (see eq. (2.14))

$$
\begin{aligned}
&\epsilon\times\epsilon = \mathbb{1}+\epsilon' , && \epsilon\times\epsilon' = \epsilon+\epsilon'' , && \epsilon\times\epsilon'' = \epsilon' ,\\
&\epsilon'\times\epsilon' = \mathbb{1}+\epsilon' , && \epsilon'\times\epsilon'' = \epsilon , && \epsilon''\times\epsilon'' = \mathbb{1} ,\\
&\epsilon\times\sigma = \sigma+\sigma' , && \epsilon\times\sigma' = \sigma , && \epsilon'\times\sigma = \sigma+\sigma' ,\\
&\epsilon'\times\sigma' = \sigma , && \epsilon''\times\sigma = \sigma , && \epsilon''\times\sigma' = \sigma' ,\\
&\sigma\times\sigma = \mathbb{1}+\epsilon+\epsilon'+\epsilon'' , && \sigma\times\sigma' = \epsilon+\epsilon' , && \sigma'\times\sigma' = \mathbb{1}+\epsilon'' .
\end{aligned}
\tag{3.20}
$$

The bulk theory is invariant under a $\mathbb{Z}_2$ global symmetry. Such $\mathbb{Z}_2$ flips the sign of σ and σ', and leaves invariant the other Virasoro primaries, see e.g. [30, 31].

The $\mathbb{Z}_2$-invariant conformal boundary conditions. The allowed elementary and $\mathbb{Z}_2$-preserving conformal boundary conditions are listed in Table 4. Corresponding non-vanishing values of bulk Virasoro primary one-point functions are reported in Table 5.

$(a_1, a_2)_m$	Boundary spectrum	$\mathbb{Z}_2$	$\hat{\Delta}$
$(2,1)_4$	$\hat{\mathbb{1}}$	$+1$	0
	$\psi_{(3,1)}$	-1	$3/2$
$(2,2)_4$	$\hat{\mathbb{1}}$	$+1$	0
	$\psi_{(1,2)} \simeq \psi_{(3,3)}$	-1	$1/10$
	$\psi_{(1,3)}$	$+1$	$3/5$
	$\psi_{(3,1)}$	-1	$3/2$

Table 4: $\mathbb{Z}_2$-preserving conformal boundary conditions for the tricritical Ising model and corresponding spectrum of boundary Virasoro primaries.

Bulk primary	Δ	$(2,1)_4$ b.c.	$(2,2)_4$ b.c.
$(1,1)$	0	1	1
$(1,2)$ or $(3,3)$	$1/5$	$-\sqrt{\frac{1}{2}\left(1+\sqrt{5}\right)}$	$\sqrt{-2+\sqrt{5}}$
$(1,3)$ or $(3,2)$	$6/5$	$\sqrt{\frac{1}{2}\left(1+\sqrt{5}\right)}$	$-\sqrt{-2+\sqrt{5}}$
$(1,4)$ or $(3,1)$	3	-1	-1

Table 5: Non-vanishing one-point functions $B_\phi^{\mathbf{a}}$ (see eq. (2.7)) of bulk Virasoro primaries ϕ in the $\mathbb{Z}_2$-preserving boundary conditions of tricritical Ising model.

Let us now discuss the $\mathbb{Z}_2$ charges in Table 4. In order to determine the $\mathbb{Z}_2$ charge for the $\psi_{(3,1)}$ boundary operator, in either $(2,1)_4$ and $(2,2)_4$ conformal boundary conditions, the relevant bulk-boundary OPE is

$$\sigma'(x+iy, x-iy) = \frac{B^{\mathbf{a}}_{\sigma'}}{(2y)^{\Delta_{\sigma'}}}\hat{\mathbb{1}} + \frac{B^{\mathbf{a}\,(3,1)}_{\sigma'}}{(2y)^{\Delta_{\sigma'}-\hat{\Delta}_{3,1}}}\psi_{(3,1)}(x) + \text{desc.} \tag{3.21}$$

One finds that [41]

$$(B^{\mathbf{a}\,(3,1)}_{\sigma'})^2 = \frac{7}{4\sqrt{2}}\ . \tag{3.22}$$

We have reproduced this result by studying the bulk two-point function of σ' in appendix D.2. Hence $\psi_{(3,1)}$ is $\mathbb{Z}_2$-odd. For $\psi_{(1,3)}$ in $(2,2)_4$ one can consider instead

$$\epsilon'(x+iy,x-iy)=\frac{B^{\mathbf{a}}_{\epsilon'}}{(2y)^{\Delta_{\epsilon'}}}\hat{\mathbb{1}}+\frac{B^{\mathbf{a}\,(1,3)}_{\epsilon'}}{(2y)^{\Delta_{\epsilon'}-\hat{\Delta}_{1,3}}}\psi_{(1,3)}(x)+\text{desc.} \tag{3.23}$$

From the bulk two-point function of ϵ' in appendix D.3 we find that $\psi_{(1,3)}$ is $\mathbb{Z}_2$-even, since [41]

$$(B^{\mathbf{a}\,(1,3)}_{\epsilon'})^2\simeq 0.663053\ . \tag{3.24}$$

For $\psi_{(3,3)}$ in $(2,2)_4$, instead of computing the bulk-boundary OPE of σ (which is complicated), we can investigate the boundary four-point correlation function with $\psi_{(1,3)}$ and $\psi_{(3,1)}$

$$\langle\psi_{(1,3)}(x_1)\psi_{(3,1)}(x_2)\psi_{(1,3)}(x_3)\psi_{(3,1)}(x_4)\rangle\ . \tag{3.25}$$

Since $\psi_{(1,3)}$ and $\psi_{(3,1)}$ are (respectively) even and odd, the s-channel blocks expansion of the above expression can contain at most $\psi_{(3,1)}$ and $\psi_{(3,3)}$. On the other hand

$$\hat{C}^{\mathbf{a}}_{(1,3)(3,1)(3,1)}=\hat{C}^{\mathbf{a}}_{(3,1)(3,1)(1,3)}=0\ , \tag{3.26}$$

since the self-OPE of $\psi_{(3,1)}$ does not contain $\psi_{(1,3)}$ – see appendix D.3.2. Being (3.25) non-vanishing, this correlator must contain $\psi_{(3,3)}$, which therefore must be $\mathbb{Z}_2$-odd. Proceeding this way, again we end up reconstructing the holomorphic counterpart of the fusion rules in eq. (3.20)

$$\begin{aligned}
&\psi_{(3,3)}\times\psi_{(3,3)}=\hat{\mathbb{1}}+\psi_{(1,3)}\ , && \psi_{(3,3)}\times\psi_{(1,3)}=\psi_{(3,3)}+\psi_{(3,1)}\ ,\\
&\psi_{(3,3)}\times\psi_{(3,1)}=\psi_{(1,3)}\ , && \psi_{(1,3)}\times\psi_{(1,3)}=\hat{\mathbb{1}}+\psi_{(1,3)}\ ,\\
&\psi_{(1,3)}\times\psi_{(3,1)}=\psi_{(3,3)}\ , && \psi_{(3,1)}\times\psi_{(3,1)}=\hat{\mathbb{1}}\ .
\end{aligned} \tag{3.27}$$

Bulk perturbations. We will consider both relevant and (leading) irrelevant, $\mathbb{Z}_2$-preserving, bulk perturbations of the tricritical Ising model in AdS, with either $(2,1)_4$ or $(2,2)_4$ conformal boundary conditions (counterterm contributions are left implicit)

$$\begin{aligned}
\delta S_{\text{rel}}&=\int d^2x\sqrt{g}\ \left[g_{(3,3)}R^{\Delta_{3,3}-2}\phi_{(3,3)}(x+iy,x-iy)+g_{(1,3)}R^{\Delta_{1,3}-2}\phi_{(1,3)}(x+iy,x-iy)\right]\\
\delta S_{\text{irrel}}&=\int d^2x\sqrt{g}\ \left[g_{(3,1)}R^{\Delta_{3,1}-2}\phi_{(3,1)}(x+iy,x-iy)+g_{T\bar{T}}R^2T\bar{T}(x+iy,x-iy)\right]\ .
\end{aligned} \tag{3.28}$$

For each allowed global boundary primary with tree-level dimension $\hat{\Delta}$ we will compute, at the leading order in the deformation

$$\hat{\Delta}_\psi(g_{(i)})=\hat{\Delta}+\sum_i g_{(i)}\delta\hat{\Delta}^{(i)}_\psi+\ldots,\quad g_{(i)}=\{g_{(3,3)},\ g_{(1,3)},\ g_{(3,1)},\ g_{(3,3)},\ g_{T\bar{T}}\}\ . \tag{3.29}$$

For the contributions of the $\phi_{(1,3)}$, $\phi_{(3,1)}$ deformation to the anomalous dimensions of $\psi_{(r,s)}$ we can use the result of ref. [26], while the $\phi_{(1,2)}$ deformation is studied in our appendix G. For the one-loop anomalous dimensions under the $T\bar{T}$ deformation we use eq. (3.5), while for that of D,D^2 under a generic bulk Virasoro primary we use eq. (3.10).

3.4.1 The $(2,1)_4$ conformal b.c. and its deformations

Tree-level analysis. Beside the boundary identity $\hat{\mathbb{1}}$, the other allowed boundary Virasoro primary is $\psi_{(3,1)}$, which is $\mathbb{Z}_2$-odd (see Table 4). We will study the $\mathbb{Z}_2$-invariant four-point correlation functions between $\psi_{(3,1)}$ and D along the RG. At tree-level, the leading OPEs are (schematically)

$$\begin{aligned} \psi_{(3,1)} \times \psi_{(3,1)} &\sim \hat{\mathbb{1}} + \mathrm{D} + \dots \ , \\ \psi_{(3,1)} \times \mathrm{D} &\sim \psi_{(3,1)} + \psi^{(2)}_{(3,1)} + \psi^{(5)}_{(3,1)} + \dots \ , \\ \mathrm{D} \times \mathrm{D} &\sim \hat{\mathbb{1}} + \mathrm{D} + \mathrm{D}^2 + \dots \ , \end{aligned} \tag{3.30}$$

The superscript (n) denotes level-n Virasoro descendants which are global primaries. The quantum numbers of the operators that appear in (3.30) are reported in Table 6. The analysis of the parity-odd channel in correlation functions with the displacement is reviewed in appendix C.

	$\hat{\Delta}$	$\mathbb{Z}_2$	P
$\psi_{(3,1)}$	$\frac{3}{2}$	-1	$+1$
D	2	$+1$	$+1$
$\psi^{(2)}_{(3,1)}$	$2+\frac{3}{2}$	-1	$+1$
D^2	4	$+1$	$+1$
$\psi^{(5)}_{(3,1)}$	$5+\frac{3}{2}$	-1	-1

Table 6: Tricritical Ising model with $(2,1)_4$ conformal boundary condition. Quantum numbers of the leading global boundary primaries appearing in the OPEs (3.30).

One-loop results. In Table 7 we report the one-loop anomalous dimensions for the boundary operators $\psi_{(r,s)}$, D and D^2 under the bulk deformations of eq. (3.28).

	$g_{(3,3)}\phi_{(3,3)}$	$g_{(1,3)}\phi_{(1,3)}$	$g_{(3,1)}\phi_{(3,1)}$	$g_{T\bar{T}}T\bar{T}$
$\delta\hat{\Delta}^{(i)}_{(3,1)}$	$\beta'/2$	$-\beta'$	$\frac{45\pi}{14}$	$\frac{3\pi}{8}$
$\delta\hat{\Delta}^{(i)}_{\mathrm{D}}$	$-\frac{3\beta'}{5}$	$-\frac{4\beta'}{5}$	$-\frac{15\pi}{7}$	π
$\delta\hat{\Delta}^{(i)}_{\mathrm{D}^2}$	$-\frac{69\beta'}{85}$	$-\frac{72\beta'}{85}$	$-\frac{45\pi}{7}$	6π

$$\beta' = \frac{12\pi}{7} 2^{4/5} B^{\mathbf{a}}_{(1,3)} \approx 11.9275 \tag{3.31}$$

Table 7: Anomalous dimensions of leading boundary primaries in $(2,1)_4$. Rows: contribution to $\delta\hat{\Delta}_{(r,s)}$ from each deformation. The number β' is defined in (3.31). The corresponding value of $B^{\mathbf{a}}_{(1,3)}$ is shown in Table 5.

3.4.2 The $(2,2)_4$ conformal b.c. and its deformations

Tree-level analysis. The allowed boundary Virasoro primaries in the $(2,2)_4$ conformal boundary condition are listed in Table 4. The leading OPEs are (schematically)

$$\begin{aligned}
&\psi_{(3,3)} \times \psi_{(3,3)} \sim \hat{\mathbb{1}} + \psi_{(1,3)} + \mathrm{D} + \psi^{(2)}_{(1,3)} + \dots \,, \\
&\psi_{(1,3)} \times \psi_{(1,3)} \sim \hat{\mathbb{1}} + \psi_{(1,3)} + \mathrm{D} + \psi^{(2)}_{(1,3)} + \dots \,, \\
&\psi_{(3,3)} \times \psi_{(1,3)} \sim \psi_{(3,3)} + \psi_{(3,1)} + \dots + \psi^{(3)}_{(3,3)} + \dots \,, \\
&\psi_{(3,1)} \times \psi_{(3,1)} \sim \hat{\mathbb{1}} + \mathrm{D} + \dots \,, \\
&\psi_{(3,3)} \times \psi_{(3,1)} \sim \psi_{(1,3)} + \psi^{(2)}_{(1,3)} \cdots \,, \\
&\psi_{(1,3)} \times \psi_{(3,1)} \sim \psi_{(3,3)} + \dots
\end{aligned} \tag{3.32}$$

The superscript (n) denotes level-n Virasoro descendants which are global primaries. In the third and fifth lines of eq. (3.32) we have also omitted leading parity-even descendants of $\psi_{(3,3)}$ and $\psi_{(3,1)}$, which are subleading with respect to $\psi^{(2)}_{(1,3)}$. The quantum numbers of the operators in eq. (3.32) are reported in Table 8 (the analysis of the parity-odd channel in correlation functions with the displacement is worked out in appendix C).

	$\hat{\Delta}$	$\mathbb{Z}_2$	P
$\psi_{(3,3)}$	$\frac{1}{10}$	-1	$+1$
$\psi_{(1,3)}$	$\frac{3}{5}$	$+1$	$+1$
$\psi_{(3,1)}$	$\frac{3}{2}$	-1	$+1$
D	2	$+1$	$+1$
$\psi^{(2)}_{(1,3)}$	$2+\frac{3}{5}$	$+1$	$+1$
$\psi^{(3)}_{(3,3)}$	$3+\frac{1}{10}$	-1	-1

Table 8: Tricritical Ising model with $(2,2)_4$ conformal boundary condition. Quantum numbers of the leading global boundary primaries appearing in the OPEs (3.32).

One-loop anomalous dimensions. In Table 9 we list the one-loop anomalous dimensions for the boundary operators $\psi_{(r,s)}$, D and D^2 under the bulk deformations of eq. (3.28).

	$g_{(3,3)}\phi_{(3,3)}$	$g_{(1,3)}\phi_{(1,3)}$	$g_{(3,1)}\phi_{(3,1)}$	$g_{T\bar{T}}T\bar{T}$
$\delta\hat{\Delta}^{(i)}_{(3,3)}$	$-\sigma$	$-\delta$	$\frac{3\pi}{14}$	$-\frac{9\pi}{200}$
$\delta\hat{\Delta}^{(i)}_{(1,3)}$	ζ	α	$\frac{6\pi}{7}$	$-\frac{3\pi}{25}$
$\delta\hat{\Delta}^{(i)}_{(3,1)}$	$-\beta/2$	β	$\frac{45\pi}{14}$	$\frac{3\pi}{8}$
$\delta\hat{\Delta}^{(i)}_{\mathrm{D}}$	$-\frac{3\beta}{5}$	$\frac{4\beta}{5}$	$-\frac{15\pi}{7}$	π
$\delta\hat{\Delta}^{(i)}_{\mathrm{D}^2}$	$-\frac{69\beta}{85}$	$\frac{72\beta}{85}$	$-\frac{45\pi}{7}$	6π

Table 9: Anomalous dimensions of leading boundary primaries in $(2,2)_4$. Rows: contribution to $\delta\hat{\Delta}_{(r,s)}$ from each deformation. The numbers $\alpha,\beta,\delta,\sigma,\zeta$ are defined in (3.33).

The parameters $\alpha,\beta,\delta,\sigma,\zeta$ of Table 9 are defined as follows

$$
\begin{aligned}
\alpha &= -B^{\mathbf{a}}_{(1,3)}\left(\frac{36\pi}{35}2^{4/5}\kappa_1+\frac{25\left(\sqrt{5}+1\right)\sqrt{\pi}\Gamma\left(-\frac{3}{10}\right)\Gamma\left(\frac{7}{10}\right)}{224\ 2^{4/5}\Gamma\left(-\frac{12}{5}\right)\Gamma\left(\frac{13}{10}\right)}\kappa_2\right)\approx 6.3241,\\
\beta &= -\frac{12\pi}{7}2^{4/5}B^{\mathbf{a}}_{(1,3)}\approx 4.55592\ ,\\
\delta &= -B^{\mathbf{a}}_{(1,3)}\left(-\frac{6}{35}2^{4/5}\pi\kappa_3+\frac{\left(\sqrt{5}+1\right)\sqrt{\pi}\Gamma\left(\frac{7}{10}\right)^2}{2\ 2^{4/5}\Gamma\left(\frac{3}{5}\right)\Gamma\left(\frac{13}{10}\right)}\kappa_4\right)\approx 0.702678\ ,\\
\sigma &= \frac{2\pi}{35}2^{4/5}B^{\mathbf{a}}_{(1,2)}\kappa_5\approx 0.209884\ ,\\
\zeta &= B^{\mathbf{a}}_{(1,2)}\left(-\frac{12\pi}{35}2^{4/5}\kappa_3+\frac{3\pi 2^{2/5}\Gamma\left(\frac{7}{10}\right)\Gamma\left(\frac{11}{10}\right)}{\Gamma\left(\frac{1}{5}\right)\Gamma\left(\frac{13}{10}\right)^2}\kappa_4\right)\approx 1.40536\ ,
\end{aligned}
\tag{3.33}
$$

with $\mathbf{a} = (2,2)_4$. Correspondingly, the values of $B^{\mathbf{a}}_{(1,2)}$, $B^{\mathbf{a}}_{(1,3)}$ are shown in Table 5, while κ_i are the following numbers:

$$\begin{aligned}
\kappa_1 &\equiv {}_4F_3\left(-\frac{1}{5},\frac{2}{5},\frac{1}{2},\frac{13}{5};\frac{3}{5},\frac{17}{10},2;1\right) \ , \\
\kappa_2 &\equiv {}_4F_3\left(-\frac{9}{10},-\frac{3}{10},-\frac{1}{5},\frac{19}{10};-\frac{1}{10},\frac{3}{10},\frac{13}{10};1\right) \ , \\
\kappa_3 &\equiv {}_3F_2\left(\frac{2}{5},\frac{1}{2},\frac{9}{5};\frac{17}{10},2;1\right) \ , \\
\kappa_4 &\equiv {}_3F_2\left(-\frac{3}{10},-\frac{1}{5},\frac{11}{10};\frac{3}{10},\frac{13}{10};1\right) \ , \\
\kappa_5 &\equiv {}_3F_2\left(\frac{1}{2},\frac{4}{5},\frac{7}{5};\frac{17}{10},2;1\right) \ .
\end{aligned} \tag{3.34}$$

4 Numerical Results

In this section we show results from the numerical bootstrap and compare to the perturbative predictions of the previous section.

4.1 Universal bounds from Displacement four-point function

The displacement operator D is a universal feature of any BCFT with a stress-energy tensor in the bulk. At the BCFT point it has (protected) scaling dimension and its four-point correlation function is completely fixed in terms of the bulk central charge c, as shown in (2.4).

As soon as we turn on a (covariant) deformation in the bulk of AdS, the displacement is no longer protected and we expect its (conformal) four-point correlation function to depend non-trivially on the RG trajectory. This correlator should remain crossing symmetric along the AdS deformation, and so we can use the bootstrap to constrain the RG itself.

The underlying logic is simple. Let us imagine that we have found a bound saturated by the 'unperturbed' correlator (we will soon show an example of such). Then, what happens if we turn on a deformation in AdS_2? We can investigate how the unperturbed bound changes along the RG, for example by maximizing a certain OPE coefficient along the direction in parameter space that is predicted by perturbation theory. This upper bound can be then compared with the prediction from perturbation theory for this OPE coefficient. Now, since the unperturbed correlator saturates the bound there is a potential tension here. In particular the first-order prediction may extend into the disallowed region, for example for a particular sign of the perturbation. In that case this particular sign of the perturbation is disallowed on general grounds, and it is this type

of bound that we are after here.[4]

As a warm-up exploration, let us focus on the unperturbed theory and look for a bound saturated by the four-point correlation function of the displacement operator. We recall that $\Delta_{\mathrm{D}} = 2$, $\Delta_{\mathrm{D}^2} = 4$ and that, from eq. (2.6),

$$\mathrm{D} \times \mathrm{D} \sim \hat{\mathbb{1}} + \mathrm{D} + \mathrm{D}^2 + \dots \tag{4.1}$$

The first bound that comes to mind to a bootstrapper is gap maximization, and so we can try to maximize the gap after D. As it turns out, the bound in this case approaches $2\Delta_{\mathrm{D}} + 1 = 5$, which is the gap of the generalized free fermion solution. In fact this can be proved rigorously: the same functional that proves that this is the maximal allowed gap in a general correlator [42] applies here because it also happens to be positive at $\Delta_{\mathrm{D}} = 2$ where we have an additional conformal block. We must conclude that the exchange of $\Delta_{\mathrm{D}^2} = 4$ in our correlator means that it is far from extremizing the gap.

The next bound that comes to mind is OPE coefficient maximization. One could for example attempt to find upper bounds on $\hat{\lambda}_{\mathrm{DDD}}$ or $\hat{\lambda}_{\mathrm{DDD}^2}$ (independently), but this cannot work because of the following. The displacement four-point function in eq. (2.4) admits a positive conformal block decomposition for arbitrary c, with the leading OPE coefficients reading:

$$\hat{\lambda}^2_{\mathrm{DDD}} = \frac{8}{c}\,, \quad \hat{\lambda}^2_{\mathrm{DDD}^2} = 2 + \frac{11}{10}\hat{\lambda}^2_{\mathrm{DDD}}\,, \tag{4.2}$$

where we took D and D^2 to have unit normalized two-point functions. One can formally take $c \to 0$ in the equation above, and this provides a legitimate solution to crossing with arbitrarily large OPE coefficients.[5]

On the other hand, what happens if we fix $\hat{\lambda}^2_{\mathrm{DDD}}$ and maximize $\hat{\lambda}^2_{\mathrm{DDD}^2}$? In that case we do find a non-trivial upper bound: it is displayed in fig. 1 and converges nicely to the relation in eq. (4.2), when extrapolated to an infinite number of derivatives. It would be interesting to prove this property using for instance extremal functionals [42–45].

Having obtained a bound saturated by the 'unperturbed' correlator, we can start exploring how it changes as we turn on a bulk deformation. An interesting example is provided by the $T\bar{T}$ deformation of section 3.2. Guided by one-loop perturbation theory, we can explore the following direction in the space of CFT data

$$\Delta_{\mathrm{D}} - 2 = \pi g_{T\bar{T}} \equiv \tilde{g}_{T\bar{T}}\,, \quad \Delta_{\mathrm{D}^2} = 4 + 6\tilde{g}_{T\bar{T}}\,, \tag{4.3}$$

[4] This idea was used earlier in [4] to constrain the sign of an irrelevant $(\partial\phi)^4$ deformation in two bulk dimensions.

[5] Alternatively, note that the unit-normalized four-point function of D contains a GFB piece and a c-dependent piece that makes the results above unbounded. This piece is exactly equal to the fully connected Wick contractions of $\langle\phi^2\phi^2\phi^2\phi^2\rangle$ in a GFB theory. This correlator has a positive conformal block decomposition with no identity operator, and so it can be multiplied by an arbitrarily large number, leading to the unboundedness property.

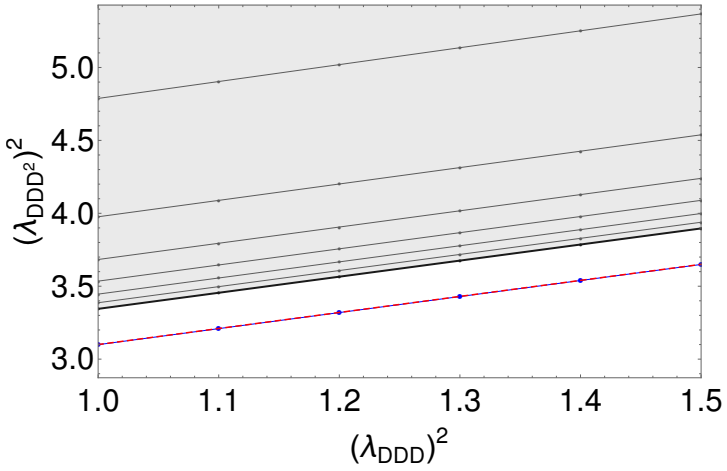

Figure 1: Upper bound on the squared OPE coefficient $(\hat{\lambda}_{\mathrm{DDD}^2})^2$ as a function of $(\hat{\lambda}_{\mathrm{DDD}})^2$. The grey dots denote bounds at increasing derivative order, which are then extrapolated to the blue dots. The red line corresponds to the analytic results of eq. (4.2). The extrapolated bounds agree with the analytic result to the third decimal place.

and maximize $\hat{\lambda}^2_{\mathrm{DDD}^2}$, as a function of $\tilde{g}_{T\bar{T}}$ and $\hat{\lambda}^2_{\mathrm{DDD}}$. Figure 2 shows the difference between the perturbative prediction

$$\hat{\lambda}^2_{\mathrm{DDD}^2} = 2 + \frac{11}{10}\hat{\lambda}^2_{\mathrm{DDD}} + \left(\frac{2510 + 209\hat{\lambda}^2_{\mathrm{DDD}}}{150}\right)\tilde{g}_{T\bar{T}}\,, \tag{4.4}$$

and the extrapolated (upper) bound. Hence, for any given central charge c, only the negative sign of the $T\bar{T}$ deformation is allowed. We emphasize that the scale of the variation with $\tilde{g}_{T\bar{T}}$ is much larger than the accuracy of the extrapolation, so we believe that our numerical results are robust. This sign constraint is a known property of the $T\bar{T}$ deformation, see e.g. [8, 9], which we have re-discovered using 1d numerical bootstrap.[6]

We can play a similar game for deformations by a generic scalar Virasoro primary, for which the first-order analysis was done in section 3.2. For a deformation ϕ with scaling dimension Δ_ϕ, the perturbative results can be rewritten as

$$\begin{aligned}
\Delta_D - 2 \equiv \tilde{g}_\phi\,, \quad \Delta_{\mathrm{D}^2} &= 4 + \tilde{g}_\phi\left(\frac{64 + 160\hat{\lambda}^{-2}_{\mathrm{DDD}} + 25\Delta_\phi(\Delta_\phi - 2)}{44 + 80\hat{\lambda}^{-2}_{\mathrm{DDD}}}\right) \\
\hat{\lambda}^2_{\mathrm{DDD}^2} &= 2 + \frac{11}{10}\hat{\lambda}^2_{\mathrm{DDD}} + \tilde{g}_\phi\left(\frac{(672 - 250\Delta_\phi + 125\Delta_\phi^2)\hat{\lambda}^2_{\mathrm{DDD}}}{1200}\right).
\end{aligned} \tag{4.5}$$

[6]Such a result is presumably related to causality. Indeed, for a positive $T\bar{T}$ coupling, the anomalous dimensions grow very quickly, destroying the good Regge behavior of the four-point function, which is associated to bulk causality. In ref. [9], the same sign of the $T\bar{T}$ coupling leads to a superluminal sound speed. Furthermore, for small but finite coupling some non-unitarity occurs for high-dimensional operators.

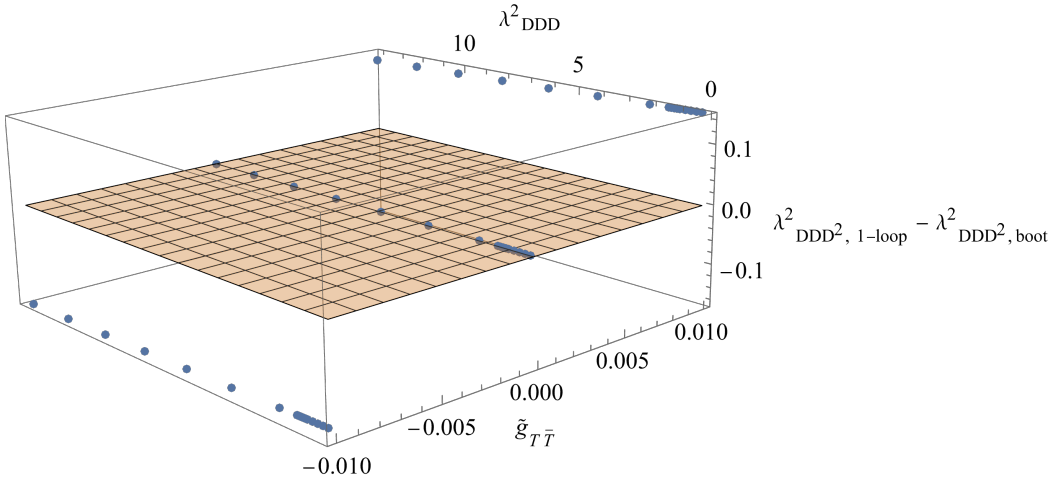

Figure 2: Difference between the perturbative prediction and the extrapolated bound on the $\hat{\lambda}^2_{\mathrm{DDD}^2}$ for varying c and $\Delta_{\mathrm{D}}, \Delta_{\mathrm{D}^2}$, following the perturbative prediction parametrized by $\tilde{g}_{T\bar{T}}$. The yellow surface serves as a guide to the eye, excluding points above it.

We have explored a few values of Δ_ϕ, including both relevant and irrelevant deformations. This time, the very same game leads to a very different result. To within our numerical precision, all these deformations saturate the numerical upper bounds, and therefore no constraint on the sign of the coupling seems to be possible.[7] In turn, we can track the perturbative RG flows, at least to leading order, by following the numerical bounds, see fig. 3 for an illustrative example with $\Delta_\phi = 1.5$. The fact that, unlike for $T\bar{T}$, no sign constraints arise for general deformations at the leading order is consistent with causality constraints. More precisely, any causality violation by irrelevant couplings, while linear for $T\bar{T}$, is at least quadratic for a generic interaction [9].

4.2 Bootstrapping the Tricritical to Critical Ising RG flow

In this section we consider the RG flow induced by the $\phi_{(1,3)}$ deformation of the tricritical Ising model in AdS_2. In the complex plane, this is the famous tricritical-to-critical Ising RG flow, see e.g. refs. [1, 2]. These flows have many interesting properties: they preserve integrability, and as such can be studied through the TBA equations [2], and can be studied perturbatively as the finite m limit of large m perturbation theory [1]. These bulk flows can also be studied in the presence of a boundary, where highly non-trivial boundary dynamics emerges [38]. Placing this flow in AdS_2 is expected to alter the nature of the boundary conditions [26], which we will assume to always be $\mathbb{Z}_2$-preserving.

[7] In a CFT one can always replace a local primary operator with minus itself, at the expense of flipping also the relevant OPE coefficients. The invariant statement we are making is that the sign of the product $g_\phi B_\phi$ is not constrained by our analysis.

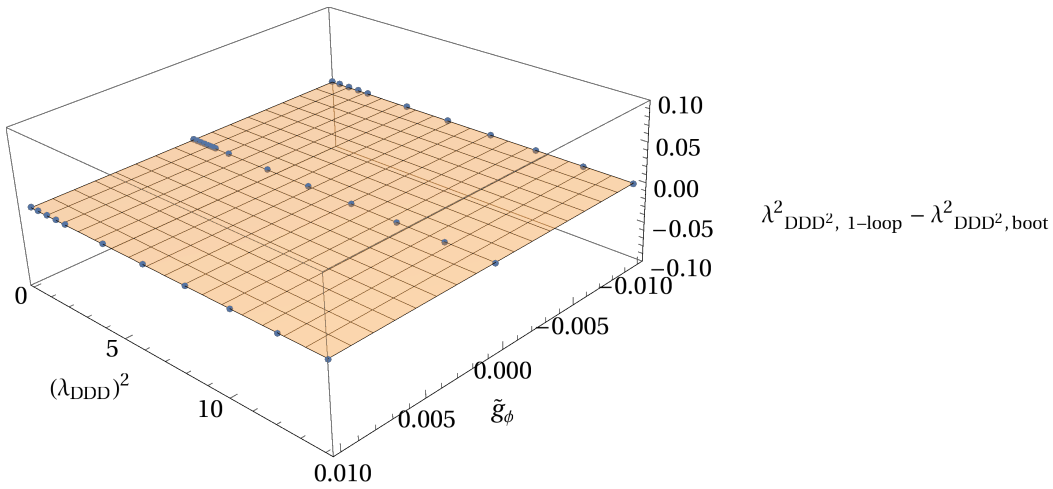

Figure 3: $\Delta_\phi = 1.5$. Difference between the perturbative prediction and the extrapolated bound on the $\hat{\lambda}^2_{\mathrm{DDD}^2}$ OPE coefficient for varying c and $\Delta_{\mathrm{D}}, \Delta_{\mathrm{D}^2}$, following the perturbative prediction parametrized by $\tilde{g}_\phi$. The yellow surface serves as a guide to the eye, excluding points above it.

4.2.1 Single correlator bound

We consider the four-point correlation function of a $\mathbb{Z}_2$-odd (global) boundary primary ψ with scaling dimension Δ_ψ

$$\langle \psi(x_1)\psi(x_2)\psi(x_3)\psi(x_4)\rangle \ . \tag{4.6}$$

As we vary Δ_ψ along the RG, ψ can interpolate between $\psi_{(3,1)}$ in the $(2,1)_4$ boundary condition for tricritical Ising (UV) and $\psi_{(1,3)}$ in the $(1,2)_3$ boundary condition for Ising (IR). Its scaling dimension correspondingly is expected to decrease from 3/2 to 1/2 along the flow.

We take the $\psi \times \psi$ OPE to be, schematically and up to subleading $\mathbb{Z}_2$-even exchanges

$$\psi \times \psi \sim \hat{\mathbb{1}} + \mathrm{D} + \mathrm{D}^2 + \dots \ . \tag{4.7}$$

Note that the scaling dimensions Δ_{D} and Δ_{D^2} must equal 2 and 4 both at the UV and at the IR fixed point, but along the flow they are not protected.

We first searched for the maximal gap $\Delta_{\mathrm{D}^2} > \Delta_{\mathrm{D}}$ as a function of Δ_ψ and Δ_{D}. The results are shown in fig. 4, which provides an overview of the landscape in which the RG flow is embedded. A section of this 3d plot at $\Delta_\psi = 3/2$ is shown in fig. 5. The interesting 'bump' in the plot of fig. 4 is delimited by:

(i) A 'floor' spanned by the generalized free fermion solution with $\Delta_{\mathrm{D}^2} = 2\Delta_\psi + 1$ for any Δ_ψ and Δ_{D}, shown as a pink surface in the figure.

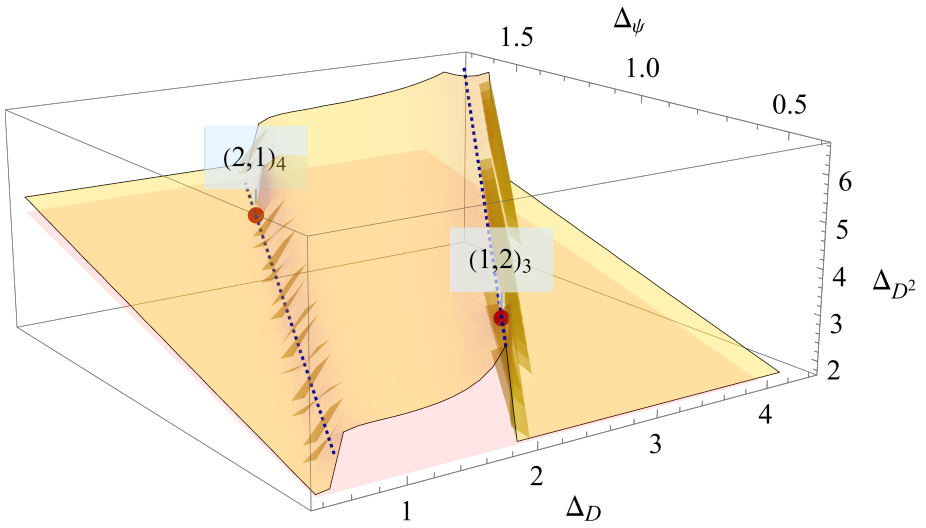

Figure 4: The light yellow surface is the 3d bound on the scalar gap from the single correlator bootstrap obtained with $\Lambda = 25$ derivatives.

(ii) The dashed blue line at the top of the cliff, which is another generalized free fermion solution with $(\Delta_\psi, \Delta_{\mathrm{D}} = 2\Delta_\psi + 1, \Delta_{\mathrm{D}^2} = 2\Delta_\psi + 3)$. The $(1,2)_3$ boundary condition for Ising corresponds to $\Delta_\psi = 1/2$ along this line.

(ii) The dashed blue line at the bottom of the cliff, which corresponds to the following four-point correlation function (conventions in appendix A.2)

$$\mathcal{G}(\eta) = \frac{\eta^{4\Delta_\psi/3}}{(1-\eta)^{2\Delta_\psi/3}} \,. \tag{4.8}$$

This solution has has $\Delta_{\mathrm{D}} = \frac{4}{3}\Delta_\psi$ and $\Delta_{\mathrm{D}^2} = \Delta_{\mathrm{D}} + 2$, for arbitrary Δ_ψ, and has previously appeared for example in [4, 46]. It merges with the $(2,1)_4$ boundary condition at $\Delta_\psi = 3/2$, as shown in fig. 5.

4.2.2 Mixed correlator system with ψ and D: the anteater

To further constrain the RG flows around the tricritical and ordinary Ising model, let us assume that ψ and D are the leading boundary primaries in the $\mathbb{Z}_2$-odd and $\mathbb{Z}_2$-even sectors, respectively. Having analyzed their individual four-point functions in sections 4.1 and 4.2.1, we now consider the following mixed system of correlators

$$\langle\psi\psi\psi\psi\rangle\,, \quad \langle\mathrm{DDDD}\rangle\,, \quad \langle\psi\psi\mathrm{DD}\rangle\,, \quad \langle\psi\mathrm{D}\psi\mathrm{D}\rangle\,. \tag{4.9}$$

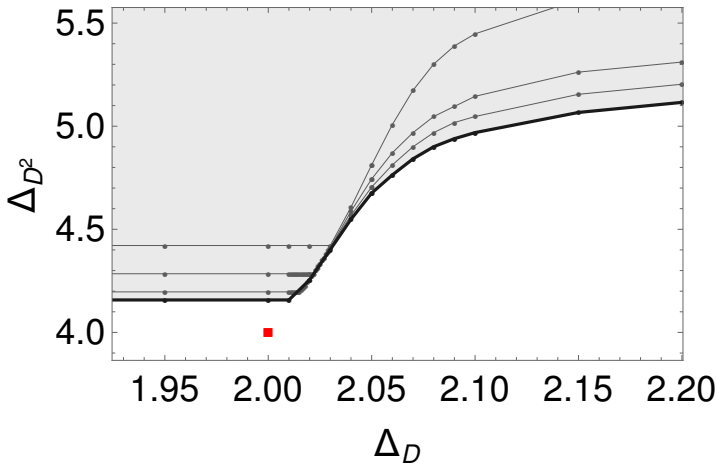

Figure 5: Bounds on the $\mathbb{Z}_2$ even gap from the numerical bootstrap for $\Delta_\psi = 3/2$. We show the results obtained with different number of derivatives, from $\Lambda = 15$ to $\Lambda = 45$ in steps of 10. The red dot corresponds to the $(2,1)_4$ b.c. of tricritical Ising.

Besides their $\mathbb{Z}_2$ charge operators are also labeled by their parity P, which is the analog of spin for the one-dimensional conformal group. The OPEs consistent with these symmetries are then:

$$\begin{aligned}
\psi \times \psi &\sim \hat{\mathbb{1}} + \mathrm{D} + \mathrm{D}^2 + \mathtt{gap}_{(+,+)} + \dots\,, \\
\mathrm{D} \times \mathrm{D} &\sim \hat{\mathbb{1}} + \mathrm{D} + \mathrm{D}^2 + \mathtt{gap}_{(+,+)} + \dots\,, \\
\psi \times \mathrm{D} &\sim \psi + \mathtt{gap}_{(-,+)} + \cdots + \mathtt{gap}_{(-,-)} \cdots\,,
\end{aligned} \tag{4.10}$$

where the ellipsis denote subleading contributions which are supposed to lie above the threshold values $\mathtt{gap}_{(\mathbb{Z}_2,P)}$ in a given $(\mathbb{Z}_2, P)$ sector. We decided on these gap assumptions as follows.

In one dimension our bounds are in particular at risk of being saturated by a generalized free solution. To gain some perspective we therefore plot the spectra of the generalized free fermion (GFF), the generalized free boson (GFB) and our minimal model boundary conditions in figure 6. This then leads us to consider the gaps (note that operators with $(\mathbb{Z}_2, P) = (+,-)$ are not exchanged here) shown in table 10.

$\mathtt{gap}_{(\mathbb{Z}_2,P)}$	$P+$	$P-$
$\mathbb{Z}_2+$	5.5	-
$\mathbb{Z}_2-$	3.5	6.5

Table 10

Below these gaps we have two operators in the $(\mathbb{Z}_2, P) = (+,+)$ sector and one operator in the $(\mathbb{Z}_2, P) = (-,+)$ sector. Altogether this means that these assumptions rule out the GFB

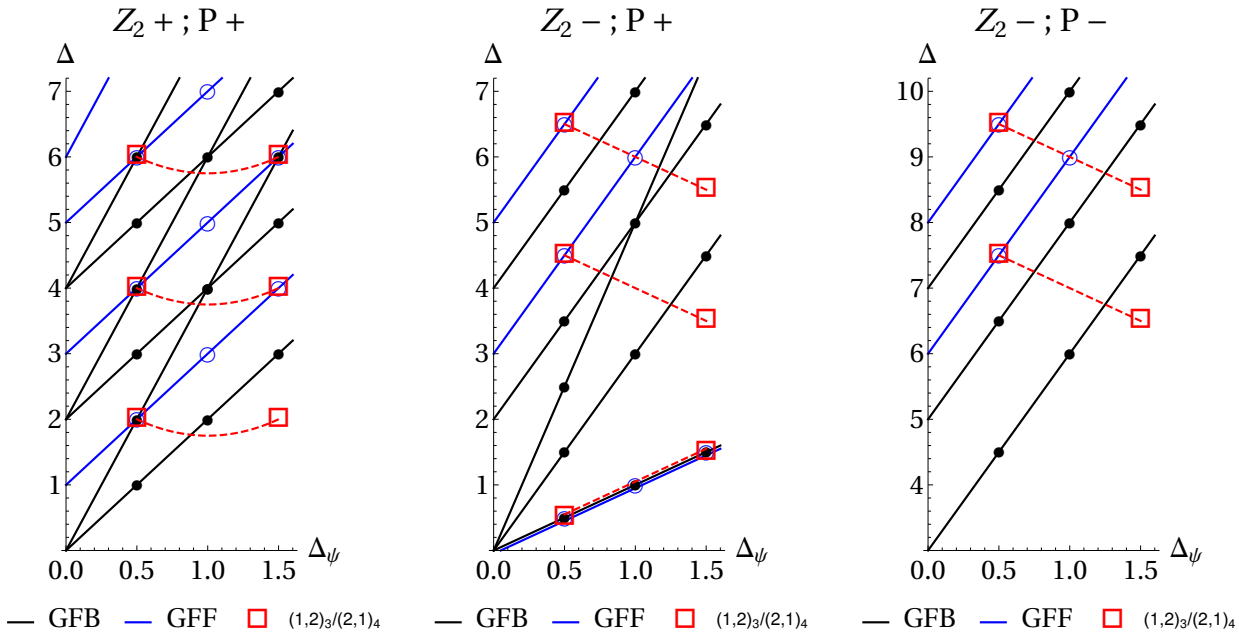

(a) (b) (c)

Figure 6: Spectra of GFF (blue lines and circles), GFB (black lines and circles) and minimal model boundary conditions (red squares) for the different $\mathbb{Z}_2$ and P sectors: (a) $\mathbb{Z}_2 : +, P : +$; (b) $\mathbb{Z}_2 : -, P : +$; (c) $\mathbb{Z}_2 : -, P : -$. The red dashed lines are suggestive of the qualitative behavior that the different dimension might take along the RG flow.

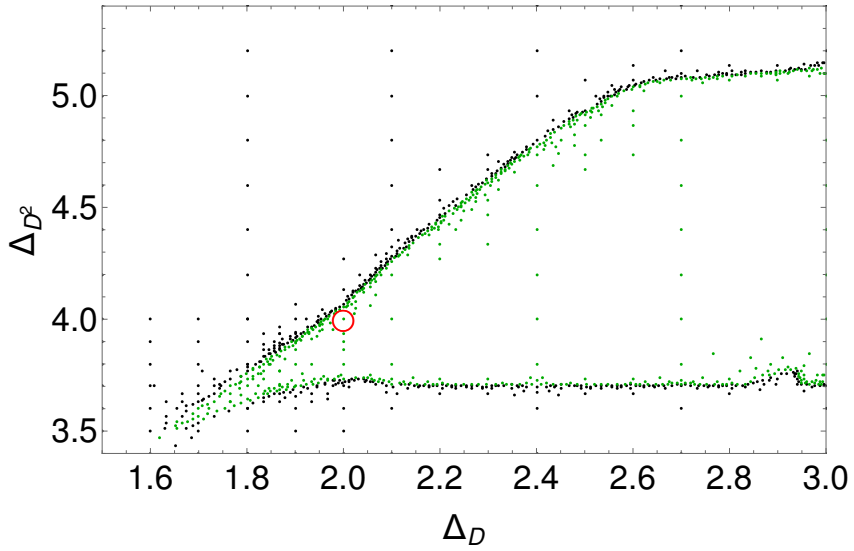

Figure 7: Bounds on $(\Delta_{\mathrm{D}}, \Delta_{\mathrm{D}^2})$ for $\Delta_\psi = 3/2$, $\Lambda = 45$. The green and black points respectively denote allowed and excluded points. The circle pinpoints the $(2,1)_4$ b.c., i.e. the eye of the 'anteater', which is attached to a very sharp 'nose'.

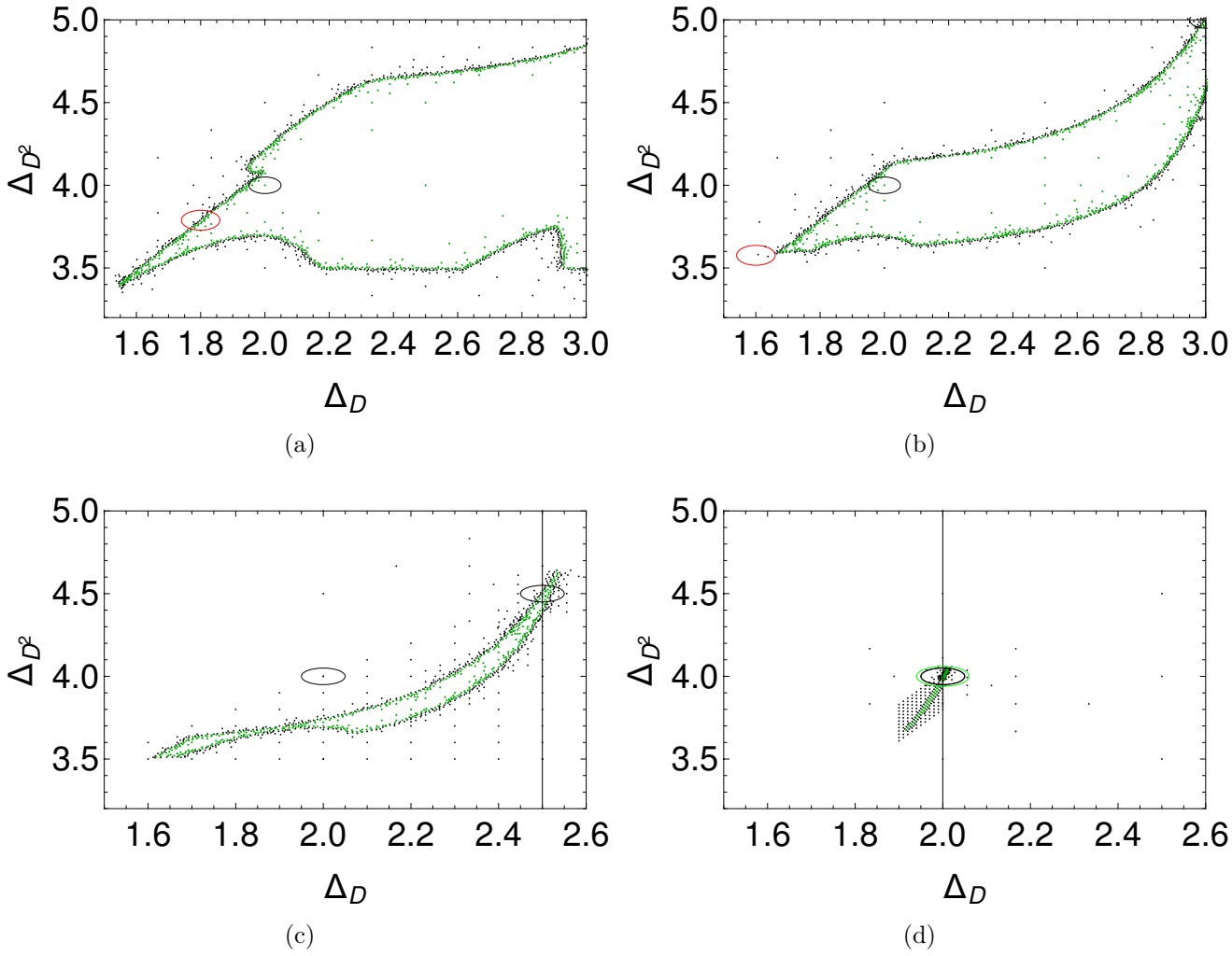

Figure 8: The anteater for different values of Δ_ψ: (a) 1.25; (b) 1.0; (c) 0.75; (d) 0.5, interpolating between the UV and IR fixed points. The plots were obtained at $\Lambda = 30$. The black circles indicate the location of a conformal boundary condition for each Δ_ψ, and the red circles denote the leading order $\phi_{1,3}$ deformation of the $(2,1)_4$ b.c, eqs.(4.14, 4.15) below, evaluated at the corresponding value of Δ_ψ. The 'anteater' shrinks as we approach the IR, and forms a tiny island around the $(1,2)_3$ b.c. of Ising, which is denoted by the green circle.

except when $\Delta_\psi \geq 1.17$, but not the GFF which has a very sparse spectrum. We can nevertheless hope that the RG flow saturates our bounds at least somewhere in the $(\Delta_{\mathrm{D}}, \Delta_{\mathrm{D}^2})$ plane as we vary Δ_ψ.

We compute bounds in the space $(\Delta_{\mathrm{D}}, \Delta_{\mathrm{D}^2})$ as we vary Δ_ψ within the interval $[1/2, 3/2]$. The numerically allowed region, the 'anteater', is shown in figures 7 and 8 for different values of Δ_ψ. We then use these points to delineate the allowed region using Delaunay triangulation [47]. A few comments are in order:

(i) In the UV, the $(2,1)_4$ boundary condition for the tricritical Ising model appears to saturate the bounds, see e.g. fig. 7.

(ii) As we go with the flow towards lower values of Δ_ψ, the allowed region shrinks, becoming substantially thinner and subsequently turns to an island, see figures 8(a-c) .

(iii) In the IR, the $(1,2)_3$ boundary condition for the Ising model is almost isolated by our gap assumptions, up to a small lobe that can be understood from combining a $\phi_{(1,3)}$ with a $T\bar{T}$ deformation, see fig. 8(d).[8]

We are going to explore these features more closely in the next sections, by focusing on specific perturbative RG flows.

4.3 Bootstrapping perturbative RG flows

In this section we refine the 'agnostic' bootstrap employed in section 4.2 by focusing on some of the $\mathbb{Z}_2$-preserving perturbative RG flows of section 3. Specifically, we again adopt the setup of section 4.2, but this time we bound CFT data along a specific RG trajectory by inputting the one-loop predictions for Δ_ψ and Δ_{D} and comparing Δ_{D^2} to predictions from perturbation theory. Of course these comparisons are only rigorous close to the origin of the perturbation.

4.3.1 Deformations of the Ising Model with $(1,2)_3$ boundary condition

In this section we study the vicinity of the Ising model with $(1,2)_3$ boundary condition using the single-correlator bootstrap setup of section 4.2.1.

(I) The relevant deformation

Turning on $\phi_{(1,3)}$ in the bulk of AdS_2 corresponds to giving a mass to the free massless Majorana fermion in the dual description of the Ising model. In terms of boundary correlators, ψ becomes a GFF whose scaling dimension Δ_ψ smoothly moves away from $1/2$, the Ising value. Since both

[8] See also the discussion on combined AdS deformations below.

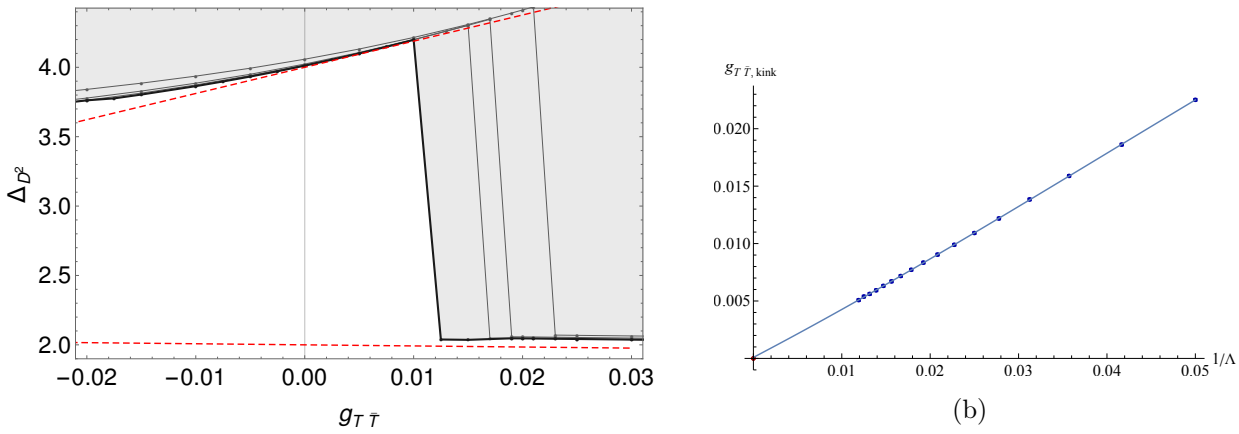

(a) (b)

Figure 9: Comparison between the numerical upper bounds (solid lines) and the predictions from the first-order $T\bar{T}$ deformation (dashed lines) near $(1,2)_3$. In (a), to the right of the kink, the bound converges to a GFF with $\Delta_\psi = \frac{1}{2} - \frac{g_{T\bar{T}}\pi}{8}$ (bottom dashed line). Figure (b) shows the convergence of the kink along the perturbation theory line towards $g_{T\bar{T}} = 0$. The data are fitted with a cubic, and the error on the intercept is $\simeq 10^{-4}$.

signs of the fermion mass are allowed, there is no constraint on the sign of $\phi_{(1,3)}$. This expectation is corroborated by our bootstrap study. One can search for the maximal gap (after D) in the four-point correlation function of ψ, along the direction suggested by the one-loop results of Table 3:

$$\Delta_\psi = 1/2 + \tilde{g}_{(1,3)} \ , \quad \Delta_{\rm D} = 2 + 2\tilde{g}_{(1,3)} \ . \tag{4.11}$$

The upper bound is saturated for both signs of the coupling by

$$\Delta_{{\rm D}^2} = 4 + 2\tilde{g}_{(1,3)} = 2\Delta_\psi + 3 \ , \tag{4.12}$$

which is just the GFF value. This solution remains valid until $\tilde{g}_{(1,3)}$ is such that Δ_ψ decreases down to zero, below which unitary is necessarily violated.

(II) The leading irrelevant deformation

We can repeat the same gap maximisation along the $T\bar{T}$ deformation of the Ising model $(1,2)_3$ conformal boundary condition, which from Table 3 reads

$$\Delta_\psi = 1/2 - g_{T\bar{T}}\pi/8 \ , \quad \Delta_{\rm D} = 2 + g_{T\bar{T}}\pi \ . \tag{4.13}$$

The comparison with the one-loop prediction for $\Delta_{{\rm D}^2}$ is shown in fig. 9. After extrapolating in the number of derivatives we see that the $g_{T\bar{T}} > 0$ region is completely excluded (on the basis

of crossing and unitarity). This is consistent with the results of section 4.1, but here the same conclusion is obtained from a different correlation function.

It is clear that this has to be the case. For a single-correlator with external dimension Δ_ψ, the maximal gap above the identity is $2\Delta_\psi + 1$, see e.g. [43]. The Ising model $(1,2)_3$ boundary condition saturates this bound when $g_{T\bar{T}} = 0$, while first-order $T\bar{T}$ perturbation clearly violates it when $g_{T\bar{T}} > 0$. Note that, in this particular case, the $T\bar{T}$ deformation can be written as a special higher derivative interaction around the free fermion, and this sign constraint can be understood using AdS_2 dispersion relations [48]. For the tree level correlator, this fermionic derivative interaction leads to a u-channel Regge behavior ($\eta \to i\infty$) of $\eta^{-2\Delta_\psi}\mathcal{G}(\eta) \sim a\eta^1$ [42]. This is precisely the maximal Regge behavior allowed in a planar CFT, corresponding to a Regge spin of 2 [42, 49] (note that higher dimensional u-channel Regge limit bounds can consistently be studied in 1d by setting $z = \bar{z}$). When this Regge behavior is saturated, bounds from causality/chaos also constrain the sign of a [50, 51], reproducing the constraint we derived from the bootstrap. The same argument also applies for the bosonic $(\partial\phi)^4$ coupling discussed in [4].

4.3.2 Deformations of tricritical Ising Model with $(2,1)_4$ boundary condition

In this section we study the vicinity of the tricritical Ising model with $(2,1)_4$ boundary condition using the mixed-correlator bootstrap setup of section 4.2.2.

(I) The relevant deformations

There are two $\mathbb{Z}_2$-even even relevant bulk deformations of tricritical Ising model: $\phi_{(1,3)}$ and $\phi_{(3,3)}$. For the former let us first consider the bootstrap analysis of section 4.2.2, but this time varying Δ_ψ and Δ_{D} along the one-loop prediction (see Table 7)

$$\Delta_\psi = \frac{3}{2} + \tilde{g}_{(1,3)}, \quad \Delta_{\mathrm{D}} = 2 + \frac{4}{5}\tilde{g}_{(1,3)} \ , \tag{4.14}$$

and comparing with

$$\Delta_{\mathrm{D}^2} = 4 + \frac{72}{85}\tilde{g}_{(1,3)} \ . \tag{4.15}$$

As shown in figure 10, which was obtained with the gaps of Table 10, the (extrapolated) upper bound is saturated by the RG prediction of eq. (4.15) for both signs of the coupling. This is not a surprise: one sign (the one for which $\Delta_\psi < 1.5$) should lead to the Ising model in the bulk, while the other is expected to gap out the bulk which corresponds to all the boundary scaling dimensions becoming large. In flat space these massive $\phi_{(1,3)}$ deformations of minimal models correspond to a family of integrable massive theories known as RSOS models, which are related to certain restricted versions of the sine-Gordon theory, as discussed in [52, 53].

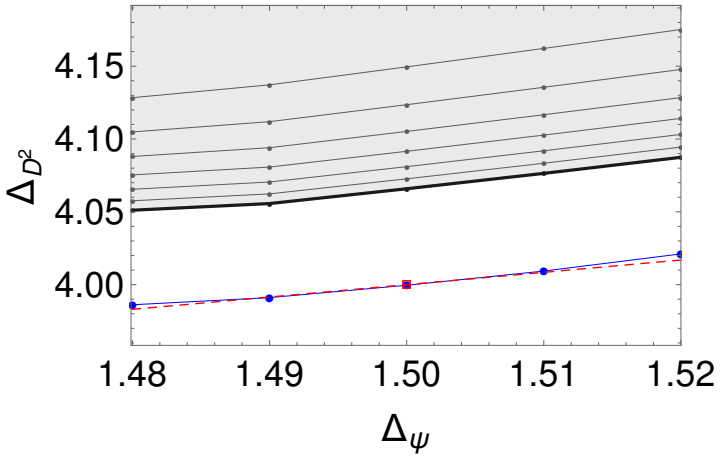

Figure 10: Bounds on Δ_{D^2} as a function of Δ_ψ, where Δ_ψ and Δ_{D} follows the perturbative prediction of eq. (4.14). The grey dots denote bounds at increasing derivative order, which are then extrapolated to the blue dots. The red line corresponds to the analytic results of eq. (4.14). The bound is saturated for both signs of the coupling.

Having two relevant singlet couplings, we can generalize the previous analysis by discussing a 'combined' RG flow in AdS, where dimensionful couplings can be made dimensionless through the AdS radius R. By tuning R we can combine the $\phi_{(1,3)}$ and $\phi_{(3,3)}$ deformations to define a space of 1d CFTs parametrized by the two couplings.[9] For the $(2,1)_4$ boundary condition, using the result of Table 7, we can trade $(g_{(3,3)}, g_{(1,3)})$ for $(\Delta_\psi, \Delta_{\mathrm{D}})$ and write

$$\Delta_{\mathrm{D}^2} = \frac{1}{17}(20 + 33\Delta_{\mathrm{D}} - 12\Delta_\psi) \ . \tag{4.16}$$

In the vicinity of the $(2,1)_4$ boundary condition, we can tune the two couplings to keep Δ_ψ fixed at 1.5 and then compare this one-loop prediction with the bootstrap bounds of section 4.2.2, in particular with those presented in fig. 7. As shown in fig. 11, this combined flow appears to saturate the boundary of the anteater, with a slightly better fit to the right of the $(2,1)_4$ boundary condition. Note that an analogous combined flow, with operators $\phi_{(1,3)}$ and $T\bar{T}$ can similarly be used to understand the structure of the allowed region around the $(1,2)_3$ boundary condition with $\Delta_\psi = 1/2$ (see fig. 8 (d)).

It is also interesting to investigate how the bounds change as we vary $\mathtt{gap}_{(+,+)}$. Figure 11 was obtained by choosing $\mathtt{gap}_{(+,+)} = 5.5$, and allows for deformations with both signs of the (combined) coupling. As shown in figure 12, upon increasing the gap to 5.8 the allowed region shrinks while still allowing for both signs of the coupling. Taking the gap all the way to 6 leads to near saturation of the tip by the $(2,1)_4$ boundary condition, and a positive sign of the combined

[9]The individual $\phi_{(3,3)}$ deformation in the complex plane is known to lead to an integrable massive system: Zamolodchikov's E_7 theory [54].

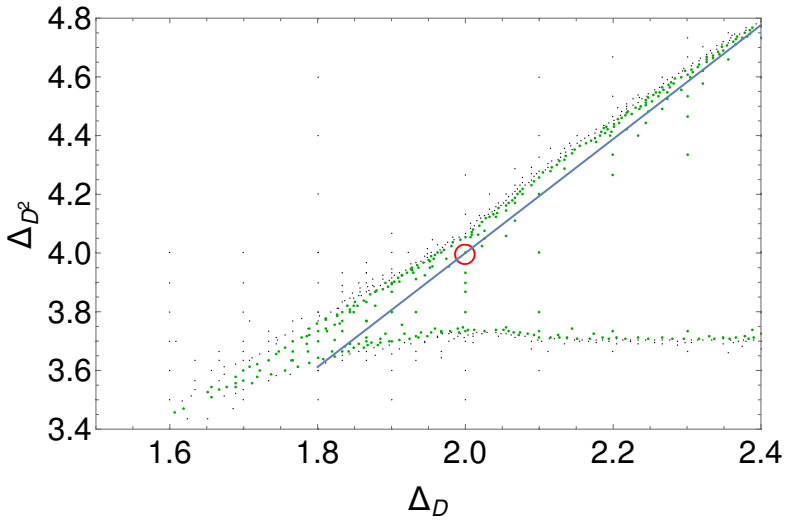

Figure 11: The combined $\phi_{(3,3)} + \phi_{(1,3)}$ deformation of the $(2,1)_4$ b.c. for $\Delta_\psi = 1.5$. The solid line is the perturbative result of eq. (4.16), which appears to saturate the upper bound to the right of the $(2,1)_4$ point, represented by the red circle.

deformation is in near contradiction with the gap assumption. In other words, as we lower the gap from 6, the 'nose' of the anteater grows, and the location of the tip gives an heuristic definition for how big 'the combined coupling' can be. We also note that the top part of the bound is insensitive to the gap assumption. This makes robust the identification of the tricritical Ising as a theory saturating the bound as it sits close precisely to the top of the exclusion plot.

(II) The leading irrelevant deformation

Next, we consider the $\phi_{(3,1)}$ deformation of $(2,1)_4$, which is $\mathbb{Z}_2$-preserving. We run again the bootstrap analysis of section 4.2.2, varying Δ_ψ and $\Delta_{\rm D}$ along the one-loop prediction (see Table 7)

$$\Delta_\psi = \frac{3}{2} + \tilde{g}_{(3,1)}, \quad \Delta_{\rm D} = 2 - \frac{2}{3}\tilde{g}_{(3,1)} \ , \tag{4.17}$$

and comparing with

$$\Delta_{{\rm D}^2} = 4 - 2\tilde{g}_{(3,1)} \ . \tag{4.18}$$

The results are shown in fig. 13 (the chosen gaps are those of Table 10). While for $\tilde{g}_{(3,1)} < 0$ the bound appears to be saturated, the other sign points towards the interior of the allowed region. This is possible due to a quick change in the slope of the bound around the $(2,1)_4$ point. The m'th minimal model flows under the relevant $\phi_{(1,3)}$ deformation to the $m-1$'th minimal model in the IR. From the IR point of view, it is the *irrelevant* $\phi_{(3,1)}$ operator that begins the flow back up the UV. Nicely enough we see that it is exactly the flow up to the tetracritical Ising

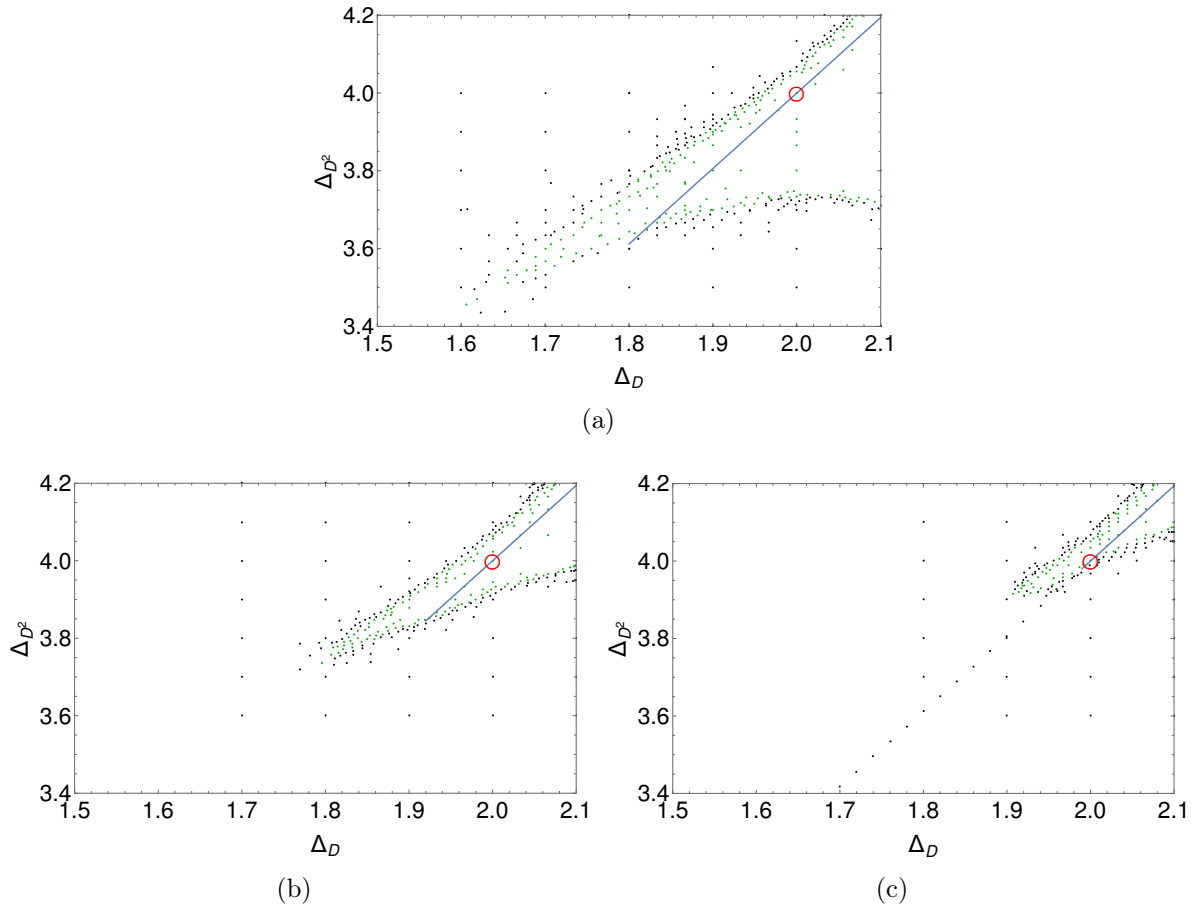

(a)

(b)

(c)

Figure 12: The combined $\phi_{(3,3)} + \phi_{(1,3)}$ deformation of the $(2,1)_4$ b.c. for $\Delta_\psi = 1.5$ at $\Lambda = 45$. In (a) $\texttt{gap}_{(+,+)} = 5.5$, in (b) $\texttt{gap}_{(+,+)} = 5.8$ and in (c) $\texttt{gap}_{(+,+)} = 6.0$. The solid line is the perturbative result of eq. (4.16).

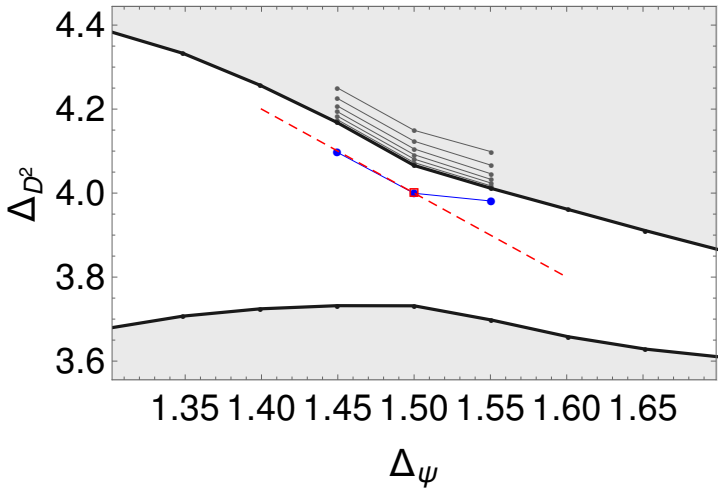

Figure 13: Bounds on Δ_{D^2} as a function of Δ_ψ, along eq. (4.17). The grey dots denote bounds at increasing derivative order, which are then extrapolated to the blue dots. The red line corresponds to the analytic results of eq. (4.18). The bound is saturated for $\tilde{g}_{(3,1)} < 0$.

model that saturates the bound, since the tricritical $\phi_{(1,3)}$ operator is becoming less irrelevant, as we go to the left of the plot where $\tilde{g}_{(3,1)} < 0$.

(III) The $T\bar{T}$ deformation

Finally we consider the $T\bar{T}$ deformation. This time we vary Δ_ψ and Δ_{D} along the one-loop prediction (see Table 7)

$$\Delta_\psi = \frac{3}{2} + \tilde{g}_{T\bar{T}}, \quad \Delta_{\mathrm{D}} = 2 + \frac{8}{3}\tilde{g}_{T\bar{T}} \ , \tag{4.19}$$

and comparing with

$$\Delta_{\mathrm{D}^2} = 4 + 16\tilde{g}_{T\bar{T}} \ . \tag{4.20}$$

As shown in fig. 14, there is a clear sign constraint, so and it must be that $g_{T\bar{T}} \leq 0$. This is the same sign determined in section 4.1, consistent with causality. It is once again reassuring to find out that different boundary correlators lead to the same inconsistency.

4.3.3 Explorations around tricritical Ising Model with $(2,2)_4$ boundary condition

We conclude this section with an exploration of the 'neighborhood' of tricritical Ising with $(2,2)_4$ boundary condition. To this end, we employ again the 'agnostic' approach of section 4.2, but this time we consider a $\mathbb{Z}_2$-invariant system of correlators with two (global) boundary primaries, one $\mathbb{Z}_2$-odd (ψ) and one $\mathbb{Z}_2$-even (χ). Hence we consider:

$$\langle\psi\psi\psi\psi\rangle\,, \quad \langle\chi\chi\chi\chi\rangle\,, \quad \langle\psi\psi\chi\chi\rangle\,, \quad \langle\psi\chi\psi\chi\rangle\,, \tag{4.21}$$

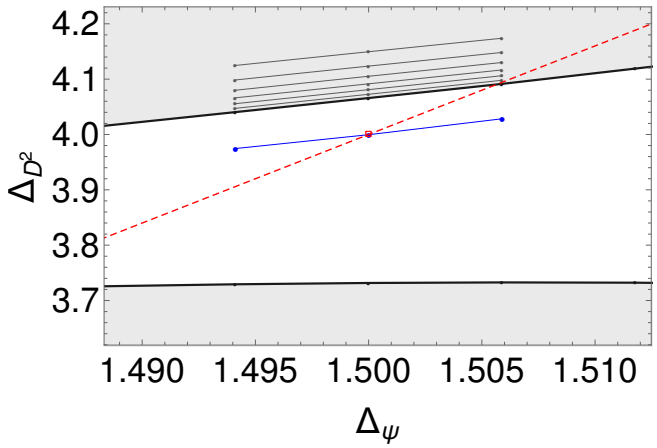

Figure 14: Bounds on Δ_{D^2} as a function of Δ_ψ, along eq. (4.19). The grey dots denote bounds at increasing derivative order, which are then extrapolated to the blue dots. The red line corresponds to the analytic results of eq. (4.20). The bound is violated for $\tilde{g}_{T\bar{T}} > 0$.

$\mathtt{gap}_{(\mathbb{Z}_2,P)}$	$P+$	$P-$
$\mathbb{Z}_2+$	2.4	-
$\mathbb{Z}_2-$	1.3	2.8

Table 11

In order to bootstrap this system of correlators it is useful to impose gaps. At the $(2,2)_4$ conformal boundary condition, we can identity ψ with $\psi_{(3,3)}$ and χ with $\psi_{(1,3)}$. With this in mind, and recalling the OPEs of eq. (3.32), we assume

$$\begin{aligned}
\psi \times \psi &\sim \hat{\mathbb{1}} + \chi + \mathrm{D} + \mathtt{gap}_{(+,+)} + \dots\,, \\
\chi \times \chi &\sim \hat{\mathbb{1}} + \chi + \mathrm{D} + \mathtt{gap}_{(+,+)} + \dots\,, \\
\psi \times \chi &\sim \psi + \mathtt{gap}_{(-,+)} + \mathtt{gap}_{(-,-)} + \dots\,.
\end{aligned} \tag{4.22}$$

A possible choice for the gaps (leaving some leeway to deformations) is displayed in Table 11. In order to explore the vicinity of $(2,2)_4$ we choose $\Delta_\psi = 1/10$ and explore the allowed values of Δ_χ and Δ_{D} around their $(2,2)_4$ values which are 0.6 and 2, respectively. A systematic binary search leads to the kinky region of fig. 15, which shows that the $(2,2)_4$ boundary condition is deep inside the allowed region. In order to gain some insights on the two kinks in this figure, we can modify slightly our gap assumptions. With all the gaps set at their exact values corresponding to the $(2,2)_4$ boundary condition, we find the upper bound in figure 16. This time the upper bound is almost linear, except for a small bump precisely around the $(2,2)_4$ boundary condition. As we increase the number of derivatives, the linear part of the bound appears to converge towards the

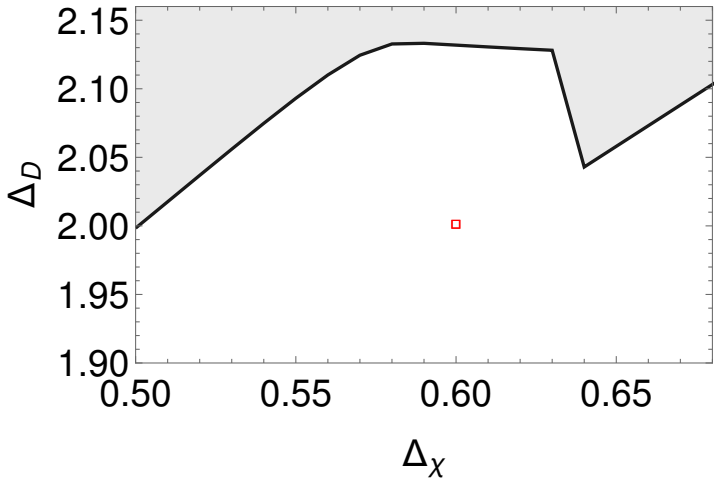

Figure 15: Allowed region in $(\Delta_\chi, \Delta_\mathrm{D})$ space for $\Delta_\psi = 1/10$ with mild gap assumptions. The red dots is the location of $(2,2)_4$. The plot was obtained at derivative order $\Lambda = 33$.

red dashed line in the figure. This line corresponds to a spurious solution to crossing with the following properties: no identity is exchanged, and leading (subleading) exchange has dimension Δ_χ ($\Delta_\mathrm{D} = 3\Delta_\chi/2 + 1$). In the conventions of appendix A.2, this spurious four-point correlation function reads:

$$\mathcal{G}(\eta) = \frac{\eta^{3\Delta_\chi/2}}{(1-\eta)^{\Delta_\chi}} + \frac{\eta^{\Delta_\chi}}{(1-\eta)^{\Delta_\chi/2}} - \frac{\eta^{3\Delta_\chi/2}}{(1-\eta)^{\Delta_\chi/2}} \ . \tag{4.23}$$

This correlator can be obtained by taking linear combinations of fully connected Wick contractions of $\langle\phi^4\phi^4\phi^4\phi^4\rangle$, where ϕ is a GFF with scaling dimension $\Delta_\phi = \Delta_\chi/4$. These spurious solutions to 1d crossing are common in the 1d bootstrap, see for example [4]. If we identify χ with $\psi_{(1,3)}$ of the $(2,2)_4$ boundary condition, the gap in (4.23) is at $3\Delta_{1,3}/2+1 = 1.9$, just below the displacement. This explains the unusual features of this bootstrap bound.

4.4 Correlator maximization and the conformal staircase

In this section we will find a different quantity to extremize such that the $(2,2)_4$ b.c saturates the bound. It turns out that a natural object is the four-point correlator of the $\mathbb{Z}_2$ odd operator ψ $\mathcal{G}(\eta) = x_{12}^{2\Delta_\psi} x_{34}^{2\Delta_\psi} \langle\psi\psi\psi\psi\rangle$ and its second derivative evaluated at the crossing symmetric point:

$$\{\mathcal{G}(z=1/2), \mathcal{G}''(z=1/2)\}. \tag{4.24}$$

Our motivation for studying the allowed region in this plane comes from the observation that the RG flows between minimal models can be embedded in the so-called staircase RG-Flows, which are connected to the sinh-Gordon/staircase model and its flat space S-matrix [3]. These

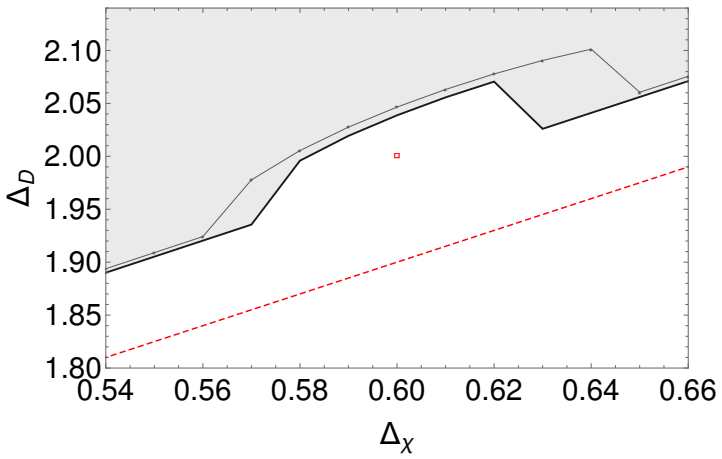

Figure 16: Allowed region in $(\Delta_\chi, \Delta_\mathrm{D})$ space for $\Delta_\psi = 1/10$, for gap assumptions that saturate the spectrum of $(2,2)_4$ (red dot), at $\Lambda = 33, 41$. The red dashed line is the family of solution described by (4.23).

S-matrices of a single massive particle without bound-states saturate bounds in the space [55]:

$$\{S(2m^2), S''(2m^2)\}.$$

Using the connection between S-matrices and correlators in the flat-space limit [56] we arrive at equation (4.24) as the natural uplift of these bounds to the QFT in AdS setup. A review of the staircase model and a more detailed explanation of its connection to the bounds below is given in appendix H.

To bound $\mathcal{G}(1/2) \equiv g$ and $\mathcal{G}''(1/2) \equiv g''$ we need to fix them to a specific value and then determine whether this value is allowed. For g we can just use the recipe described in [4], where one works with shifted conformal blocks:

$$(1-\eta)^{2\Delta_\psi} G_\Delta(\eta) \to (1-\eta)^{2\Delta_\psi} G_\Delta(\eta) - \delta_{\Delta,0} 2^{-2\Delta_\psi} g \equiv F^*_\Delta(\eta)\,, \tag{4.25}$$

and then adds the zero derivative functional to the search space. Studying the Taylor series of the crossing equation leads to the following generalization that allows us to fix both g and g'':

$$(1-\eta)^{2\Delta_\psi} G_\Delta(\eta) \to F^*_\Delta(\eta) - \delta_{\Delta,0}\left(\eta - \frac{1}{2}\right)^2 2^{-1-2\Delta_\psi}\left(g'' - 8\Delta_\psi(2\Delta_\psi+1)g\right) \equiv F''_\Delta(\eta)\,, \tag{4.26}$$

Then, alongside with the usual odd derivative functionals, we must include the zero- and two-derivative terms to the basis. We can subsequently perform a two-dimensional feasibility search in this space, for several external dimensions Δ_ψ. We will always assuming a gap of $2\Delta_\psi$ in the spectrum since that is appropriate for a theory with no bound states. With these assumptions the generalized free boson (GFB) and generalized free fermion (GFF) theories are always in the

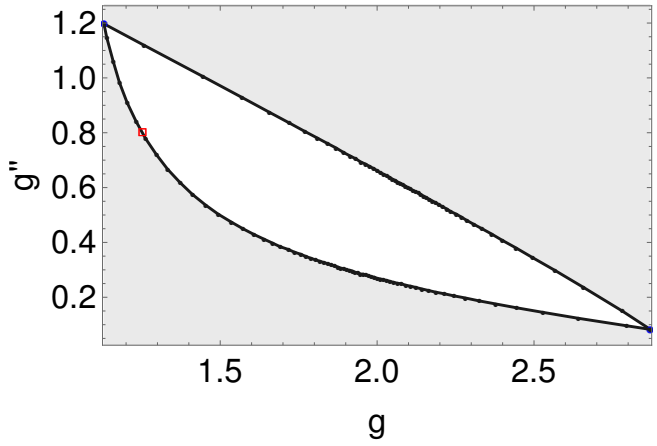

Figure 17: Bounds on the space of values of the correlator and its second derivative at the crossing symmetric point for $\Delta_\psi = 0.1$. GFF/GFB sit on the kinks and the $(2,2)_4$ tricritical Ising point, in red, also saturates the bound. The points shown were obtained upon extrapolation to infinite Λ.

allowed space. By convexity that means that the line connecting these theories is also allowed, which allows one to find a line strictly in the interior of the allowed region. An efficient numerical exploration can then be performed by doing a radial/angular search around this interior point.

For $\Delta_\psi = 1/10$, which corresponds to the $\psi_{(1,2)}$ operator in the tricritical Ising model, we find the bound in figure 17 after extrapolation in the derivative order Λ.[10] We find an island with two sharp corners corresponding to the GFB and GFF solutions, as expected. Furthermore, we can compute the four point function of the $\psi_{(1,2)}$ operator using the techniques of appendix D, and plot the result. This is the red square which neatly saturates the bound.

Computing deformations of these bounds perturbatively is challenging because it involves integrating five-point functions in AdS. In theory it should however be possible to follow the RG flow between the $(2,2)_4$ boundary condition and the $(1,2)_3$ boundary condition by studying the same bounds for different values of Δ_ψ.[11] This leads to a family of islands similar to the one above which we present in figure 18. These islands always have two sharp kinks corresponding to the GFB and GFF solutions and drift in the direction of increasing g''.

[10] We obtained bounds at finite derivative order $\Lambda = 9, 13, \ldots, 33$, which converged rather quickly, except very close to the corners. On the other hand, the $(2,2)_4$ boundary condition is already very close to saturation even at finite Λ.

[11] It would also be interesting to understand how these bounds change for higher m minimal models. This presumably sheds some light on the UV of the staircase model.

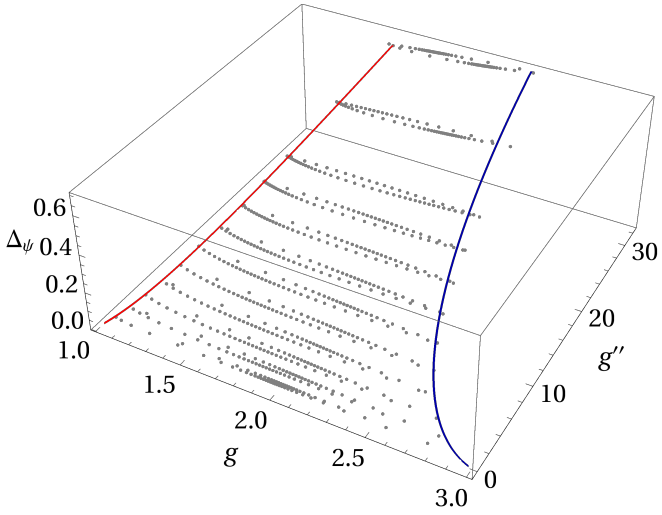

Figure 18: Allowed space of $\mathbb{Z}_2$ symmetric correlators parametrized by g and g'' for varying Δ_ψ. We see a tower of island shaped regions drifting in the g'' direction. The red and blue lines respectively correspond to the GFF and GFB families of correlators which not only saturate the bounds, but actually sit in kinks at the endpoints of these islands.

This drift is related to the "center of mass" of the GFF and GFB solutions. For explicitness we write the values of $\{g, g''\}$ for these solutions:

$$\begin{aligned} GFF(\Delta_\phi) &= \left\{2 - 4^{-\Delta_\phi}, 2^{3-2\Delta_\phi}\Delta_\phi\left(2\left(4^{\Delta_\phi+1}-1\right)\Delta_\phi+1\right)\right\} \\ GFB(\Delta_\phi) &= \left\{2 + 4^{-\Delta_\phi}, 8\Delta_\phi\left(8\Delta_\phi + 4^{-\Delta_\phi}\left(2\Delta_\phi - 1\right)\right)\right\}, \end{aligned} \tag{4.27}$$

whose center of mass is $\{2, 64\Delta_\phi^2\}$. After subtracting the quadratically growing second component we find figure 19.

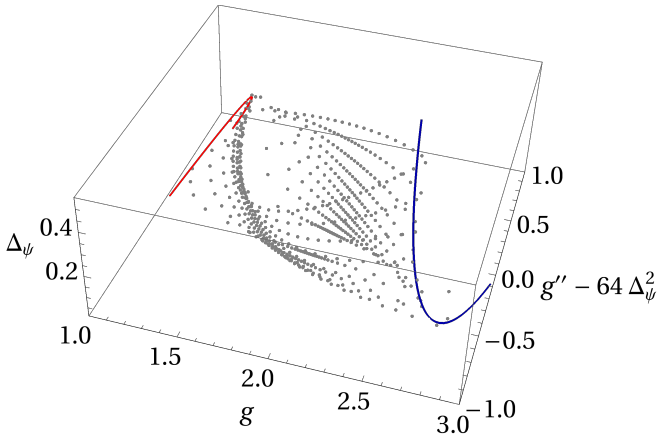

Figure 19: Subtracting the center of mass drift of the previous figure. We now see interesting rotation and stretching patterns of the islands.

Finally, we focus on $\Delta_\psi = 0.5$ which contains the $(1,2)_3$ boundary condition. We show the bounds in figure 20, where we see that the Ising theory sits in the kink (red square), since it coincides with GFF. We also plot the $T\bar{T}$ deformation which is tangent to bound, with only one sign being allowed, as we have seen many times by now. In this case, the perturbative calculation is feasible since we can use a fermionic contact Witten diagrams to compute the correction to the correlator, as discussed in more detail in appendix H.

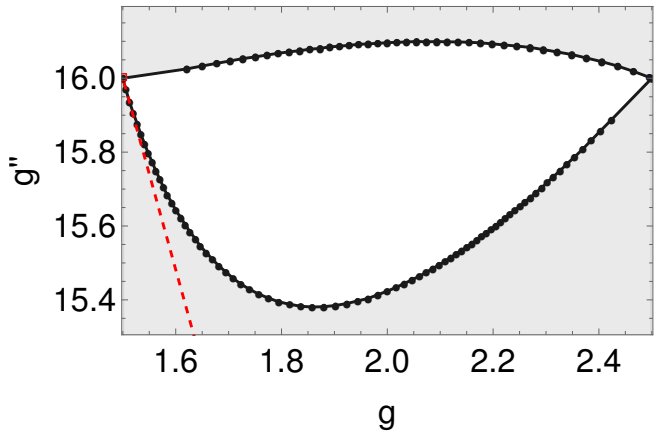

Figure 20: Bounds for $\Delta_\psi = 0.5$. GFF/Ising sits on the kink and the $T\bar{T}$ deformation is tangent. As always, only one sign of the $T\bar{T}$ coupling is consistent with the bounds. The points shown are obtained after extrapolation in Λ.

These results suggest that we can track two RG flows that end on the same $(1,2)_3$ boundary condition of Ising by studying different bootstrap problems. Starting with $(2,1)_4$ in tricritical, we follow gap maximization. Instead, starting with $(2,2)_4$, we can study correlator maximization.

5 Outlook

We conclude with a discussion on future directions.

A natural extension of our work is to consider $\mathbb{Z}_2$-breaking deformations of minimal models boundary conditions in AdS. The simplest example would be the magnetic deformation of the Ising model, which was studied in AdS with Hamiltonian truncation in [35]. More generally, we could combine the thermal and magnetic deformations hence studying Ising field theory [57]. The regime of weak magnetic field with only one stable particle in the infrared is particularly amenable to the bootstrap, since we can parametrize the $\mathbb{Z}_2$ breaking through a self OPE coefficient $\lambda_{\psi\psi\psi}$ of the $\mathbb{Z}_2$-odd field.

One limitation of our setup is that we cannot impose locality of the bulk theory along the RG flow. Our strategy in this work is to look for bootstrap bounds which are saturated at the

fixed points of the RG flow when the bulk theory is Weyl-equivalent to a local BCFT, but we are not guaranteed saturation throughout the flow. In order to make progress on this, a promising strategy recently discussed in [58, 59] is to include bulk observables into the bootstrap. These authors considered sum rules on the three-point functions between one bulk operator and two boundary operators (called AdS 2-particle form factors) which capture bulk locality. In [59] sum rules stemming from the two-point function of the bulk stress-energy tensor were also found, allowing the formulation of a positive semi-definite system of correlators involving bulk and boundary data. This extended the formalism of [60, 61] to AdS, where bounds as a function of the central charge were obtained. It would be very interesting to see to what extent these additional constraints would improve the bounds obtained in this paper.

Our strategy works well for computing certain non-perturbative numerical bounds on irrelevant couplings of generic CFTs. There has been a lot of progress in the context of EFT corrections for free bosons and fermions in AdS [15, 48], and our approach could be used in order to search for such constraints in interacting CFTs. As an application, we have found a constraint on the sign of the $T\bar{T}$ deformation. For other types of deformations, for instance those of section 3.2, we found no sign constraints along our one-loop perturbation theory, and higher-order corrections might be useful to detect further bulk inconsistencies.

Finally, it would be interesting to understand if integrability, which plays a key role in the solution of minimal model RG flows both in flat space and on the upper half-plane, survives in AdS. To understand this it would be necessary to follow the behavior of bulk higher-spin currents which exist at the fixed point, due to Virasoro symmetry. Another notion of solvability for conformal correlators is extremality, i.e. saturation of the bootstrap bounds, which is known to lead to sparse spectra. While the relation between these concepts is well understood in the flat-space limit, it is still an open problem to understand this connection at finite AdS radius.

Acknowledgements

We would like to thank C. Behan, C. Bercini, M. Billò, A. Cavaglià, M. Costa, L. Di Pietro, A. Gimenez-Grau, M. Hogervorst, A. Kaviraj, P. Liendo, A. Manenti, M. Milam, M. Paulos, V. Schomerus, A. Tilloy, E. Trevisani, and P. van Vliet for discussions. We also thank V. Fofana and Y. Fitamant for assistance in the use of the Cholesky cluster at the Ecole Polytechnique. AA thanks the University of Turin, where part of this work was presented, for hospitality. AA received funding from the German Research Foundation DFG under Germany's Excellence Strategy – EXC 2121 Quantum Universe – 390833306. Centro de Física do Porto is partially funded by Fundação para a Ciência e Tecnologia (FCT) under the grant UID04650-FCUP. BvR is supported by the Simons Foundation grant #488659 (Simons Collaboration on the non-perturbative

bootstrap). EL is funded by the European Union (ERC, QFT.zip project, Grant Agreement no. 101040260, held by A. Tilloy). Views and opinions expressed are however those of the author(s) only and do not necessarily reflect those of the European Union or the European Research Council Executive Agency. Neither the European Union nor the granting authority can be held responsible for them.

A Conventions

m	$(a_1, a_2)_m$	$\mathbb{Z}_2$ - preserving	Boundary spectrum
3	$(1,2)_3$	✓	$\hat{\mathbb{1}}, \psi_{(1,3)}$
4	$(1,2)_4$		$\hat{\mathbb{1}}, \psi_{(1,3)}$
	$(1,3)_4$		$\hat{\mathbb{1}}, \psi_{(1,3)}$
	$(2,1)_4$	✓	$\hat{\mathbb{1}}, \psi_{(3,1)}$
	$(2,2)_4$	✓	$\hat{\mathbb{1}}, \psi_{(1,3)}, \psi_{(3,1)}, \psi_{(3,3)}$
5	$(1,2)_5$		$\hat{\mathbb{1}}, \psi_{(1,3)}$
	$(1,3)_5$	✓	$\hat{\mathbb{1}}, \psi_{(1,3)}, \psi_{(1,5)}$
	$(1,4)_5$		$\hat{\mathbb{1}}, \psi_{(1,3)}$
	$(2,1)_5$		$\hat{\mathbb{1}}, \psi_{(3,1)}$
	$(2,2)_5$		$\hat{\mathbb{1}}, \psi_{(1,3)}, \psi_{(3,1)}, \psi_{(3,3)}$
	$(2,3)_5$	✓	$\hat{\mathbb{1}}, \psi_{(1,3)}, \psi_{(1,5)}, \psi_{(3,1)}, \psi_{(3,3)}, \psi_{(3,5)}$
	$(2,4)_5$		$\hat{\mathbb{1}}, \psi_{(1,3)}, \psi_{(3,1)}, \psi_{(3,3)}$
	$(2,5)_5$		$\hat{\mathbb{1}}, \psi_{(3,1)}$

Table 12: Elementary conformal boundary conditions for diagonal and unitary minimal models with $m \leq 5$. We dropped the conformal b.c. labeled by the identity (and its $\mathbb{Z}_2$-conjugate $(1,m)_m$): they are always possible, and allow only for $\hat{\mathbb{1}}$ at the boundary.

A.1 OPEs and basic correlation functions

Consider a generic BCFT on the upper half-plane. Here $\phi_i(z,\bar{z})$ denotes a scalar bulk global primary with dimension Δ_i, and $\psi_i(x)$ denotes a scalar global boundary primary with dimension $\hat{\Delta}_i$. Unless otherwise specified, primary bulk and boundary operators are taken to be unit-normalized. The bulk and boundary identity operators satisfy: $\langle \mathbb{1} \rangle = \langle \hat{\mathbb{1}} \rangle = 1$.

The bulk-bulk, bulk-boundary, and boundary-boundary OPEs are

$$\begin{aligned}
\phi_i(z_1,\bar{z}_1)\phi_j(z_2,\bar{z}_2) &= \sum_k C_{ij}{}^k \phi_k(z_2,\bar{z}_2)|z_1-z_2|^{\Delta_k-\Delta_i-\Delta_j}+\cdots\,,\\
\phi_i(x+iy,x-iy) &= \sum_k B_i{}^k \psi_k(x)(2y)^{\hat{\Delta}_k-\Delta_i}+\cdots\,,\\
\psi_i(x_1)\psi_j(x_2) &= \sum_k \hat{C}_{ij}{}^k \psi_k(x_2)(x_1-x_2)^{\hat{\Delta}_k-\hat{\Delta}_i-\hat{\Delta}_j}+\cdots \qquad (x_1>x_2)\,.
\end{aligned} \tag{A.1}$$

The ellipsis in the first (second and third) line above denotes $SL(2,\mathbb{C})$ ($SL(2,\mathbb{R})$) descendants. Indices are raised and lowered using the Zamolodchikov metric.

The simplest correlation functions on the upper half-plane are:

$$\begin{aligned}
\langle\psi(x_1)\psi(x_2)\rangle_{\mathbb{H}^+} &= \frac{1}{(x_{12}^2)^{\hat{\Delta}}}\,, && (x_1>x_2)\\
\langle\phi(x+iy,x-iy)\rangle_{\mathbb{H}^+} &= \frac{B_\phi}{(2y)^{\Delta}}\,, && (y>0)\\
\langle\phi(x_1+iy_1,x_1-iy_1)\psi(x_2)\rangle_{\mathbb{H}^+} &= \frac{B_{\phi\psi}}{(2y_1)^{\Delta-\hat{\Delta}}(x_{12}^2+y_1^2)^{\hat{\Delta}}}\,, && (y_1>0)\\
\langle\psi_i(x_1)\psi_j(x_2)\psi_k(x_3)\rangle_{\mathbb{H}^+} &= \frac{\hat{C}_{ijk}}{(x_{12})^{\hat{\Delta}_{ijk}}(x_{23})^{\hat{\Delta}_{jki}}(x_{13})^{\hat{\Delta}_{ikj}}}\,, && (x_i>x_{i+1})\,.
\end{aligned} \tag{A.2}$$

with $x_{ij}\equiv x_i-x_j$ and $\hat{\Delta}_{ijk}\equiv\hat{\Delta}_i+\hat{\Delta}_j-\hat{\Delta}_k$. In a generic BCFT, the coefficients B, $\hat{C}$ and C are determined via the 'sewing' constraints of Lewellen [34]. For unitary and diagonal minimal models with elementary conformal boundary conditions, the solution to these constraints appeared in [41] (see [62] for the extension to the D-series of minimal models), where $\hat{C}$ and B are written in terms of F-matrices (the one-point function of $\phi_{(r,s)}$ is determined by the Cardy state, as written in (2.17)). The C coefficients are the same of the homogeneous minimal model, and they can be computed via the 'Coulomb gas formalism' of refs. [63–65] (see also the Mathematica notebook attached to the submission of [66], where many Coulomb gas formulae are implemented.)

A.2 Global conformal blocks on the upper half-plane

Next, we discuss the four-point correlation function between four boundary conformal primaries ψ_i (not necessarily Virasoro primaries) with scaling dimensions $\hat{\Delta}_i$ in a generic 2d BCFT. By $SL(2,\mathbb{R})$ symmetry we have

$$\langle\psi_1(x_1)\psi_2(x_2)\psi_3(x_3)\psi_4(x_4)\rangle_{\mathbb{H}^+} = \left(\frac{x_{14}}{x_{24}}\right)^{\hat{\Delta}_{21}}\left(\frac{x_{14}}{x_{13}}\right)^{\hat{\Delta}_{34}}\frac{\mathcal{G}^{1234}(\eta)}{(x_{12})^{\hat{\Delta}_1+\hat{\Delta}_2}(x_{34})^{\hat{\Delta}_3+\hat{\Delta}_4}}\,,\quad x_i>x_{i+1}\,, \tag{A.3}$$

with $\hat{\Delta}_{ij} \equiv \hat{\Delta}_i - \hat{\Delta}_j$ and the cross-ratio η is defined as in eq. (2.5) and repeated here for convenience

$$\eta = \frac{x_{12}x_{34}}{x_{13}x_{24}} , \quad 0 < \eta < 1 . \tag{A.4}$$

We have the following s-channel expansion

$$\mathcal{G}^{1234}(\eta) = \sum_k \hat{C}_{12}{}^k \hat{C}_{34k} G(\hat{\Delta}_{21}, \hat{\Delta}_{34}, \hat{\Delta}_k, \eta) , \tag{A.5}$$

with global blocks given by [67]

$$G(a, b, \Delta, \eta) = \eta^{\Delta}\, {}_2F_1(a + \Delta, b + \Delta; 2\Delta; \eta) . \tag{A.6}$$

We will sometimes use the following notation

$$G_\Delta(\eta) \equiv G(0, 0, \Delta, \eta) . \tag{A.7}$$

B Correlation functions for generalized free theories

B.1 Generalized free fermion

Consider a 1d generalized free fermion ψ of scaling dimension Δ. We take ψ to be unit normalized. By Wick's theorem the four-point correlation function is

$$\mathcal{G}^{\psi\psi\psi\psi}(\eta) = 1 - \eta^{2\Delta} + \left(\frac{\eta}{1-\eta}\right)^{2\Delta} . \tag{B.1}$$

The cross-ration η is defined as in eq. (2.5). The global conformal blocks expansion reads [68]

$$\mathcal{G}^{\psi\psi\psi\psi}(\eta) = 1 + \sum_{n=0}^{\infty} \frac{2(2\Delta)^2_{2n+1}}{(2n+1)!(4\Delta+2n)_{2n+1}} G_{2\Delta+2n+1}(\eta) , \tag{B.2}$$

with global blocks given in (A.6). We want to compute mixed four-point correlation functions between ψ and the leading primary in the $\psi \times \psi$ OPE, i.e.

$$\psi(x)\psi(0) = \frac{\hat{\mathbb{1}}}{x^{2\Delta}} + x\,(\psi\partial\psi)(0) + \dots . \tag{B.3}$$

From the four-point function above we can easily obtain

$$\langle \psi\partial\psi(x)\psi\partial\psi(0)\rangle = \frac{2\Delta}{x^{4\Delta+2}} . \tag{B.4}$$

Using Wick's theorem, from the eight-point correlation function of ψ we can obtain the four-point correlation function of $\psi\partial\psi$

$$\langle\psi\partial\psi(x_1)\psi\partial\psi(x_2)\psi\partial\psi(x_3)\psi\partial\psi(x_4)\rangle \ . \tag{B.5}$$

When $\Delta = 1/2$ we get

$$\mathcal{G}^{[\psi\partial\psi][\psi\partial\psi][\psi\partial\psi][\psi\partial\psi]}(\eta) = 1 + \frac{\eta^2\left(\eta^6 - 4\eta^5 + 22\eta^4 - 52\eta^3 + 66\eta^2 - 48\eta + 16\right)}{(\eta-1)^4} \ . \tag{B.6}$$

The r.h.s. above can be expanded into s-channel conformal blocks of eq. (A.6) as follows

$$\mathcal{G}^{[\psi\partial\psi][\psi\partial\psi][\psi\partial\psi][\psi\partial\psi]}(\eta) = 1 + 16G_2(\eta) + \frac{98}{5}G_4(\eta) + \frac{512}{63}G_6(\eta) + \frac{1270}{429}G_8(\eta) + \dots \ . \tag{B.7}$$

Hence the first parity-even primary operator after the identity is the displacement operator D, and after it there is D^2.

Consider now the following mixed four-point function

$$\langle\psi(x_1)\psi(x_2)\psi\partial\psi(x_3)\psi\partial\psi(x_4)\rangle \ . \tag{B.8}$$

When $\Delta = 1/2$ we find

$$\mathcal{G}^{\psi\psi[\psi\partial\psi][\psi\partial\psi]}(\eta) = 1 + \frac{(\eta-2)^2\eta^2}{(\eta-1)^2} \ . \tag{B.9}$$

In the s-channel we find the following decomposition

$$\mathcal{G}^{\psi\psi[\psi\partial\psi][\psi\partial\psi]}(\eta) = 1 + 4G_2(\eta) + \frac{7}{5}G_4(\eta) + \frac{16}{63}G_6(\eta) + \frac{29}{858}G_8(\eta) + \frac{46G_{10}(\eta)}{12155} + \dots \ . \tag{B.10}$$

The first parity-even primary operator after the identity is D, and after it there is D^2. For generic Δ we find

$$\mathcal{G}^{\psi\psi[\psi\partial\psi][\psi\partial\psi]}(\eta) = 2\Delta\left(1 + (2\Delta(\eta-1)-1)\eta^{2\Delta} + (1-\eta)^{-1}(2\Delta-\eta+1)\left(\frac{\eta}{1-\eta}\right)^{2\Delta}\right) \ , \tag{B.11}$$

with the following s-channel decomposition

$$\begin{aligned}
\mathcal{G}^{\psi\psi[\psi\partial\psi][\psi\partial\psi]}(\eta) &= 2\Delta + 4(2\Delta+3)\Delta^2 G_{2\Delta+1}(\eta) \\
&+ \frac{4(\Delta+1)(\Delta+3)(2\Delta+1)^2\Delta^2}{12\Delta+9}G_{2\Delta+3}(\eta) + \\
&+ \frac{(\Delta+1)(\Delta+2)(2\Delta+1)^2(2\Delta+3)(\Delta(2\Delta+11)+10)\Delta^2}{15(4\Delta+5)(4\Delta+7)}G_{2\Delta+5}(\eta) \\
&+ \frac{(\Delta+1)^2(\Delta+2)(\Delta+3)(2\Delta+1)^2(2\Delta+3)(2\Delta+5)(\Delta(2\Delta+15)+21)\Delta^2}{315(4\Delta+7)(4\Delta+9)(4\Delta+11)}G_{2\Delta+7}(\eta) \\
&+ \dots \ .
\end{aligned} \tag{B.12}$$

In order to investigate on parity-odd operators we consider the s-channel decomposition of

$$\langle \psi(x_1)\psi\partial\psi(x_2)\psi(x_3)\psi\partial\psi(x_4)\rangle \ . \tag{B.13}$$

When $\Delta = 1/2$ we find

$$\mathcal{G}^{\psi[\psi\partial\psi]\psi[\psi\partial\psi]}(\eta) = \frac{\sqrt{\eta}\,(\eta^4 - 2\eta^3 + 5\eta^2 - 4\eta + 1)}{(\eta-1)^2} \ , \tag{B.14}$$

whose s-channel decomposition gives

$$\begin{aligned}\mathcal{G}^{\psi[\psi\partial\psi]\psi[\psi\partial\psi]}(\eta) = {} & G\left(\frac{3}{2}, -\frac{3}{2}, \frac{1}{2}, \eta\right) + G\left(\frac{3}{2}, -\frac{3}{2}, \frac{9}{2}, \eta\right) \\ & + \frac{1}{5}G\left(\frac{3}{2}, -\frac{3}{2}, \frac{13}{2}, \eta\right) - \frac{4}{429}G\left(\frac{3}{2}, -\frac{3}{2}, \frac{15}{2}, \eta\right) \\ & + \dots \ .\end{aligned} \tag{B.15}$$

Squared OPE coefficients associated with parity-odd, global primary boundary exchanges appear with a minus sign, see e.g. appendix K of [69]. Hence, after ψ itself we have a parity-even operator of dimension $3\Delta + 3$ and a parity-odd operator of dimension $3\Delta + 6$. For generic Δ we find

$$\mathcal{G}^{\psi[\psi\partial\psi]\psi[\psi\partial\psi]}(\eta) = -2\Delta\left((2\Delta(\eta-1)+\eta)\eta^{\Delta} - \eta^{3\Delta+1} - \left(\frac{1}{\eta-1}\right)^{2\Delta+1}(2\Delta\eta + \eta - 1)\right) \ , \tag{B.16}$$

with the following s-channel decomposition ($e^{2i\pi\Delta} = -1$)

$$\begin{aligned}\mathcal{G}^{\psi[\psi\partial\psi]\psi[\psi\partial\psi]}(\eta) = {} & 4\Delta^2 G\left(\Delta_{21}, \Delta_{34}, \Delta, \eta\right) + 2(2\Delta+1)\Delta^2 G\left(\Delta_{21}, \Delta_{34}, 3\Delta+3, \eta\right) \\ & + \frac{\Delta^2(\Delta+1)(2\Delta+1)^2(2\Delta+3)}{3(6\Delta+7)} G\left(\Delta_{21}, \Delta_{34}, 3\Delta+5, \eta\right) \\ & - \frac{2\Delta^3(\Delta+1)(\Delta+2)(2\Delta+1)^2(2\Delta+3)}{45(3\Delta+4)(3\Delta+5)} G\left(\Delta_{21}, \Delta_{34}, 3\Delta+6, \eta\right) \\ & + \dots \ .\end{aligned} \tag{B.17}$$

B.2 Generalized free boson

Consider a 1d generalized free boson ϕ of scaling dimension Δ. We take ϕ to be unit normalized. By Wick's theorem the four-point correlation function is

$$\mathcal{G}^{\phi\phi\phi\phi}(\eta) = 1 + \eta^{2\Delta} + \left(\frac{\eta}{1-\eta}\right)^{2\Delta} \ . \tag{B.18}$$

The cross-ration η is defined as in eq. (2.5). The global conformal blocks expansion reads [68]

$$\mathcal{G}^{\phi\phi\phi\phi}(\eta) = 1 + \sum_{n=0}^{\infty} \frac{2(2\Delta)_{2n}^2}{(2n)!(4\Delta+2n-1)_{2n}} G_{2\Delta+2n}(\eta) \ . \tag{B.19}$$

Next, we compute

$$\langle \phi^2(x_1)\phi^2(x_2)\phi^2(x_3)\phi^2(x_4)\rangle \ , \tag{B.20}$$

to find

$$\mathcal{G}^{\phi^2\phi^2\phi^2\phi^2}(\eta) = 4\left(1+4\eta^{2\Delta}+\left(4(1-\eta)^{-2\Delta}+1\right)\eta^{4\Delta}+4\left(\frac{\eta}{1-\eta}\right)^{2\Delta}+\left(\frac{\eta}{1-\eta}\right)^{4\Delta}\right) \ . \tag{B.21}$$

The r.h.s. above has the following s-channel decomposition

$$\begin{aligned}\mathcal{G}^{\phi^2\phi^2\phi^2\phi^2}(\eta) = {} & 4+32G_{2\Delta}(\eta)+24G_{4\Delta}(\eta)+\frac{32(2\Delta+1)\Delta^2}{4\Delta+1}G_{2\Delta+2}(\eta) \\ & +\frac{64\Delta^2(2\Delta+1)}{8\Delta+1}G_{4\Delta+2}(\eta)+\frac{8\Delta^2(\Delta+1)(2\Delta+1)^2(2\Delta+3)}{3(4\Delta+3)(4\Delta+5)}G_{2\Delta+4}(\eta) \\ & +\frac{16\Delta^2(2\Delta+1)(\Delta(8\Delta(4\Delta+5)+17)+3)}{3(8\Delta+3)(8\Delta+5)}G_{4\Delta+4}(\eta) \\ & +\dots \ .\end{aligned} \tag{B.22}$$

When $\Delta = 1$ the first parity-even primary operator after the identity is the displacement operator. Note that there are two dimension-four operators: ϕ^4 and $\phi\partial^2\phi$. Consider now

$$\langle \phi(x_1)\phi(x_2)\phi^2(x_3)\phi^2(x_4)\rangle \ . \tag{B.23}$$

Using Wick's theorem we find

$$\mathcal{G}^{\phi\phi\phi^2\phi^2}(\eta) = 2+4\eta^{2\Delta}+4\left(\frac{\eta}{1-\eta}\right)^{2\Delta} \ . \tag{B.24}$$

The s-channel decomposition reads

$$\begin{aligned}\mathcal{G}^{\phi\phi\phi^2\phi^2}(\eta) = {} & 2+8G_{2\Delta}(\eta)+\frac{8(2\Delta+1)\Delta^2}{4\Delta+1}G_{2\Delta+2}(\eta) \\ & +\frac{2\Delta^2(\Delta+1)(2\Delta+1)^2(2\Delta+3)}{3(4\Delta+3)(4\Delta+5)}G_{2\Delta+4}(\eta)+\dots \ .\end{aligned} \tag{B.25}$$

When $\Delta = 1$ the first parity-even primary operator after the identity is the displacement operator, and after it there is $\phi\partial^2\phi$. In order to uncover the spectrum of parity-odd operators we consider

$$\langle \phi(x_1)\phi^2(x_2)\phi(x_3)\phi^2(x_4)\rangle \ . \tag{B.26}$$

Using Wick's theorem we find

$$\mathcal{G}^{\phi\phi^2\phi\phi^2}(\eta) = 2\eta^{\Delta}\left(2+2\left(1-\frac{1}{\eta}\right)^{-2\Delta}+\eta^{2\Delta}\right) \ . \tag{B.27}$$

The s-channel decomposition reads ($e^{-2\pi i\Delta}=1$)

$$\mathcal{G}^{\phi\phi^2\phi\phi^2}(\eta)=4G(\Delta,-\Delta,\Delta,\eta)+6G(\Delta,-\Delta,3\Delta,\eta)+\frac{8\Delta^2(2\Delta+1)}{6\Delta+1}G(\Delta,-\Delta,3\Delta+2,\eta)$$
$$-\frac{8\Delta^3(\Delta+1)(2\Delta+1)}{27\Delta(\Delta+1)+6}G(\Delta,-\Delta,3\Delta+3,\eta)+\dots\ . \tag{B.28}$$

When $\Delta=1$ the first parity-even primary operator after ϕ itself is ϕ^3, while the first parity-odd primary is constructed from three derivatives acting on ϕ^3.

C Parity-odd channel in correlators with the displacement

In this appendix we discuss the spectrum of parity-odd primaries in the D $\times\ \psi$ OPE, being ψ a Virasoro primary of scaling dimension $\hat{\Delta}$. To this end we consider the conformal block expansion of the correlator

$$\langle \mathrm{D}(x_1)\psi(x_2)\mathrm{D}(x_3)\psi(x_4)\rangle_{\mathbb{H}^+}=\left(\frac{x_{14}}{x_{24}}\right)^{\hat{\Delta}-2}\left(\frac{x_{14}}{x_{13}}\right)^{2-\hat{\Delta}}\frac{\mathcal{G}^{\mathrm{D}\psi\mathrm{D}\psi}(\eta)}{(x_{12})^{2+\hat{\Delta}}(x_{34})^{2+\hat{\Delta}}}\ ,\quad x_i>x_{i+1}$$
$$\mathcal{G}^{\mathrm{D}\psi\mathrm{D}\psi}(\eta)=\eta^{\hat{\Delta}+2}\left(\frac{c}{2}+\frac{\hat{\Delta}(2(\eta-1)\eta+\hat{\Delta})}{\eta^2(\eta-1)^2}\right)\ , \tag{C.1}$$

which was computed in appendix A.3 of [26]. For generic $\hat{\Delta}$, the s-channel block decomposition was found to be:

$$\mathcal{G}^{\mathrm{D}\psi\mathrm{D}\psi}(\eta)=\hat{\Delta}^2G(\hat{\Delta}-2,2-\hat{\Delta},\hat{\Delta},\eta)+\sum_{n=2,3,4,\dots}\hat{C}_{\mathrm{D}\psi}{}^n\hat{C}_{\mathrm{D}\psi n}G(\hat{\Delta}-2,2-\hat{\Delta},\hat{\Delta}+n,\eta)\ , \tag{C.2}$$

where the first non-zero coefficients read

$$\hat{C}_{\mathrm{D}\psi}{}^2\hat{C}_{\mathrm{D}\psi 2}=\frac{c}{2}+\hat{\Delta}\left(4-\frac{9}{2\hat{\Delta}+1}\right)\ ,$$
$$\hat{C}_{\mathrm{D}\psi}{}^3\hat{C}_{\mathrm{D}\psi 3}=-\frac{2\hat{\Delta}}{(\hat{\Delta}+1)(\hat{\Delta}+2)}\left((c-7)\hat{\Delta}+c+3\hat{\Delta}^2+2\right)\ ,$$
$$\hat{C}_{\mathrm{D}\psi}{}^4\hat{C}_{\mathrm{D}\psi 4}=\frac{\hat{\Delta}(5c(4\hat{\Delta}(\hat{\Delta}+2)+3)+4\hat{\Delta}(\hat{\Delta}(8\hat{\Delta}-19)+26)-15)}{(\hat{\Delta}+3)(2\hat{\Delta}+3)(2\hat{\Delta}+5)}\ . \tag{C.3}$$

Hence, for generic $\hat{\Delta}$, the first parity-even global primary (after ψ itself) appears at level 2, while the first parity-odd appears at level 3. For $c=1/2$ when $\hat{\Delta}=1/2$ (i.e. $\psi_{(1,3)}$ in the Ising model with $(1,2)_3$ boundary condition) the first few coefficients vanish and the first parity-even global primary after $\psi_{(1,3)}$ appears at level four, while the first parity-odd appears at level seven, correspondingly

$$\hat{C}_{\mathrm{D}\psi}{}^4\hat{C}_{\mathrm{D}\psi 4}=\frac{1}{4}\ ,\quad \hat{C}_{\mathrm{D}\psi}{}^7\hat{C}_{\mathrm{D}\psi 7}=-\frac{1}{429}\ ,\quad \psi=\psi_{(1,3)}\text{ in }(1,2)_3\ . \tag{C.4}$$

For $c = 7/10$, leading parity-even (odd) quasi-primaries have

$$\begin{aligned}
&\hat{C}_{\mathrm{D}\psi}{}^2\hat{C}_{\mathrm{D}\psi 2} = \frac{119}{40} , && \hat{C}_{\mathrm{D}\psi}{}^5\hat{C}_{\mathrm{D}\psi 5} = -\frac{68}{231} , && \psi = \psi_{(3,3)} , \\
&\hat{C}_{\mathrm{D}\psi}{}^4\hat{C}_{\mathrm{D}\psi 4} = \frac{39}{2480} , && \hat{C}_{\mathrm{D}\psi}{}^3\hat{C}_{\mathrm{D}\psi 3} = -\frac{2}{11} , && \psi = \psi_{(3,1)} , \\
&\hat{C}_{\mathrm{D}\psi}{}^2\hat{C}_{\mathrm{D}\psi 2} = \frac{13}{44} , && \hat{C}_{\mathrm{D}\psi}{}^5\hat{C}_{\mathrm{D}\psi 5} = -\frac{28}{897} , && \psi = \psi_{(1,3)} .
\end{aligned} \tag{C.5}$$

D Correlators in minimal model boundary conditions

In this section we discuss some correlation functions in minimal model boundary conditions $\mathbf{a} = (a_1, a_2)_m$. Computing correlation functions with bulk Virasoro primaries is a standard application of the method of images [23] (see also Chapter 11.2 of [20]). Boundary Virasoro primaries behave as holomorphic Virasoro primaries as far as the Ward identities are concerned, hence for their correlation functions we will not need to employ the method of images.

D.1 Bulk two-point function of $\phi_{(1,2)}$

We start with the bulk two-point functions of $\phi_{(1,2)}$ on the upper half-plane:

$$\langle \phi_{(1,2)}(x_1 + iy_1, x_1 - iy_1)\phi_{(1,2)}(x_2 + iy_2, x_2 - iy_2)\rangle_{\mathbb{H}^+} . \tag{D.1}$$

In order to compute this correlator we employ the method of images and consider the differential equation satisfied by the four-point function of $\phi_{(1,2)}(z)$ in the homogeneous theory, i.e:

$$\left(\mathcal{L}_{-2}^{(z_4)} - \frac{3}{2(2h_{1,2}+1)}\mathcal{L}_{-1}^2\right)\langle \phi_{(1,2)}(z_1)\phi_{(1,2)}(z_2)\phi_{(1,2)}(z_3)\phi_{(1,2)}(z_4)\rangle = 0 , \tag{D.2}$$

where $h_{1,2}$ is given in eq. (2.11), $\mathcal{L}_{-1} = \partial_{z_4}$, and $\mathcal{L}_{-2}^{(\cdot)}$ is the following differential operator:

$$\mathcal{L}_{-k}^{(w)} \equiv \sum_{i=1}^{3}\left(\frac{(k-1)h_i}{(z_i - w)^k} - \frac{1}{(z_i - w)^{k-1}}\partial_i\right) . \tag{D.3}$$

By $SL(2,\mathbb{R})$ symmetry, the holomorphic correlator takes the following form

$$\langle \phi_{(1,2)}(z_1)\phi_{(1,2)}(z_2)\phi_{(1,2)}(z_3)\phi_{(1,2)}(z_4)\rangle = \frac{\tilde{\mathcal{G}}(\tilde{\eta})}{(z_{12}z_{34})^{2h_{1,2}}} . \tag{D.4}$$

The cross-ratio $\tilde{\eta}$ is

$$\tilde{\eta} = \frac{\eta^2}{1-\eta} , \quad \eta = \frac{z_{12}z_{34}}{z_{13}z_{24}} . \tag{D.5}$$

It is not difficult to solve the differential equation (D.2) for generic m and $\mathbf{a}$. The particular solution is obtained by imposing bulk-boundary crossing symmetry, upon setting $z_2 = z_1^*$, $z_4 = z_3^*$ (being $z_1 = x_1 + iy_1$ and $z_3 = x_2 + iy_2$). For the case at hand, the two Virasoro blocks that correspond to the exchange of $\mathbb{1}$ and $\phi_{(1,3)}$ in the bulk are

$$\begin{aligned} V^{\rm bulk}_{(1,1)}(\tilde\eta) &= \tilde\eta^{2h_{1,2}}\,{}_2F_1\left(\frac{2-m}{2m+2},\frac{2-m}{2m+2}-\frac{m+3}{2m+2}+1;\frac{2-m}{2m+2}-\frac{m}{2m+2}+1;-\frac{4}{\tilde\eta}\right)\ , \\ V^{\rm bulk}_{(1,3)}(\tilde\eta) &= \tilde\eta^{2h_{1,2}-h_{1,3}}\,{}_2F_1\left(\frac{m}{2m+2},\frac{m}{2m+2}-\frac{m+3}{2m+2}+1;-\frac{2-m}{2m+2}+\frac{m}{2m+2}+1;-\frac{4}{\tilde\eta}\right)\ , \end{aligned} \tag{D.6}$$

where

$$\tilde\eta \equiv \frac{16y_1^2y_2^2}{((y_1-y_2)^2+(x_1-x_2)^2)\,((y_1+y_2)^2+(x_1-x_2)^2)}\ . \tag{D.7}$$

The final result is

$$\begin{aligned} &\langle\phi_{(1,2)}(x_1+iy_1,x_1-iy_1)\phi_{(1,2)}(x_2+iy_2,x_2-iy_2)\rangle_{\mathbb{H}^+} = \\ &\qquad\frac{1}{(4y_1y_2)^{2h_{1,2}}}\left(V^{\rm bulk}_{(1,1)}(\tilde\eta)+B^{\mathbf{a}}_{(1,3)}C_{(1,2)(1,2)(1,3)}V^{\rm bulk}_{(1,3)}(\tilde\eta)\right)\ , \end{aligned} \tag{D.8}$$

where

$$\begin{aligned} B^{\mathbf{a}}_{(1,3)} &= \left(1+2\cos\left(\frac{2\pi a_2 m}{m+1}\right)\right)\sqrt{\frac{\sin\left(\frac{\pi}{m}\right)\sin\left(\frac{\pi m}{m+1}\right)}{\sin\left(\frac{\pi}{m}\right)\sin\left(\frac{3\pi m}{m+1}\right)}}\ , \\ C_{(1,2)(1,2)(1,3)} &= \sqrt{\frac{\Gamma\left(\frac{2}{m+1}\right)\Gamma\left(\frac{m}{m+1}\right)\Gamma\left(2-\frac{3}{m+1}\right)\Gamma\left(\frac{2}{m+1}-1\right)}{\Gamma\left(\frac{1}{m+1}\right)\Gamma\left(\frac{m-1}{m+1}\right)\Gamma\left(\frac{2m}{m+1}\right)\Gamma\left(\frac{3}{m+1}-1\right)}}\ . \end{aligned} \tag{D.9}$$

In the boundary channel, corresponding to the exchange of $\hat{\mathbb{1}}$ and $\psi_{(1,3)}$ we have

$$\begin{aligned} V_{(1,1)}(\tilde\eta) &= {}_2F_1\left(\frac{2-m}{2m+2},\frac{m}{2m+2};\frac{m+3}{2m+2};-\frac{\tilde\eta}{4}\right)\ , \\ V_{(1,3)}(\tilde\eta) &= \tilde\eta^{\frac{h_{1,3}}{2}}\,{}_2F_1\left(\frac{2m-1}{2m+2},\frac{1}{2m+2};\frac{3m+1}{2m+2};-\frac{\tilde\eta}{4}\right)\ . \end{aligned} \tag{D.10}$$

The final result is

$$\begin{aligned} &\langle\phi_{(1,2)}(x_1+iy_1,x_1-iy_1)\phi_{(1,2)}(x_2+iy_2,x_2-iy_2)\rangle_{\mathbb{H}^+} = \\ &\qquad\frac{1}{(4y_1y_2)^{2h_{1,2}}}\left((B^{\mathbf{a}}_{(1,2)})^2V_{(1,1)}(\tilde\eta)+(B^{\mathbf{a}\,(1,3)}_{(1,2)})^2V_{(1,3)}(\tilde\eta)\right)\ , \end{aligned} \tag{D.11}$$

with

$$B^{\mathbf{a}}_{(1,2)} = 2(-1)^{a_1}\cos\left(\frac{\pi a_2 m}{m+1}\right)\sqrt{-\frac{\sin\left(\frac{\pi m}{m+1}\right)}{\sin\left(\frac{2\pi m}{m+1}\right)}}\ , \tag{D.12}$$

and, as it follows from bulk-boundary crossing symmetry

$$(B^{\mathbf{a}\,(1,3)}_{(1,2)})^2 = \frac{\Gamma\left(\frac{2m-1}{2m+2}\right)\Gamma\left(\frac{3m}{2m+2}\right)}{2^{\frac{1}{m+1}}\Gamma\left(\frac{m-1}{m+1}\right)\Gamma\left(\frac{3m+1}{2m+2}\right)} - \frac{(B^{\mathbf{a}}_{(1,2)})^2\Gamma\left(\frac{3m}{2m+2}\right)\Gamma\left(1-\frac{3}{2m+2}\right)\Gamma\left(\frac{1}{2}+\frac{1}{m+1}\right)}{2^{1-\frac{2}{m+1}}\Gamma\left(\frac{m}{2m+2}\right)\Gamma\left(\frac{3}{2}-\frac{1}{m+1}\right)\Gamma\left(1-\frac{1}{2m+2}\right)} \ . \tag{D.13}$$

This result is consistent with the F-matrices computation of ref. [41]. As a particular case, for the Ising model with $\mathbb{Z}_2$-preserving conformal boundary conditions we find

$$(B^{\mathbf{a}\,(1,3)}_{\sigma})^2 = \frac{1}{\sqrt{2}} \ , \tag{D.14}$$

as predicted by [34, 29]. Hence $\psi_{(1,3)}$ is $\mathbb{Z}_2$-odd in this boundary condition.

D.2 Bulk two-point function of $\phi_{(2,1)}$

Next, we consider the bulk two-point functions of $\phi_{(2,1)}$ on the upper half-plane:

$$\langle\phi_{(2,1)}(x_1+iy_1,x_1-iy_1)\phi_{(2,1)}(x_2+iy_2,x_2-iy_2)\rangle_{\mathbb{H}^+} \ . \tag{D.15}$$

By the method of images, this correlator satisfies the same second order differential equation as the four-point function of $\phi_{(2,1)}(z)$ in the homogeneous theory

$$\left(\mathcal{L}^{(z_4)}_{-2} - \frac{3}{2(2h_{2,1}+1)}\mathcal{L}^2_{-1}\right)\langle\phi_{(2,1)}(z_1)\phi_{(2,1)}(z_2)\phi_{(2,1)}(z_3)\phi_{(2,1)}(z_4)\rangle = 0 \ . \tag{D.16}$$

By $SL(2,\mathbb{R})$ symmetry, this holomorphic correlator takes the following form

$$\langle\phi_{(2,1)}(z_1)\phi_{(2,1)}(z_2)\phi_{(2,1)}(z_3)\phi_{(2,1)}(z_4)\rangle = \frac{\tilde{\mathcal{G}}(\tilde{\eta})}{(z_{12}z_{34})^{2h_{2,1}}} \ . \tag{D.17}$$

The cross-ratio $\tilde{\eta}$, defined as in eq. (D.5), becomes (D.7) on the upper half-plane. The two Virasoro blocks that correspond to the exchange of $\hat{\mathbb{1}}$ and $\psi_{(3,1)}$ on the boundary read

$$\begin{aligned} V_{(1,1)}(\tilde{\eta}) &= {}_2F_1\left(\frac{m+1}{2m},-\frac{m+3}{2m};\frac{1}{2}-\frac{1}{m};-\frac{\tilde{\eta}}{4}\right) \ , \\ V_{(3,1)}(\tilde{\eta}) &= \tilde{\eta}^{\frac{h_{3,1}}{2}}\,{}_2F_1\left(1+\frac{3}{2m},-\frac{1}{2m};\frac{3}{2}+\frac{1}{m};-\frac{\tilde{\eta}}{4}\right) \ . \end{aligned} \tag{D.18}$$

In the bulk channel, corresponding to the exchange of $\mathbb{1}$ and $\phi_{(3,1)}$ we have

$$\begin{aligned} V^{\text{bulk}}_{(1,1)}(\tilde{\eta}) &= \tilde{\eta}^{2h_{1,2}}\,{}_2F_1\left(-\frac{m+3}{2m},-\frac{m+3}{2m}+\frac{1}{m}+\frac{1}{2};-\frac{m+1}{2m}-\frac{m+3}{2m}+1;-\frac{4}{\tilde{\eta}}\right) \ , \\ V^{\text{bulk}}_{(3,1)}(\tilde{\eta}) &= \tilde{\eta}^{2h_{2,1}-h_{3,1}}\,{}_2F_1\left(\frac{m+1}{2m},\frac{m+1}{2m}+\frac{1}{m}+\frac{1}{2};\frac{m+1}{2m}+\frac{m+3}{2m}+1;-\frac{4}{\tilde{\eta}}\right) \ . \end{aligned} \tag{D.19}$$

The final solution is

$$\langle\phi_{(2,1)}(x_1+iy_1,x_1-iy_1)\phi_{(2,1)}(x_2+iy_2,x_2-iy_2)\rangle_{\mathbb{H}^+} = \\ \frac{1}{(4y_1y_2)^{2h_{2,1}}}\left(V^{\rm bulk}_{(1,1)}(\tilde\eta)+B^{\mathbf{a}}_{(3,1)}C_{(2,1)(2,1)(3,1)}V^{\rm bulk}_{(3,1)}(\tilde\eta)\right)\ , \tag{D.20}$$

where

$$B^{\mathbf{a}}_{(3,1)} = \left(1+2\cos\left(\frac{2\pi a_1(m+1)}{m}\right)\right)\sqrt{\frac{\sin\left(\frac{\pi}{m}\right)\sin\left(\frac{\pi m}{m+1}\right)}{\sin\left(\frac{3\pi}{m}\right)\sin\left(\frac{\pi m}{m+1}\right)}}, \\ C_{(2,1)(2,1)(3,1)} = \sqrt{\frac{\Gamma\left(1+\frac{1}{m}\right)\Gamma\left(2+\frac{3}{m}\right)\Gamma\left(-\frac{2}{m}\right)\Gamma\left(-\frac{m+2}{m}\right)}{\Gamma\left(2+\frac{2}{m}\right)\Gamma\left(-\frac{1}{m}\right)\Gamma\left(\frac{m+2}{m}\right)\Gamma\left(-\frac{m+3}{m}\right)}}\ . \tag{D.21}$$

In the boundary channel we have

$$\langle\phi_{(2,1)}(x_1+iy_1,x_1-iy_1)\phi_{(2,1)}(x_2+iy_2,x_2-iy_2)\rangle_{\mathbb{H}^+} = \\ \frac{1}{(4y_1y_2)^{2h_{2,1}}}\left((B^{\mathbf{a}}_{(2,1)})^2V_{(1,1)}(\tilde\eta)+(B^{\mathbf{a}\,(3,1)}_{(2,1)})^2V_{(3,1)}(\tilde\eta)\right)\ , \tag{D.22}$$

with

$$B^{\mathbf{a}}_{(2,1)} = 2(-1)^{a_2}\sqrt{\frac{\sin\left(\frac{\pi}{m}\right)\sin\left(\frac{\pi m}{m+1}\right)}{\sin\left(\frac{2\pi}{m}\right)\sin\left(\frac{\pi m}{m+1}\right)}}\cos\left(\frac{\pi a_1(m+1)}{m}\right)\ , \tag{D.23}$$

and, as determined by bulk-boundary crossing symmetry

$$(B^{\mathbf{a}\,(3,1)}_{(2,1)})^2 = \frac{\sqrt{\pi}\Gamma\left(2+\frac{3}{m}\right)}{2^{\frac{m+2}{m}}\Gamma\left(\frac{3}{2}+\frac{1}{m}\right)\Gamma\left(\frac{m+2}{m}\right)} - \frac{(B^{\mathbf{a}}_{(2,1)})^2\Gamma\left(\frac{1}{2}-\frac{1}{m}\right)\Gamma\left(2+\frac{3}{m}\right)}{\sqrt{\pi}2^{\frac{m+2}{m}}\Gamma\left(2+\frac{2}{m}\right)}\ . \tag{D.24}$$

This result is consistent with the F-matrices computation of ref. [41]. For the tricritical Ising model with $\mathbb{Z}_2$-preserving conformal boundary conditions one finds

$$(B^{\mathbf{a}\,(3,1)}_{\sigma'})^2 = \frac{7}{4\sqrt{2}}\ . \tag{D.25}$$

Hence $\psi_{(3,1)}$ is $\mathbb{Z}_2$-odd in this boundary condition.

D.3 Tricritical Ising model with $\mathbb{Z}_2$-preserving conformal b.c.

D.3.1 Bulk two-point functions of ϵ'

Consider the bulk two-point correlation function of $\epsilon' = \phi_{(1,3)}$ in the tricritical Ising model with $\mathbb{Z}_2$-preserving conformal boundary conditions

$$\langle\epsilon'(x_1+iy_1,x_1-iy_1)\epsilon'(x_2+iy_2,x_2-iy_2)\rangle_{\mathbb{H}^+}\ . \tag{D.26}$$

This correlator satisfies a third order differential equation, whose solution is known in closed form (for a generic minimal model [26]). In the boundary channel, the Virasoro blocks that are relevant to the $m = 4$ case are[12]

$$\begin{aligned} V_{(1,1)}(\tilde{\eta}) &= {}_3F_2\left(\frac{2m}{m+1}, \frac{2}{m+1}-1, \frac{4}{m+1}-2; \frac{1}{m+1}+\frac{1}{2}, \frac{3}{m+1}-1; -\frac{\tilde{\eta}}{4}\right) , \\ V_{(1,3)}(\tilde{\eta}) &= \tilde{\eta}^{\frac{h_{1,3}}{2}}\, {}_3F_2\left(\frac{5}{2}-\frac{3}{m+1}, \frac{1}{m+1}-\frac{1}{2}, \frac{3}{m+1}-\frac{3}{2}; \frac{3}{2}-\frac{1}{m+1}, \frac{2}{m+1}-\frac{1}{2}; -\frac{\tilde{\eta}}{4}\right) , \end{aligned} \tag{D.27}$$

with $\tilde{\eta}$ defined as in eq. (D.5). The final correlator reads

$$\begin{aligned} &\langle \phi_{(1,3)}(x_1+iy_1, x_1-iy_1)\phi_{(1,3)}(x_2+iy_2, x_2-iy_2)\rangle_{\mathbb{H}^+} = \\ &\qquad \frac{1}{(4y_1y_2)^{2h_{1,3}}}\left((B^{\mathbf{a}}_{(1,3)})^2 V_{(1,1)}(\tilde{\eta}) + (B^{\mathbf{a}\,(1,3)}_{(1,3)})^2 V_{(1,3)}(\tilde{\eta})\right) , \end{aligned} \tag{D.28}$$

where the coefficient $B^{\mathbf{a}}_{(1,3)}$ is given in Table 5 and crossing symmetry implies for the $(2,2)_4$ boundary condition that[13]

$$(B^{\mathbf{a}\,(1,3)}_{\epsilon'})^2 \simeq 0.663053 . \tag{D.29}$$

This results, which is compatible with the F-matrix computation of [41], implies that in the $(2,2)_4$ conformal boundary condition $\psi_{(1,3)}$ is $\mathbb{Z}_2$-even.

D.3.2 The boundary four-point function of $\psi_{(3,1)}$

Consider the boundary four-point correlation function of $\psi_{(3,1)}$ in the tricritical Ising model with $\mathbb{Z}_2$-preserving conformal boundary conditions

$$\langle \psi_{(3,1)}(x_1)\psi_{(3,1)}(x_2)\psi_{(3,1)}(x_3)\psi_{(3,1)}(x_4)\rangle_{\mathbb{H}^+} , \quad x_i > x_{i+1} . \tag{D.30}$$

This correlator satisfies the same third-order differential equation as the four-point correlation function $\psi_{(3,1)}(z)$ in the homogeneous tricritical Ising model, and its solution is known in closed form for any m (see for instance [26]). The most generic solution for $m = 4$ is

$$\langle \psi_{(3,1)}(x_1)\psi_{(3,1)}(x_2)\psi_{(3,1)}(x_3)\psi_{(3,1)}(x_4)\rangle_{\mathbb{H}^+} = \frac{1}{(x_{12}x_{34})^{2h_{3,1}}}\left(V_{(1,1)}(\tilde{\eta}) + (\hat{C}^{\mathbf{a}}_{(3,1)(3,1)(3,1)})^2 V_{(3,1)}(\tilde{\eta})\right) , \tag{D.31}$$

[12] Another linearly independent solution corresponds to the exchange of $\psi_{(1,5)}$, which however does not exists for $m \leq 4$.

[13] Note that $\psi_{(1,3)}$ does not exist in the $(2,1)_4$ b.c., and correspondingly $(B^{\mathbf{a}\,(1,3)}_{\epsilon'})^2 = 0$.

(we have set to zero the coefficient of the third linearly independent solution which would correspond to the exchange of $\psi_{(5,1)}$ on the boundary), with

$$V_{(1,1)}(\tilde{\eta}) = {}_3F_2\left(-\frac{4}{m}-2,-\frac{2}{m}-1,\frac{2}{m}+2;-\frac{3}{m}-1,\frac{1}{2}-\frac{1}{m};-\frac{\tilde{\eta}}{4}\right) ,$$
$$V_{(3,1)}(\tilde{\eta}) = \tilde{\eta}^{\frac{h_{3,1}}{2}}\,{}_3F_2\left(-\frac{3}{m}-\frac{3}{2},-\frac{1}{m}-\frac{1}{2},\frac{3}{m}+\frac{5}{2};-\frac{2}{m}-\frac{1}{2},\frac{1}{m}+\frac{3}{2};-\frac{\tilde{\eta}}{4}\right) , \tag{D.32}$$

and

$$\tilde{\eta} = \frac{x_{12}^2 x_{34}^2}{x_{12}x_{14}x_{23}x_{24}} , \tag{D.33}$$

which is positive if $x_i > x_{i+1}$. The remaining coefficient in eq. (D.31) is fixed by crossing symmetry to be

$$(\hat{C}^{\mathbf{a}}_{(3,1)(3,1)(3,1)})^2 = \frac{\pi 2^{\frac{m-2}{m}}\cos\left(\frac{2\pi}{m}\right)\Gamma\left(3+\frac{4}{m}\right)\Gamma\left(-\frac{m+2}{2m}\right)}{\left(2\cos\left(\frac{2\pi}{m}\right)+1\right)\Gamma\left(\frac{1}{2}+\frac{1}{m}\right)\Gamma\left(\frac{3}{2}+\frac{1}{m}\right)\Gamma\left(2+\frac{3}{m}\right)\Gamma\left(-\frac{m+4}{2m}\right)} . \tag{D.34}$$

which vanishes identically for $m = 4$, but is positive otherwise. Hence, the self-OPE of $\psi_{(3,1)}$ in the tricritical Ising model contains only the identity. We have checked that eq. (D.34) agrees with the results of ref. [41].

E One-loop computations for the $T\bar{T}$ deformation

In this section we compute the following correlation functions at one loop in $T\bar{T}$ deformation of eq. (3.2)

$$\langle \mathrm{D}(x_1)\mathrm{D}(x_2)\rangle \ , \ \langle \mathrm{D}^2(x_1)\mathrm{D}^2(x_2)\rangle \ ,$$
$$\langle \mathrm{D}(x_1)\mathrm{D}(x_2)\mathrm{D}(x_3)\rangle \ , \ \langle \mathrm{D}(x_1)\mathrm{D}(x_2)\mathrm{D}^2(x_3)\rangle \ . \tag{E.1}$$

Here and in the following of this section, the ordering along the boundary of AdS_2 is taken such that $x_i > x_{i+1}$. As we are dealing with covariant bulk RG flows, these correlators take the form 1d conformal correlation functions, i.e. (our conventions are written in appendix A)

$$\langle \psi_i(x_1)\psi_j(x_2)\rangle = \delta_{ij}\frac{\hat{C}_i(g_{T\bar{T}})}{(x^2)^{\hat{\Delta}_i(g_{T\bar{T}})}} \ , \ \langle \psi_i(x_1)\psi_j(x_2)\psi_k(x_3)\rangle = \frac{\hat{C}_{ijk}(g_{T\bar{T}})}{(x_{12})^{\hat{\Delta}_{ijk}(g_{T\bar{T}})}(x_{23})^{\hat{\Delta}_{jki}(g_{T\bar{T}})}(x_{13})^{\hat{\Delta}_{ikj}(g_{T\bar{T}})}} . \tag{E.2}$$

In particular, they are specified by the scaling dimensions of D and D^2 which we parametrize along the RG as follows

$$\hat{\Delta}_{\mathrm{D}}(g_{T\bar{T}}) = 2 + g_{T\bar{T}}\,\delta\hat{\Delta}_{\mathrm{D}} + O(g_{T\bar{T}}^2) ,$$
$$\hat{\Delta}_{\mathrm{D}^2}(g_{T\bar{T}}) = 4 + g_{T\bar{T}}\,\delta\hat{\Delta}_{\mathrm{D}^2} + O(g_{T\bar{T}}^2) , \tag{E.3}$$

as well by as their normalizations (tree-level values are computed in appendix A.3 of [26])

$$\begin{aligned}
\hat{C}_{\mathrm{D}}(g_{T\bar{T}}) \equiv \hat{C}_{\mathrm{DD}}(g_{T\bar{T}}) &= c/2 + g_{T\bar{T}}\,\delta\hat{C}_{\mathrm{D}} + O(g_{T\bar{T}}^2)\ , \\
\hat{C}_{\mathrm{D}^2}(g_{T\bar{T}}) \equiv \hat{C}_{\mathrm{D}^2\mathrm{D}^2}(g_{T\bar{T}}) &= \frac{c}{10}(22+5c) + g_{T\bar{T}}\,\delta\hat{C}_{\mathrm{D}^2} + O(g_{T\bar{T}}^2)\ , \\
\hat{C}_{\mathrm{DDD}}(g_{T\bar{T}}) &= c + g_{T\bar{T}}\,\delta\hat{C}_{\mathrm{DDD}} + O(g_{T\bar{T}}^2)\ , \\
\hat{C}_{\mathrm{DDD}^2}(g_{T\bar{T}}) &= \frac{c}{10}(22+5c) + g_{T\bar{T}}\,\delta\hat{C}_{\mathrm{DDD}^2} + O(g_{T\bar{T}}^2)\ .
\end{aligned} \tag{E.4}$$

For conformal b.c. that support a boundary Virasoro primary ψ of scaling dimension $\hat{\Delta}$ we will also compute, along the same $T\bar{T}$ deformation in AdS_2

$$\langle\psi(x_1)\psi(x_2)\rangle\ ,\ \langle\mathrm{D}(x_1)\psi(x_2)\psi(x_3)\rangle\ ,\ \langle\mathrm{D}^2(x_1)\psi(x_2)\psi(x_3)\rangle\ . \tag{E.5}$$

We will assume ψ to be unit-normalized at tree level, and so we will let

$$\begin{aligned}
\hat{\Delta}_\psi(g_{T\bar{T}}) &= \hat{\Delta} + g_{T\bar{T}}\,\delta\hat{\Delta}_\psi + O(g_{T\bar{T}}^2)\ , \\
\hat{C}_\psi(g_{T\bar{T}}) \equiv \hat{C}_{\psi\psi}(g_{T\bar{T}}) &= 1 + g_{T\bar{T}}\,\delta\hat{C}_\psi + O(g_{T\bar{T}}^2)\ , \\
\hat{C}_{\mathrm{D}\psi\psi}(g_{T\bar{T}}) &= \hat{\Delta} + g_{T\bar{T}}\,\delta\hat{C}_{\mathrm{D}\psi\psi} + O(g_{T\bar{T}}^2)\ , \\
\hat{C}_{\mathrm{D}^2\psi\psi}(g_{T\bar{T}}) &= \frac{\hat{\Delta}}{5}(5\hat{\Delta}+1) + g_{T\bar{T}}\,\delta\hat{C}_{\mathrm{D}^2\psi\psi} + O(g_{T\bar{T}}^2)\ ,
\end{aligned} \tag{E.6}$$

where for the tree-level OPE coefficients we used the results of appendix A.3 of [26].

E.1 Two-point functions

Starting with the two-point correlation functions, Poincaré coordinates of AdS with radius R the one-loop corrections are computed by

$$\begin{aligned}
&-g_{T\bar{T}}R^4\int_{y>a}^{\infty}\frac{\mathrm{d}y}{y^2}\int_{-\infty}^{\infty}\mathrm{d}x\ \langle\mathrm{D}(x_1)\mathrm{D}(x_2)T\bar{T}(x+iy,x-iy)\rangle^{\mathrm{c}}_{0,\mathrm{AdS}_2}\ , \\
&-g_{T\bar{T}}R^4\int_{y>a}^{\infty}\frac{\mathrm{d}y}{y^2}\int_{-\infty}^{\infty}\mathrm{d}x\ \langle\mathrm{D}(x_1)\mathrm{D}^2(x_2)T\bar{T}(x+iy,x-iy)\rangle^{\mathrm{c}}_{0,\mathrm{AdS}_2}\ , \\
&-g_{T\bar{T}}R^4\int_{y>a}^{\infty}\frac{\mathrm{d}y}{y^2}\int_{-\infty}^{\infty}\mathrm{d}x\ \langle\mathrm{D}^2(x_1)\mathrm{D}^2(x_2)T\bar{T}(x+iy,x-iy)\rangle^{\mathrm{c}}_{0,\mathrm{AdS}_2}\ , \\
&-g_{T\bar{T}}R^4\int_{y>a}^{\infty}\frac{\mathrm{d}y}{y^2}\int_{-\infty}^{\infty}\mathrm{d}x\ \langle\psi(x_1)\psi(x_2)T\bar{T}(x+iy,x-iy)\rangle^{\mathrm{c}}_{0,\mathrm{AdS}_2}\ ,
\end{aligned} \tag{E.7}$$

where $\langle\dots\rangle^c$ means 'connected'. We have introduced a IR cut-off at $y=a$. The correlation functions in the integrands above are obtained from those on the upper half-plane $\mathbb{H}^+$, upon Weyl rescaling to AdS_2. These are (limits) of correlation functions with many insertions of T on

$\mathbb{H}^+$: four, five, six, and two, respectively. Explicit expressions for such correlation functions on the $\mathbb{H}^+$ can be found, for example, in the appendices of [26].

Computing the integral is not difficult, and up to $O(a, g^2_{T\bar{T}})$ corrections we find for the one-loop contribution

$$\begin{aligned}
x_{12}^4\langle \mathrm{D}(x_1)\mathrm{D}(x_2)\rangle_{1\text{ loop}} &= -\pi\,\hat{C}_{\mathrm{DDD}}(0)\left(\frac{c}{24}+1+\frac{1}{2}\log\left(\frac{x_{12}^2}{4a^2}\right)\right) g_{T\bar{T}}\ ,\\
x_{12}^6\langle \mathrm{D}(x_1)\mathrm{D}^2(x_2)\rangle &= -\pi\hat{C}_{\mathrm{D}^2}(0)\left(1-\frac{5x_{12}^2}{8a^2}\right) g_{T\bar{T}}\ ,\\
x_{12}^8\langle \mathrm{D}^2(x_1)\mathrm{D}^2(x_2)\rangle_{1\text{ loop}} &= -6\pi\hat{C}_{\mathrm{D}^2}(0)\left(\frac{131}{90}+\frac{c}{36}+\log\left(\frac{x_{12}^2}{4a^2}\right)\right) g_{T\bar{T}}\ ,\\
(x_{12}^2)^{\hat{\Delta}}\langle \psi(x_1)\psi(x_2)\rangle_{1\text{ loop}} &= -\frac{\pi\hat{\Delta}}{2}\left[\hat{\Delta}+(\hat{\Delta}-1)\log\left(\frac{x_{12}^2}{4a^2}\right)\right] g_{T\bar{T}}\ .
\end{aligned} \tag{E.8}$$

Note that an off-diagonal two-point function is generated at one-loop.

E.1.1 Renormalization and mixings

We define the renormalized operators

$$\mathrm{D}_R = Z_{\mathrm{D}}\mathrm{D} + Z_{\mathrm{D}\hat{\mathbb{1}}}\hat{\mathbb{1}} + \dots\ , \quad {\mathrm{D}^2}_R = Z_{\mathrm{D}^2}\mathrm{D}^2 + Z_{\mathrm{D}^2\mathrm{D}}\mathrm{D} + Z_{\mathrm{D}^2\mathrm{D}''}\mathrm{D}'' + Z_{\mathrm{D}^2\hat{\mathbb{1}}}\hat{\mathbb{1}} + \dots \tag{E.9}$$

(D'' denotes the second derivative of D). The wave-functions $Z_{AA'}$ are fixed by requiring correlation functions with insertions of D_R and D_R^2 to be finite and to match the expected form of 1d conformal correlators. By letting

$$\begin{aligned}
Z_{\mathrm{D}} &= 1 + g_{T\bar{T}} z_{\mathrm{D}}\log(a/R)\ , \quad Z_{\mathrm{D}^2} = 1 + g_{T\bar{T}}\ z_{\mathrm{D}^2}\log(a/R)\ ,\\
Z_{\mathrm{D}^2\mathrm{D}} &= g_{T\bar{T}}\ \frac{z_{\mathrm{D}^2\mathrm{D}}}{a^2}\ , \quad Z_{\mathrm{D}^2\mathrm{D}''} = g_{T\bar{T}}\ z_{\mathrm{D}^2\mathrm{D}''}\ ,
\end{aligned} \tag{E.10}$$

being R the AdS_2 radius we see for example that

$$\langle \mathrm{D}_R(x_1)\mathrm{D}_R(x_2)\rangle = Z_{\mathrm{D}}^2\langle \mathrm{D}(x_1)\mathrm{D}(x_2)\rangle\ , \tag{E.11}$$

is completely finite if $z_{\mathrm{D}} = -\pi$, and in particular (taking the $a \to 0$ limit) we get the following one-loop correction

$$x_{12}^4\langle \mathrm{D}_R(x_1)\mathrm{D}_R(x_2)\rangle_{1\text{ loop}} = -c\pi g_{T\bar{T}}\left(\frac{c}{24}+1-\log 2+\frac{1}{2}\log\left(x_{12}^2/R^2\right)\right)\ . \tag{E.12}$$

Hence, by comparing to the $O(g_{T\bar{T}})$ expansion of eq. (E.2) we find

$$\delta\hat{\Delta}_{\mathrm{D}} = \pi\ , \quad \delta\hat{C}_{\mathrm{D}} = \pi c\left(1-\log 2-\frac{c}{24}\right)\ . \tag{E.13}$$

Analogously,

$$\langle \mathrm{D}^2{}_R(x_1)\mathrm{D}^2{}_R(x_2)\rangle = Z^2_{\mathrm{D}^2}\langle \mathrm{D}^2(x_1)\mathrm{D}^2(x_2)\rangle \tag{E.14}$$

is completely finite in the $a \to 0$ limit if we set $z_{\mathrm{D}} = -6\pi$. By comparing to the $O(g_{T\bar{T}})$ expansion of eq. (E.2) we find

$$\delta\Delta_{\mathrm{D}^2} = 6\pi \ , \quad \delta\hat{C}_{\mathrm{D}^2} = \pi\left(\frac{11c}{75}(180\log 2 - 131) + c^2\left(6\log 2 - \frac{71}{15}\right) - \frac{c^3}{12}\right) \ . \tag{E.15}$$

For the mixed two-point function, requiring that

$$\begin{aligned} 0 &= \langle \mathrm{D}_R(x_1)\mathrm{D}^2{}_R(x_2)\rangle \\ &= Z_{\mathrm{D}^2}Z_{\mathrm{D}}\langle \mathrm{D}(x_1)\mathrm{D}^2(x_2)\rangle + Z_{\mathrm{D}^2}Z_{\mathrm{D}^2\mathrm{D}}\langle \mathrm{D}(x_1)\mathrm{D}(x_2)\rangle + Z_{\mathrm{D}^2}Z_{\mathrm{D}^2\mathrm{D}''}\langle \mathrm{D}(x_1)\mathrm{D}''(x_2)\rangle \ , \end{aligned} \tag{E.16}$$

fixes

$$z_{\mathrm{D}^2\mathrm{D}} = -\frac{\pi(5c+22)}{8} \ , \quad z_{\mathrm{D}^2\mathrm{D}''} = \frac{\pi(5c+22)}{100} \ . \tag{E.17}$$

Finally, in order to renormalize the two-point function of ψ we introduce $\psi_R = Z_\psi\psi$ with

$$Z_\psi = 1 + g_{T\bar{T}}z_\psi\log(a/R) \ , \quad z_\psi = -\frac{\pi}{2}(\hat{\Delta}-1)\hat{\Delta} \ . \tag{E.18}$$

By plugging into the renormalized correlator

$$\langle \psi_R(x_1)\psi_R(x_2)\rangle = Z^2_\psi\langle \psi(x_1)\psi(x_2)\rangle \ , \tag{E.19}$$

and comparing to the $O(g_{T\bar{T}})$ expansion of eq. (E.2) we find

$$\delta\hat{\Delta} = -z_\psi \ , \quad \delta\hat{C}_\psi = -\frac{\pi\hat{\Delta}}{2}(2\log 2 - \hat{\Delta}(2\log 2 - 1)) \ . \tag{E.20}$$

E.2 Three-point functions

For the one-loop corrections to three-point functions we shall compute

$$\begin{aligned} &-g_{T\bar{T}}R^4\int_{y>a}^{\infty}\frac{\mathrm{d}y}{y^2}\int_{-\infty}^{\infty}\mathrm{d}x\ \langle \mathrm{D}(x_1)\mathrm{D}(x_2)\mathrm{D}(x_3)T\bar{T}(x+iy,x-iy)\rangle^{\mathrm{c}}_{0,\mathrm{AdS}_2} \ , \\ &-g_{T\bar{T}}R^4\int_{y>a}^{\infty}\frac{\mathrm{d}y}{y^2}\int_{-\infty}^{\infty}\mathrm{d}x\ \langle \mathrm{D}(x_1)\mathrm{D}(x_2)\mathrm{D}^2(x_3)T\bar{T}(x+iy,x-iy)\rangle^{\mathrm{c}}_{0,\mathrm{AdS}_2} \ , \\ &-g_{T\bar{T}}R^4\int_{y>a}^{\infty}\frac{\mathrm{d}y}{y^2}\int_{-\infty}^{\infty}\mathrm{d}x\ \langle \mathrm{D}(x_1)\psi(x_2)\psi(x_3)T\bar{T}(x+iy,x-iy)\rangle^{\mathrm{c}}_{0,\mathrm{AdS}_2} \ , \\ &-g_{T\bar{T}}R^4\int_{y>a}^{\infty}\frac{\mathrm{d}y}{y^2}\int_{-\infty}^{\infty}\mathrm{d}x\ \langle \mathrm{D}^2(x_1)\psi(x_2)\psi(x_3)T\bar{T}(x+iy,x-iy)\rangle^{\mathrm{c}}_{0,\mathrm{AdS}_2} \ . \end{aligned} \tag{E.21}$$

The integrands are again obtained from appropriate limits of correlation functions with many insertions of T on $\mathbb{H}^+$: five, six, three, four, respectively. Computing the integral is easy if we set for example $x_3 = 0$ and $x_1 = 1$, so up to $O(a, g^2_{T\bar{T}})$ corrections we find

$$
\begin{aligned}
&(x-1)^2x^2\ \langle \mathrm{D}(1)\mathrm{D}(x)\mathrm{D}(0)\rangle_{1\text{ loop}} = \\
&-\frac{\pi c^2 g_{T\bar{T}}}{4}\left(1-\frac{c\,(x^8-4x^7+6x^6-4x^5+3x^4-4x^3+6x^2-4x+1)}{8c(x-1)^2x^2a^2}+\frac{4}{c}\log\left(\frac{(x-1)x}{8a^3}\right)\right)\ ,
\end{aligned}
$$

$$
\begin{aligned}
&x^4\ \langle \mathrm{D}(1)\mathrm{D}(x)\mathrm{D}^2(0)\rangle_{1\text{ loop}} = \\
&-\frac{\pi c(5c+22)}{10}g_{T\bar{T}}\left(\frac{5cx^4}{128(x-1)^4a^4}-\frac{5x^2}{4(x-1)^2a^2}\right) \\
&-\frac{\pi c(5c+22)g_{T\bar{T}}}{60}\left(\frac{(c+20)x^2-2(c+14)x+c+20}{6(x-1)^2}-4\log(x-1)+6\log x-8\log(2a)\right)\ ,
\end{aligned}
$$

$$
\begin{aligned}
&(x-1)^2(x^2)^{\hat{\Delta}-1}\ \langle \mathrm{D}(1)\psi(x)\psi(0)\rangle_{1\text{ loop}} = \\
&+\frac{\pi c g_{T\bar{T}}}{16}\frac{(x-1)^2}{x^2a^2}-\frac{\pi g_{T\bar{T}}\hat{\Delta}}{12}\left(\frac{c}{12}+\frac{1}{2}(\hat{\Delta}-2)^2-((\hat{\Delta}-1)\hat{\Delta}+1)\log 2\right) \\
&+\pi g_{T\bar{T}}\hat{\Delta}\left(\left(1-\hat{\Delta}^2+\hat{\Delta}\right)\log x-\log(x-1)+(1+(\hat{\Delta}-1)\hat{\Delta})\log a\right)\ ,
\end{aligned}
$$

$$
\begin{aligned}
&(x-1)^4(x^2)^{\hat{\Delta}-2}\ \langle \mathrm{D}^2(1)\psi(x)\psi(0)\rangle_{1\text{ loop}} = \\
&+\frac{\pi c(5c+22)}{10}\left(\frac{5\hat{\Delta}(x-1)^2}{4ca^2}-\frac{5(x-1)^4}{64x^2a^4}\right)g_{T\bar{T}} \\
&-\frac{\pi\hat{\Delta}}{30}(5c(x((\hat{\Delta}+2)x-6)+6)+x((\hat{\Delta}(3\hat{\Delta}(5\hat{\Delta}-39)+238)+92)x-132)+132)g_{T\bar{T}} \\
&+\frac{\pi\hat{\Delta}(5\hat{\Delta}+1)x^2}{5}\left(((\hat{\Delta}-1)\hat{\Delta}+6)\log(2a)+\left(-\hat{\Delta}^2+\hat{\Delta}+6\right)\log x-6\log(x-1)\right)g_{T\bar{T}}\ .
\end{aligned}
\tag{E.22}
$$

E.2.1 Renormalization and mixings

To resolve the infrared divergences we include the mixings of eq. (E.9) i.e. write

$$
\begin{aligned}
\langle \mathrm{D}_R(x_1)\mathrm{D}_R(x_2)\mathrm{D}_R(x_3)\rangle = &\ Z^3_{\mathrm{D}}\langle \mathrm{D}(x_1)\mathrm{D}(x_2)\mathrm{D}(x_3)\rangle \\
&+ Z^2_{\mathrm{D}}Z_{\mathrm{D}\hat{\mathbb{1}}}\left(\langle \mathrm{D}(x_1)\mathrm{D}(x_2)\hat{\mathbb{1}}\rangle+\langle \mathrm{D}(x_1)\mathrm{D}(x_3)\hat{\mathbb{1}}\rangle+\langle \mathrm{D}(x_2)\mathrm{D}(x_3)\hat{\mathbb{1}}\rangle\right) \\
&+ Z^3_{\mathrm{D}\hat{\mathbb{1}}}\langle \hat{\mathbb{1}}\hat{\mathbb{1}}\hat{\mathbb{1}}\rangle\ ,
\end{aligned}
\tag{E.23}
$$

with $Z_{\rm D}$ as in the previous section and

$$Z_{{\rm D}\hat{\mathbb{1}}} = g_{T\bar{T}}\frac{\pi c}{16a^2}\ . \tag{E.24}$$

With these chosen counterterms we find (up to $O(g_{T\bar{T}}^2)$ corrections)

$$(x-1)^2x^2\langle {\rm D}_R(1){\rm D}_R(x){\rm D}_R(0)\rangle = c - \frac{c\pi g_{T\bar{T}}}{4}\left(c + 2\log(x^2(1-x^2)/R^4) - 12\log 2\right)\ , \tag{E.25}$$

and so, comparing to the $O(g_{T\bar{T}})$ expansion of eq. (E.2) we find

$$\delta\hat{C}_{\rm DDD} = \pi c\left(3\log 2 - \frac{c}{4}\right)\ . \tag{E.26}$$

The choices above are of course enough in order to renormalize

$$\langle {\rm D}_R(1)\psi_R(x)\psi_R(0)\rangle = Z_{\rm D}D_\psi^2\langle {\rm D}(x_1)\psi(x_2)\psi(x_3)\rangle + Z_\psi^2 Z_{{\rm D}\hat{\mathbb{1}}}\langle\psi(x_1)\psi(x_2)\hat{\mathbb{1}}\rangle\ , \tag{E.27}$$

from which we can extract

$$\delta\hat{C}_{\psi\psi{\rm D}} = -\frac{\pi\hat{\Delta}}{2}\left((\hat{\Delta}-2)^2 - 2(\hat{\Delta}-1)\hat{\Delta}\log 2 - 2\log 2 + 6c\right)\ . \tag{E.28}$$

More mixings are needed in order to remove divergences as well as spurious finite terms in the second of eq. (E.22), but the essence is the same. We write

$$\begin{aligned}\langle {\rm D}_R(x_1){\rm D}_R(x_2){\rm D}_R^2(x_3)\rangle = {}& Z_{\rm D}^2 Z_{{\rm D}^2}\langle {\rm D}(x_1){\rm D}(x_2){\rm D}^2(x_3)\rangle \\ &+ Z_{\rm D}^2 Z_{{\rm D}^2{\rm D}}\langle {\rm D}(x_1){\rm D}(x_2){\rm D}(x_3)\rangle + Z_{\rm D}^2 Z_{{\rm D}^2{\rm D}''}\langle {\rm D}(x_1){\rm D}(x_2){\rm D}''(x_3)\rangle \\ &+ Z_{\rm D}^2 Z_{{\rm D}^2\hat{\mathbb{1}}}\langle {\rm D}(x_1){\rm D}(x_2)\hat{\mathbb{1}}\rangle + \text{subleading}\ .\end{aligned} \tag{E.29}$$

Almost all divergent terms, and all the spurious finite terms, are subtracted with the previous choices for the wave functions. We are left with one divergent contribution, which we subtract by including a mixing term with the identity, i.e.

$$Z_{{\rm D}^2\hat{\mathbb{1}}} = g_{T\bar{T}}\frac{\pi c(5c+22)}{128a^4}\ . \tag{E.30}$$

The counterterms above will also renormalize

$$\begin{aligned}\langle {\rm D}^2{}_R(x_1)\psi_R(x_2)\psi_R(x_3)\rangle = {}& Z_\psi^2 Z_{{\rm D}^2}\langle {\rm D}^2(x_1)\psi(x_2)\psi(x_3)\rangle \\ &+ Z_\psi^2 Z_{{\rm D}^2{\rm D}}\langle {\rm D}(x_1)\psi(x_2)\psi(x_3)\rangle + Z_\psi^2 Z_{{\rm D}^2{\rm D}''}\langle {\rm D}''(x_1)\psi(x_2)\psi(x_3)\rangle \\ &+ Z_\psi^2 Z_{{\rm D}^2\hat{\mathbb{1}}}\langle\hat{\mathbb{1}}\psi(x_2)\psi(x_3)\rangle\ .\end{aligned} \tag{E.31}$$

The above renormalized correlators have the right conformal structure, and we from them we extract

$$\begin{aligned}\delta\hat{C}_{{\rm DD}{\rm D}^2} &= \pi c\left(-\frac{c^2}{12} + c\left(4\log 2 - \frac{26}{15}\right) + \frac{11}{75}(120\log 2 - 41)\right)\ , \\ \delta\hat{C}_{\psi\psi{\rm D}^2} &= \frac{\pi\hat{\Delta}(5\hat{\Delta}+1)}{5\times 30}\left(180\log 2 - 5c + 15\hat{\Delta}(8 - \hat{\Delta} + (\hat{\Delta}-1)\log 4) - 262\right)\ .\end{aligned} \tag{E.32}$$

E.2.2 Final results for the OPE coefficients

Taking into account the renormalization of the external operators computed earlier, the OPE coefficients for unit-normalized operators are

$$\begin{aligned}
\frac{\hat{C}_{\mathrm{DDD}}(g_{T\bar{T}})}{\hat{C}_{\mathrm{DD}}(g_{T\bar{T}})^{3/2}} &= \frac{2\sqrt{2}}{c}\left(1-\frac{\pi(c-24)}{8}g_{T\bar{T}}+O(g_{T\bar{T}}^2)\right)\ , \\
\frac{\hat{C}_{\psi\psi\mathrm{D}}(g_{T\bar{T}})}{\hat{C}_{\psi}(g_{T\bar{T}})\hat{C}_{\mathrm{D}}(g_{T\bar{T}})^{1/2}} &= \frac{\sqrt{2}\hat{\Delta}}{\sqrt{c}}\left(1-\pi\left(1+\frac{c}{24}-2\hat{\Delta}\right)g_{T\bar{T}}+O(g_{T\bar{T}}^2)\right)\ , \\
\frac{\hat{C}_{\psi\psi\mathrm{D}^2}(g_{T\bar{T}})}{\hat{C}_{\psi}(g_{T\bar{T}})\hat{C}_{\mathrm{D}^2}(g_{T\bar{T}})^{1/2}} &= \frac{\sqrt{\frac{2}{5}}\hat{\Delta}(5\hat{\Delta}+1)}{\sqrt{c(5c+22)}}\left(1-\frac{\pi}{60}(5c-240\hat{\Delta}+262)g_{T\bar{T}}+O(g_{T\bar{T}}^2)\right)\ , \\
\frac{\hat{C}_{\mathrm{DDD}^2}(g_{T\bar{T}})}{\hat{C}_{\mathrm{DD}}(g_{T\bar{T}})\hat{C}_{\mathrm{D}^2\mathrm{D}^2}(g_{T\bar{T}})^{1/2}} &= \frac{1}{c}\sqrt{\frac{2}{5}}\sqrt{c(5c+22)}\left(1+\frac{109\pi}{30}g_{T\bar{T}}+O(g_{T\bar{T}}^2)\right)\ .
\end{aligned} \tag{E.33}$$

F One-loop computations for Virasoro deformations

In this section we compute the following correlation functions at one loop in the Virasoro deformation of eq. (3.8)

$$\begin{aligned}
&\langle \mathrm{D}(x_1)\mathrm{D}(x_2)\rangle\ ,\ \langle \mathrm{D}^2(x_1)\mathrm{D}^2(x_2)\rangle\ , \\
&\langle \mathrm{D}(x_1)\mathrm{D}(x_2)\mathrm{D}(x_3)\rangle\ ,\ \langle \mathrm{D}(x_1)\mathrm{D}(x_2)\mathrm{D}^2(x_3)\rangle\ .
\end{aligned} \tag{F.1}$$

For covariant RG flows in AdS_2, these take the form of 1d correlation functions. The ordering along the boundary of AdS is taken such that $x_i > x_{i+1}$. Following the conventions of appendix E, we parametrize the CFT data along the RG as

$$\begin{aligned}
\hat{\Delta}_{\mathrm{D}}(g_\phi) &= 2+g_\phi\,\delta\hat{\Delta}_{\mathrm{D}}+O(g_\phi^2)\ , \\
\hat{\Delta}_{\mathrm{D}^2}(g_\phi) &= 4+g_\phi\,\delta\hat{\Delta}_{\mathrm{D}^2}+O(g_\phi^2)\ ,
\end{aligned} \tag{F.2}$$

$$\begin{aligned}
\hat{C}_{\mathrm{D}}(g_\phi)\equiv\hat{C}_{\mathrm{DD}}(g_\phi) &= c/2+g_\phi\,\delta\hat{C}_{\mathrm{D}}+O(g_\phi^2)\ , \\
\hat{C}_{\mathrm{D}^2}(g_\phi)\equiv\hat{C}_{\mathrm{D}^2\mathrm{D}^2}(g_\phi) &= \frac{c}{10}(22+5c)+g_\phi\,\delta\hat{C}_{\mathrm{D}^2}+O(g_\phi^2)\ , \\
\hat{C}_{\mathrm{DDD}}(g_\phi) &= c+g_\phi\,\delta\hat{C}_{\mathrm{DDD}}+O(g_\phi^2)\ , \\
\hat{C}_{\mathrm{DDD}^2}(g_\phi) &= \frac{c}{10}(22+5c)+g_\phi\,\delta\hat{C}_{\mathrm{DDD}^2}+O(g_\phi^2)\ .
\end{aligned} \tag{F.3}$$

F.1 Two-point functions

The one-loop corrections are computed by

$$
\begin{aligned}
&-g_\phi R^{\Delta_\phi}\int_{y>a}^{\infty}\frac{\mathrm{d}y}{y^2}\int_{-\infty}^{\infty}\mathrm{d}x\ \langle \mathrm{D}(x_1)\mathrm{D}(x_2)\phi(x+iy,x-iy)\rangle^{\mathrm{c}}_{0,\mathrm{AdS}_2}\ ,\\
&-g_\phi R^{\Delta_\phi}\int_{y>a}^{\infty}\frac{\mathrm{d}y}{y^2}\int_{-\infty}^{\infty}\mathrm{d}x\ \langle \mathrm{D}(x_1)\mathrm{D}^2(x_2)\phi(x+iy,x-iy)\rangle^{\mathrm{c}}_{0,\mathrm{AdS}_2}\ ,\\
&-g_\phi R^{\Delta_\phi}\int_{y>a}^{\infty}\frac{\mathrm{d}y}{y^2}\int_{-\infty}^{\infty}\mathrm{d}x\ \langle \mathrm{D}^2(x_1)\mathrm{D}^2(x_2)\phi(x+iy,x-iy)\rangle^{\mathrm{c}}_{0,\mathrm{AdS}_2}\ ,
\end{aligned}
\tag{F.4}
$$

where $\langle\dots\rangle^c$ means 'connected' and $y=a$ is an IR cut-off. The correlation functions in the integrands above are obtained from correlation functions on the upper-half plane $\mathbb{H}^+$ via Weyl rescaling. These are in turn computed from appropriate limits of correlation functions with one insertion of the Virasoro primary ϕ and (respectively) two, three and four insertions of T on $\mathbb{H}^+$. Explicit expressions of such can be found for example in [26].

Computing the integral we find (up to $O(a,g_\phi^2)$ corrections)

$$
\begin{aligned}
x_{12}^4\langle \mathrm{D}(x_1)\mathrm{D}(x_2)\rangle_{1\text{ loop}} &= -\frac{\pi\Delta_\phi B_\phi}{2^{\Delta_\phi-1}}\left(\Delta_\phi+(\Delta_\phi-2)\log\left(\frac{x_{12}^2}{4a^2}\right)\right)g_\phi\ ,\\
x_{12}^6\langle \mathrm{D}(x_1)\mathrm{D}^2(x_2)\rangle_{1\text{ loop}} &= -\frac{\pi\Delta_\phi B_\phi}{5\times 2^{\Delta_\phi+2}}\left(8(\Delta_\phi-2)(5\Delta_\phi+2)-5(2c+5(\Delta_\phi-2)\Delta_\phi+4)\frac{x_{12}^2}{a^2}\right)g_\phi\ ,\\
x_{12}^8\langle \mathrm{D}^2(x_1)\mathrm{D}^2(x_2)\rangle_{1\text{ loop}} &= -\frac{\pi\Delta_\phi B_\phi}{75\times 2^{\Delta_\phi+1}}\left[1344+\Delta_\phi(600c+5\Delta_\phi(185\Delta_\phi-692)+4468)\right.\\
&\qquad\left.+30(\Delta_\phi-2)(20c+25(\Delta_\phi-2)\Delta_\phi+64)\log\left(\frac{x_{12}^2}{4a^2}\right)\right]g_\phi\ .
\end{aligned}
\tag{F.5}
$$

Note that an off-diagonal two-point function is generated at one-loop.

F.1.1 Renormalization and mixings

In order to renormalize the two-point functions above we shall essentially repeat the analysis of appendix E. We define the renormalized operators

$$
\mathrm{D}_R=Z_{\mathrm{D}}\mathrm{D}+Z_{\mathrm{D}\hat{\mathbb{1}}}\hat{\mathbb{1}}+\dots\ ,\quad \mathrm{D}^2{}_R=Z_{\mathrm{D}^2}\mathrm{D}^2+Z_{\mathrm{D}^2\mathrm{D}}\mathrm{D}+Z_{\mathrm{D}^2\mathrm{D}''}\mathrm{D}''+Z_{\mathrm{D}^2\hat{\mathbb{1}}}\hat{\mathbb{1}}+\dots \tag{F.6}
$$

and fix the wave-functions $Z_{AA'}$ by requiring correlation functions with insertions of D_R and D_R^2 to be finite and to match the expected form of 1d conformal correlators. By letting

$$
\begin{aligned}
&Z_{\mathrm{D}}=1+g_\phi z_{\mathrm{D}}\log(a/R)\ ,\quad Z_{\mathrm{D}^2}=1+g_\phi\ z_{\mathrm{D}^2}\log(a/R)\ ,\\
&Z_{\mathrm{D}^2\mathrm{D}}=g_\phi\ \frac{z_{\mathrm{D}^2\mathrm{D}}}{a^2}\ ,\quad Z_{\mathrm{D}^2\mathrm{D}''}=g_\phi\ z_{\mathrm{D}^2\mathrm{D}''}\ ,
\end{aligned}
\tag{F.7}
$$

being R the AdS radius, the wave-functions are found to be

$$z_{\mathrm{D}} = -\frac{B_\phi}{2^{\Delta_\phi}}\frac{4\pi}{c}(\Delta_\phi-2)\Delta_\phi \ , \quad z_{\mathrm{D}^2} = -\frac{B_\phi}{2^{\Delta_\phi}}\frac{2\pi\Delta_\phi(\Delta_\phi-2)(20c+25(\Delta_\phi-2)\Delta_\phi+64)}{c(5c+22)} \ ,$$
$$z_{\mathrm{D}^2\mathrm{D}} = \frac{\pi B_\phi\Delta_\phi}{2^{\Delta_\phi+1}c}(2c+5(\Delta_\phi-2)\Delta_\phi+4) \ , \quad z_{\mathrm{D}^2\mathrm{D}''} = \frac{\pi B_\phi}{2^\Delta_\phi\times 25c}(\Delta_\phi-2)\Delta_\phi(5\Delta_\phi+2) \ . \tag{F.8}$$

From the renormalized two-point correlation functions, comparing to the $O(g_{T\bar{T}})$ expansion of eq. (E.2) we find

$$\begin{aligned}
\delta\hat{\Delta}_{\mathrm{D}} &= -z_{\mathrm{D}} \ , \qquad \delta\hat{\Delta}_{\mathrm{D}^2} = -z_{\mathrm{D}^2} \ , \\
\delta\hat{C}_{\mathrm{D}} &= -\frac{\pi B_\phi\Delta_\phi}{2^{\Delta_\phi-1}}(\Delta_\phi-2(\Delta_\phi-2)\log 2) \ , \\
\delta\hat{C}_{\mathrm{D}^2} &= -\frac{\pi B_\phi\Delta_\phi}{75\times 2^{\Delta_\phi+1}}\left(1344+\Delta_\phi(600c+5\Delta_\phi(185\Delta_\phi-692)+4468)\right. \\
&\quad \left.-60(\Delta_\phi-2)(20c+25(\Delta_\phi-2)\Delta_\phi+64)\log 2\right) \ .
\end{aligned} \tag{F.9}$$

F.2 Three-point functions

For the one-loop corrections to three-point functions we shall compute

$$\begin{aligned}
&-g_\phi R^{\Delta_\phi}\int_{y>a}^{\infty}\frac{\mathrm{d}y}{y^2}\int_{-\infty}^{\infty}\mathrm{d}x\ \langle \mathrm{D}(x_1)\mathrm{D}(x_2)\mathrm{D}(x_3)\phi(x+iy,x-iy)\rangle^{\mathrm{c}}_{0,\mathrm{AdS}_2} \ , \\
&-g_\phi R^{\Delta_\phi}\int_{y>a}^{\infty}\frac{\mathrm{d}y}{y^2}\int_{-\infty}^{\infty}\mathrm{d}x\ \langle \mathrm{D}(x_1)\mathrm{D}(x_2)\mathrm{D}^2(x_3)\phi(x+iy,x-iy)\rangle^{\mathrm{c}}_{0,\mathrm{AdS}_2} \ .
\end{aligned} \tag{F.10}$$

The integrand are again obtain from appropriate limits of correlation functions with many insertions of T and one insertion of ϕ on $\mathbb{H}^+$. From the integrals we find

$$\begin{aligned}
&(x-1)^2x^2\ \langle \mathrm{D}(1)\mathrm{D}(x)\mathrm{D}(0)\rangle_{1\text{ loop}} = \\
&\qquad + \frac{12\pi B_\phi(\Delta_\phi-4)\Delta_\phi^2}{2^{\Delta_\phi+2}}\left[1-\frac{4(\Delta_\phi-2)}{3(\Delta_\phi-4)\Delta_\phi}\log\left(\frac{(x-1)x}{8a^3}\right)\right. \\
&\qquad \left. + \frac{c((x-1)x+1)\left((x-1)x\left(x^4-2x^3+x+3\right)+1\right)}{12(\Delta_\phi-4)\Delta_\phi(x-1)^2x^2a^2}\right]g_\phi \ ,
\end{aligned}$$

$$\begin{aligned}
&x^4\ \langle \mathrm{D}(1)\mathrm{D}(x)\mathrm{D}^2(0)\rangle_{1\text{ loop}} = \\
&\qquad \frac{\pi B_\phi\Delta_\phi}{15\times 2^{\Delta_\phi+5}}\left(\frac{240(5(\Delta_\phi-2)\Delta_\phi+4)x^2+480cx^2}{(x-1)^2\epsilon^2}-\frac{15c(5\Delta_\phi+2)x^4}{(x-1)^4\epsilon^4}\right. \\
&\qquad \left. + \frac{(c_0+c_1x+c_2x^2)}{(x-1)^2}+d_0+d_1\log a+d_2\log(x-1)+d_3\log x\right)g_\phi \ ,
\end{aligned} \tag{F.11}$$

with

$$
\begin{aligned}
c_0 &= -32(\Delta_\phi(\Delta_\phi(40\Delta_\phi - 229) + 466) + 120) \ , \\
c_1 &= 64(\Delta_\phi(\Delta_\phi(40\Delta_\phi - 259) + 514) + 144) \ , \\
c_2 &= -32(\Delta_\phi(\Delta_\phi(40\Delta_\phi - 229) + 466) + 120) \ , \\
d_0 &= 96(20c(\Delta_\phi(2\log 2 - 1) - \log 16) + (\Delta_\phi - 2)(25(\Delta_\phi - 2)\Delta_\phi + 152)\log 2) \ , \\
d_1 &= 96(\Delta_\phi - 2)(40c + 25(\Delta_\phi - 2)\Delta_\phi + 152) \ , \\
d_2 &= 96(\Delta_\phi - 2)(25(\Delta_\phi - 2)\Delta_\phi - 24) \ , \\
d_3 &= 96(\Delta_\phi - 2)(-20c - 25(\Delta_\phi - 2)\Delta_\phi - 64) \ .
\end{aligned} \tag{F.12}
$$

F.2.1 Renormalization and mixings

One can verify that the wave-functions in the previous section, together with the following mixing terms with the identity

$$
Z_{\mathrm{D}\hat{\mathbb{1}}} = g_\phi \frac{2\pi B_\phi \Delta_\phi}{2^{2+\Delta_\phi} a^2} \ , \quad Z_{\mathrm{D}^2\hat{\mathbb{1}}} = g_\phi \frac{\pi B_\phi \Delta_\phi (5\Delta_\phi + 2)}{2^{4+\Delta_\phi} a^4}, \tag{F.13}
$$

are enough to remove all divergences in eq. (F.11). The resulting functions are conformally covariant, and by comparing them to the $O(g_{T\bar{T}})$ expansion of eq. (E.2) we extract

$$
\begin{aligned}
\delta\hat{C}_{\mathrm{DDD}} &= \frac{3\pi B_\phi \Delta_\phi}{2^{\Delta_\phi}} \left((\Delta_\phi - 4)\Delta_\phi + 4(\Delta_\phi - 2)\log 2\right) \ , \\
\delta\hat{C}_{\mathrm{DDD}^2} &= \frac{\pi B_\phi \Delta_\phi}{75 \times 2^{\Delta_\phi}} \left(-\Delta_\phi(300c + 5\Delta_\phi(40\Delta_\phi - 247) + 2474)\right. \\
&\quad \left. + 15(\Delta_\phi - 2)(40c + 25(\Delta_\phi - 2)\Delta_\phi + 152)\log 2 - 672\right) \ .
\end{aligned} \tag{F.14}
$$

F.2.2 Final results for the OPE coefficients

Taking into account the renormalization of the external operators computed earlier, the OPE coefficients for unit-normalized operators are

$$
\begin{aligned}
\frac{\hat{C}_{\mathrm{DDD}}(g_\phi)}{\hat{C}_{\mathrm{DD}}(g_\phi)^{3/2}} &= \frac{2\sqrt{2}}{c}\left(1 + \frac{B_\phi}{2^{\Delta_\phi}}\frac{3\pi}{c}(\Delta_\phi - 2)\Delta_\phi^2\, g_\phi + O(g_\phi^2)\right) \ , \\
\frac{\hat{C}_{\mathrm{DDD}^2}(g_\phi)}{\hat{C}_{\mathrm{DD}}(g_\phi)\hat{C}_{\mathrm{D}^2\mathrm{D}^2}(g_\phi)^{1/2}} &= \frac{1}{c}\sqrt{\frac{2}{5}}\sqrt{c(5c + 22)} \\
&\quad \times \left(1 + \frac{B_\phi}{2^{\Delta_\phi}}\frac{\pi(\Delta_\phi - 2)\Delta_\phi(5\Delta_\phi + 2)(25\Delta_\phi + 336)}{30c(5c + 22)} g_\phi + O(g_\phi^2)\right) \ .
\end{aligned} \tag{F.15}
$$

G $\phi_{(1,2)}$ deformations of minimal models

In this section we study the $\phi \equiv \phi_{(1,2)}$ deformation of a diagonal minimal model with elementary conformal boundary condition $\mathbf{a} = (a_1, a_2)_m$, on AdS_2

$$\delta S = g R^{\Delta-2} \int d^2x \sqrt{g}\, \phi(x+iy, x-iy) + \text{counterterms} \ . \tag{G.1}$$

The scaling dimension of ϕ is, from eq. (2.11)

$$\Delta \equiv \Delta_{1,2} = 2h_{1,2} = \frac{m-2}{2(m+1)} \ . \tag{G.2}$$

We will work with m finite. The main result of this section pertains the one-loop anomalous dimension of the boundary Virasoro primary $\psi_{(r,s)}$ (assuming it exists) in a generic conformal boundary condition $\mathbf{a}$ and at finite m i.e.

$$\hat{\Delta}_{r,s} = h_{r,s} + g\delta\hat{\Delta}_{r,s} + O(g^2) \ . \tag{G.3}$$

The tree-level scaling dimension $h_{(r,s)}$ is given in eq. (2.11). In Poincaré coordinates of AdS_2 we shall then study

$$G_1(x_{12}) = R^{\Delta} \int_{y>a} \frac{\mathrm{d}y}{y^2} \int_{-\infty}^{\infty} \mathrm{d}x \ \langle \psi_{(r,s)}(x_1)\psi_{(r,s)}(x_2)\phi_{(1,2)}(x+iy, x-iy)\rangle^{\mathrm{c}}_{0,\mathrm{AdS}_2} + \text{counterterms} \ . \tag{G.4}$$

As usual, here $\langle \dots \rangle^c$ means 'connected' and $y = a$ is an IR cut-off. The correlation functions in the integrand above is obtained from correlation functions on the upper-half plane via Weyl rescaling.

G.1 Correlator between two $\psi_{(r,s)}$ and one $\phi_{(1,2)}$

Our first task is to compute

$$\langle \psi_{(r,s)}(x_1)\psi_{(r,s)}(x_2)\phi_{(1,2)}(x+iy, x-iy)\rangle_{\mathbb{H}^+} \ , \quad x_1 > x_2 \ . \tag{G.5}$$

By the method of images, this correlator satisfies the following second order differential equation.

$$\left(\mathcal{L}^{(z_4)}_{-2} - \frac{3}{2(2h_{r,s}+1)} \mathcal{L}^2_{-1} \right) \langle \psi_{(r,s)}(z_1)\psi_{(1,2)}(z_2)\phi_{(1,3)}(z_3)\phi_{(1,3)}(z_4)\rangle = 0 \ , \tag{G.6}$$

where $\mathcal{L}^{(\cdot)}_{-n}$ is the differential operator defined in eq. (D.3) and $\mathcal{L}_{-1} = \partial_{z_4}$. By $SL(2,\mathbb{R})$ symmetry we have

$$\langle \psi_{(r,s)}(z_1)\psi_{(r,s)}(z_2)\phi_{(1,2)}(z_3)\phi_{(1,2)}(z_4)\rangle = \frac{\mathcal{G}(\eta)}{(z_{12})^{2h_{r,s}}(z_{34})^{2h_{1,2}}} \ . \tag{G.7}$$

The cross-ratio η is

$$\eta = \frac{z_{12}z_{34}}{z_{13}z_{24}} = \frac{2iyx_{12}}{(x_1 - z)(x_2 - z^*)} \ . \tag{G.8}$$

From (G.6) we get

$$4\eta(\eta-1)^2(m+1)^2G''(\eta) + 4(\eta-1)(m+1)(\eta(m+2)-2)G'(\eta) + \eta(2-m)mG(\eta) = 0 \ . \tag{G.9}$$

In order to solve this equation, it is convenient to define another function

$$\mathcal{G}(\eta) = \tilde{\mathcal{G}}(\tilde{\eta}) \ , \tag{G.10}$$

where

$$\tilde{\eta} = \frac{\eta^2}{\eta - 1} = \frac{4y^2(x_{12})^2}{((x_1 - x)^2 + y^2)\left((x_2 - x)^2 + y^2\right)} \ , \quad 0 \leq \tilde{\eta} \leq 4 \ . \tag{G.11}$$

The Virasoro blocks corresponding to the exchange of $\hat{\mathbb{1}}$ and $\psi_{(1,3)}$ read

$$\begin{aligned} V_{(1,1)}(\tilde{\eta}) &= {}_2F_1\left(\frac{mr - ms + r + 1}{2m+2}, \frac{-((m+1)r) + ms + 1}{2(m+1)}; \frac{m+3}{2m+2}; \frac{\tilde{\eta}}{4}\right) \ , \\ V_{(1,3)}(\tilde{\eta}) &= \tilde{\eta}^{h_{1,3}/2}\, {}_2F_1\left(\frac{rm - sm + m + r}{2m+2}, \frac{-rm + sm + m - r}{2m+2}; \frac{3m+1}{2m+2}; \frac{\tilde{\eta}}{4}\right) \ . \end{aligned} \tag{G.12}$$

The final solution is then

$$\begin{aligned} \langle \psi_{(r,s)}(x_1)\psi_{(r,s)}(x_2)\phi_{(1,2)}(x+iy, x-iy)\rangle_{\mathbb{H}^+} &= \frac{\tilde{\mathcal{G}}(\tilde{\eta})}{(x_{12})^{2h_{r,s}}(2y)^{2h_{1,2}}} \ , \\ \tilde{\mathcal{G}}(\tilde{\eta}) &= B^{\mathbf{a}}_{(1,2)} V_{(1,1)}(\tilde{\eta}) + \hat{C}^{\mathbf{a}}_{(r,s)(r,s)(1,3)} B^{\mathbf{a}\,(1,3)}_{(1,2)} V_{(1,3)}(\tilde{\eta}) \ , \end{aligned} \tag{G.13}$$

where $B^{\mathbf{a}}_{(1,2)}$ was given in eq. (D.13). The remaining coefficient in the equation above is determined by the following requirement. The function $\tilde{\mathcal{G}}(\tilde{\eta})$ has a branch cut along $\tilde{\eta} \in [4, \infty]$. None of these singularities correspond to an OPE channel: they are unphysical and so they should disappear [34].[14] Requiring that Disc $\tilde{\mathcal{G}} = 0$ across the cut one finds

$$\hat{C}^{\mathbf{a}}_{(r,s)(r,s)(1,3)} B^{\mathbf{a}\,(1,3)}_{(1,2)} = -B^{\mathbf{a}}_{(1,2)} \frac{2^{\frac{2}{m+1}-1}\Gamma\left(\frac{1}{2} + \frac{1}{m+1}\right)\Gamma\left(\frac{rm-sm+m+r}{2m+2}\right)\Gamma\left(\frac{-rm+sm+m-r}{2m+2}\right)}{\Gamma\left(\frac{3}{2} - \frac{1}{m+1}\right)\Gamma\left(\frac{mr+r-ms+1}{2m+2}\right)\Gamma\left(\frac{-((m+1)r)+ms+1}{2(m+1)}\right)} \ . \tag{G.14}$$

This formula is consistent with the results from F-matrices [41].

[14] This condition has been exploited in higher dimensions as well: to prove 'triviality' of certain free theory conformal defects [70, 71], to constrain the space of conformal boundary conditions for a theory of a free massless scalar field [72, 73], to compute perturbative data in $O(N)$ models with boundaries of defects [74, 75], in the context of QFTs in AdS [58].

G.2 Anomalous dimensions

We have all the ingredients to compute the anomalous dimension of boundary Virasoro primaries along the deformation of eq. (G.1). Following the same steps as those of section 4.2 in [26] we arrive at the following result for the anomalous dimension of $\psi_{(r,s)}$

$$\delta\hat{\Delta}_{r,s} = \delta\hat{\Delta}_{1,1} + \delta\hat{\Delta}_{1,3} \ , \tag{G.15}$$

where

$$\begin{aligned}
\delta\hat{\Delta}_{1,1} &= B^{\mathbf{a}}_{(1,2)} \sum_{n=0}^{\infty} \frac{\pi\,(1/2)_n\,(mr-ms+r-1)(mr-ms+r+1)}{2^{\frac{3m}{2m+2}}(m+1)(m+3)n!(2)_n\left(\frac{3}{2}+\frac{1}{m+1}\right)_n} \\
&\quad\times\left(\frac{r+m(r-s+2)+3}{2(m+1)}\right)_n\left(\frac{-r+m(-r+s+2)+3}{2(m+1)}\right)_n \ , \\
\delta\hat{\Delta}_{1,3} &= \hat{C}^{\mathbf{a}}_{(r,s)(r,s)(1,3)} B^{\mathbf{a}\,(1,3)}_{(1,2)} \sum_{n=0}^{\infty} \frac{\pi(m-1)\Gamma\left(\frac{m-1}{m+1}\right)\left(-\frac{1}{m+1}\right)_n\left(\frac{rm-sm+m+r}{2m+2}\right)_n\left(\frac{-rm+sm+m-r}{2m+2}\right)_n}{2^{2-\frac{4}{m+1}}\Gamma(n+1)\Gamma\left(n+\frac{1}{2}-\frac{1}{m+1}\right)\Gamma\left(n+\frac{3}{2}-\frac{1}{m+1}\right)} \ .
\end{aligned} \tag{G.16}$$

H Review of the Staircase model

In the main text we discussed how to study the $(2,2)_4$ b.c. of the tricritical Ising by analyzing the space of values of the four-point function and its derivatives at the crossing symmetric point. We motivated this by recalling that RG flows between minimal models can be embedded in the so-called staircase RG flows which are associated to the S-matrix of the staircase model. In this appendix we review the definition and properties of this model and flesh out the connection to our original problem of minimal model RG flows in AdS.

H.1 Defining properties

The staircase model is an integrable 2-dimensional quantum field theory, whose S-matrix is obtained by analytic continuation in the coupling of sinh-Gordon (shG) theory as first done by Alyosha Zamolodchikov in an unpublished paper [3]. It describes the scattering of a single massive scalar without bound-states. The shG S-matrix is a pure CDD-zero:

$$S_{\text{shG}}(\theta) = \frac{\sinh\theta - i\sin\gamma}{\sinh\theta + i\sin\gamma} \, , \tag{H.1}$$

where γ is related to the sinh-Gordon coupling and θ is the usual rapidity defined in terms of Mandelstam's $s = (p_1+p_2)^2$ through $s = 2m^2(1+\cosh\theta)$. This S-matrix is invariant under the

duality $\gamma \to \pi - \gamma$, which is a weak-strong duality in the original coupling. One then goes to the self-dual point and gives the coupling an imaginary part: $\gamma \to \frac{\pi}{2} + i\theta_0$, leading to the S-matrix:

$$S_{\text{stc}}(\theta) = \frac{\sinh\theta - i\cosh\theta_0}{\sinh\theta + i\cosh\theta_0}\,. \tag{H.2}$$

This is a perfectly healthy S-matrix with all the right reality and crossing properties. However the Lagrangian nature of the UV theory is completely obscured by this procedure, as it would correspond to a sine-Gordon theory with a complex potential. It is important to recall that since this is a purely elastic theory, one has access to some off-shell quantities through the Thermodynamic Bethe Ansatz (TBA). In particular, one can obtain the ground state energy on a circle of radius R which is related to the effective central-charge of the theory [76]:

$$E(R) = -\frac{\pi c_{\text{eff}}(x)}{6R}\,, \tag{H.3}$$

where $x = \log(mR/2)$ is a convenient dimensionless scale. This quantity, in the UV and IR matches the central charges of the UV and IR CFTs (which can of course be trivial and have $c = 0$), and is an RG monotone. In fact it is the monotonic quantity defined in Sasha Zamolodchikov's c-theorem [77]. Solving the TBA equations (numerically), one finds that the IR central charge is 0, as it should for a massive theory, and the UV one is 1, as one might expect from the relation to the shG model. We emphasize that this does not mean that the theory can be described by a UV lagrangian with a massless scalar, since such a theory would have a rather sick potential.

Looking at the explicit solutions replicated in figure 21, one sees that the central charge develops a staircase pattern, spending RG time at central charge plateaus which precisely match the central charges of the unitary minimal models $\mathcal{M}_m$. Indeed, as $\theta_0 \to \infty$, the RG flow of this theory approaches the integrable RG flows between $\mathcal{M}_m \to \mathcal{M}_{m-1}$ which are triggered by the integrable, nearly marginal deformation driven by the $\phi_{(1,3)}$ operator in the UV. This operator obviously becomes irrelevant and manifests itself as the $\phi_{(3,1)}$ operator in the IR. In the Ising model (the last plateau), this operator does not exist, and the irrelevant deformation is instead driven by the $T\bar{T}$ operator, as we have seen in the main text.

H.2 A hint from the S-matrix Bootstrap

As a simple CDD factor, we expect the shG and staircase S-matrices to saturate S-matrix bounds [78]. Since they have no poles/bound-states, the natural observable is the effective quartic coupling which we can take to be $S(s = 2m^2)$. However this leads to very trivial bounds $-1 \leq S(2) \leq 1$ which are saturated by a free Majorana fermion on the left and a free boson on the right. A natural extension of this is to consider a low energy expansion, which we can take to be the Taylor series around $s = 2m^2$. Crossing ensures that $S'(2) = 0$, so we can focus on the two

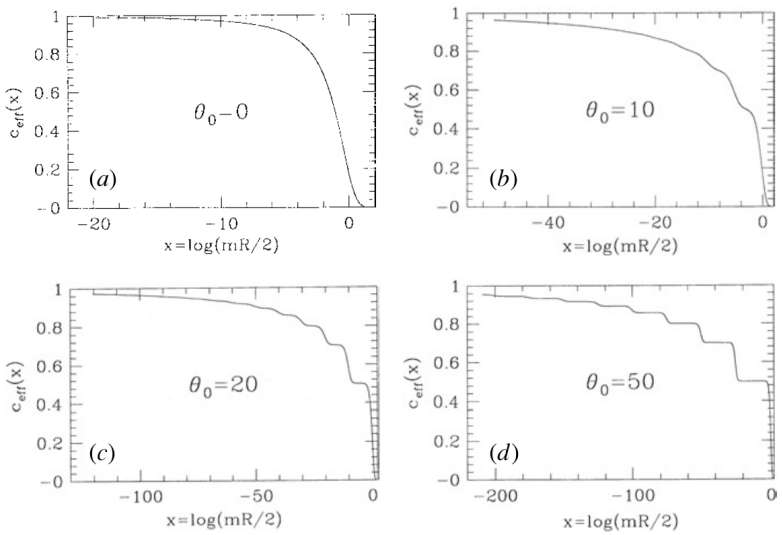

Figure 21: Effective central charge from the TBA equation for the staircase model at several values of θ_0, taken from [3]. As θ_0 increases, the function develops plateaus which take precisely the minimal model values.

dimensional space of parameters $\{S(2), S''(2)\}$. Using the standard numerical S-matrix bootstrap we find the region in figure 22. Indeed, the staircase model saturates the bounds, interpolating between the self-dual point of shG and the massive Majorana. A deformed version of this plot was presented previously in the work of [55]. This feature is reminiscent of the $O(2)$ symmetric S-matrices of the sine-Gordon kinks. Indeed, this one parameter family of S-matrices saturates similar bounds, where the 2-dimensional space is instead spanned by 2 components associated to different representations of the $O(2)$ symmetry (say singlet and rank 2 tensor components). In the work of [4], the authors understood how to embed such bounds as a flat space limit of 1d CFT bounds, with the role of the AdS radius being played by the dimension of the external $O(2)$ fundamentals. There it was clear that the UV is well described by free vertex operators, deformed by the sine-Gordon interaction. One can then wonder whether repeating this strategy for the $\mathbb{Z}_2$ symmetric space of correlators labeled by $g(z = 1/2)$ and $g''(z = 1/2)$ might illuminate the UV origin of the staircase model. This also leads us to the Minimal Model flows in AdS which we studied in the main text.

H.3 More on Minimal Model RG flows

From our analysis so far, one thing that remains unclear, is why it should be the specific $(2, 2)_4$ b.c. of tricritical Ising and the specific $(1, 2) \equiv (3, 3)$ operator saturating this bound. While this is not completely clear, there is some evidence we can follow:

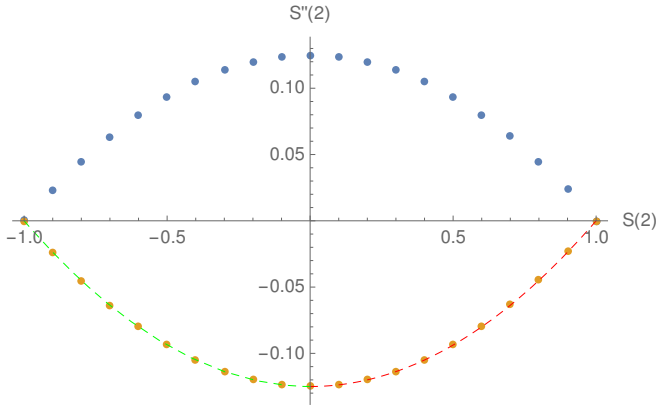

Figure 22: Allowed space of S-matrices for a single scalar particle without bound states projected to the $\{S(2), S''(2)\}$ subspace. The right and left endpoints are a real free boson and fermion, respectively. The bottom right section, in dashed red, are the shG S-matrices as γ varies from 0 to $\pi/2$. Going beyond this brings us back, by duality. Reaching the self-dual point and giving an imaginary part θ_0 from 0 to ∞ builds the green dashed line, corresponding to the staircase models. At large θ_0 we recover the gapped fermion.

- Our S-matrix has a $\mathbb{Z}_2$ symmetry, so it seems natural to keep it along the flow. Therefore we should pick $\mathbb{Z}_2$ preserving boundary conditions.
- The particles are $\mathbb{Z}_2$ odd. We therefore should consider $\mathbb{Z}_2$ odd boundary operators.
- For a massless boson in AdS, the natural $\mathbb{Z}_2$ preserving boundary conditions are the Dirichlet ones $\phi|_{\text{bdry}} = 0$. Although the UV of the staircase model is **not** a free massless boson, one might be tempted to impose the analogue of the Dirichlet BC along the flow. For the Minimal Models this can be understood from the Landau-Ginzburg formulation. The L-G field ϕ corresponds to the lightest $\mathbb{Z}_2$ odd operator which is $\phi_{(2,2)}$ in the Kac table. Indeed, $(2,2)$ boundary conditions are always $\mathbb{Z}_2$ preserving. In this case, the bulk $\mathbb{Z}_2$ even operators will appear in the BOE of $\phi_{(2,2)}$. It seems tempting to consider the lightest boundary operator $\psi_{(3,3)}$ which becomes $\mathbb{Z}_2$ odd in these boundary conditions. These operators satisfy the property that their dimensions become small in the UV limit $m \to \infty$.

We can now check this in more detail for the Ising and tricritical Ising cases.

H.3.1 Ising Model and $T\bar{T}$ deformation

There is only one $\mathbb{Z}_2$ preserving boundary condition $(2,2)_3 = (1,2)_3$ for the Ising model. The boundary theory contains only the identity and the $\psi_{(2,1)}$ modules. The 1d operator $\psi_{(2,1)}$ has dimension $\Delta_{(1,2)} = 1/2$, which is unsurprisingly dual to a bulk massless free fermion, which

corresponds to the boundary GFF correlator. In this language, the irrelevant deformation which takes us back up the RG flow is the $T\bar{T}$ deformation which can be written as a quartic fermion interaction leading to the action

$$S_{FF} + S_{T\bar{T}} = \int_{AdS_2} \frac{dxdy}{y^2}(y\psi\bar{\partial}\psi + y\bar{\psi}\partial\bar{\psi}) + g_{T\bar{T}} \int_{AdS_2} \frac{dxdy}{y^2}(y\psi\partial\psi)(y\bar{\psi}\bar{\partial}\bar{\psi})\,, \tag{H.4}$$

Note that on the boundary there can only be one fermionic degree of freedom, corresponding to the identification $\hat{\psi} = -\hat{\bar{\psi}}$. Using standard, but somewhat involved Witten diagram techniques, we can find the first order deformation of the conformal data. Taking the four fermion operator to be normal-ordered is a convenient renormalization scheme in which the external operator doesn't get a leading order anomalous dimensions. Computing the full four-point function, we get:

$$\begin{aligned}\delta_{T\bar{T}}\mathcal{G}(\eta) \propto &-\frac{8\eta^3((5-2\eta)\eta-5)\log(\eta)}{(\eta-1)^2\eta} \\ &- \frac{8\left((2\eta^2+\eta+2)(\eta-1)^3\log(1-\eta)+2\eta((\eta-1)\eta+1)(\eta-1)\right)}{(\eta-1)^2\eta}\end{aligned} \tag{H.5}$$

The anomalous dimensions and correction to OPE coefficients of two-fermion operators corresponding to this interaction were actually bootstrapped using analytic functionals in [42]. Expanding our answer into blocks matches all their anomalous dimensions and all their OPE coefficients except for the OPE coefficient of the first non-trivial exchanged operator. This is to be expected since they include certain subtraction terms. These results lead to the saturation of the bounds of figure 20, in the main text.

H.3.2 Tricritical Ising

For the tricritical Ising, there are of course two different $\mathbb{Z}_2$ preserving boundary conditions, associated to $(2,1)_4$ and $(2,2)_4$. However, only the $(2,2)_4$ BC contains the lightest ($\mathbb{Z}_2$ odd) boundary operator $\psi_{(1,2)} = \psi_{(3,3)}$ of dimension $\Delta_{(1,2)} = 1/10$. In this case, the symmetry of the Kac table means that we can still solve a second order BPZ equation of the (1,2) type as in Appendix D. Imposing crossing and normalization for the unit operator once again leads to a unique solution:

$$\begin{aligned}&x_{12}^{1/5}x_{34}^{1/5}\langle\psi_{(1,2)}(x_1)\psi_{(1,2)}(x_3)\psi_{(1,2)}(x_3)\psi_{(1,2)}(x_4)\rangle_{(2,2)_4} \\ &\quad= \frac{{}_2F_1\left(-\frac{2}{5},\frac{1}{5};\frac{2}{5};1-\eta\right)}{\sqrt[5]{1-\eta}} + \frac{(1-\eta)^{2/5}\Gamma\left(\frac{7}{10}\right)\Gamma\left(\frac{7}{5}\right)\,{}_2F_1\left(\frac{1}{5},\frac{4}{5};\frac{8}{5};1-\eta\right)}{\sqrt[10]{2}\sqrt{\left(3+\sqrt{5}\right)\pi}\Gamma\left(\frac{8}{5}\right)}\,.\end{aligned} \tag{H.6}$$

We can then plot this point in the bounds for $\Delta_\psi = 1/10$ as we did in figure 17 in the main text. It saturates the bound, and is an expected position, somewhat close to the GFF point, in the direction predicted by the $T\bar{T}$ deformation.

If we were to try to backtrack the flows of this boundary conditions to the UV, the prediction of [26] would tell us that (a_1, a_2) flows to (a_2, a_1). This is consistent with the picture outlined above, since the RG flows would stick to the $(2, 2)$ boundary conditions, containing the lightest $\mathbb{Z}_2$ odd operator. This in contrast to the results in the UHP [38], where our scattering of the lightest $\mathbb{Z}_2$ odd particle can not be consistently embedded in the chain of bulk and boundary RG flows.

References

[1] A. B. Zamolodchikov, *Renormalization Group and Perturbation Theory Near Fixed Points in Two-Dimensional Field Theory*, *Sov. J. Nucl. Phys.* **46** (1987) 1090.

[2] A. B. Zamolodchikov, *From tricritical Ising to critical Ising by thermodynamic Bethe ansatz*, *Nucl. Phys. B* **358** (1991) 524–546.

[3] A. B. Zamolodchikov, *Resonance factorized scattering and roaming trajectories*, *J. Phys. A* **39** (2006) 12847–12862.

[4] A. Antunes, M. S. Costa, J. a. Penedones, A. Salgarkar, and B. C. van Rees, *Towards bootstrapping RG flows: sine-Gordon in AdS*, *JHEP* **12** (2021) 094, [arXiv:2109.13261].

[5] A. B. Zamolodchikov, *Expectation value of composite field T anti-T in two-dimensional quantum field theory*, hep-th/0401146.

[6] F. A. Smirnov and A. B. Zamolodchikov, *On space of integrable quantum field theories*, *Nucl. Phys. B* **915** (2017) 363–383, [arXiv:1608.05499].

[7] A. Cavaglià, S. Negro, I. M. Szécsényi, and R. Tateo, *$T\bar{T}$-deformed 2D Quantum Field Theories*, *JHEP* **10** (2016) 112, [arXiv:1608.05534].

[8] J. Cardy, *Quantum Quenches to a Critical Point in One Dimension: some further results*, *J. Stat. Mech.* **1602** (2016), no. 2 023103, [arXiv:1507.07266].

[9] L. V. Delacretaz, A. L. Fitzpatrick, E. Katz, and M. T. Walters, *Thermalization and hydrodynamics of two-dimensional quantum field theories*, *SciPost Phys.* **12** (2022), no. 4 119, [arXiv:2105.02229].

[10] Y. Jiang, *Expectation value of* $\mathrm{T}\overline{\mathrm{T}}$ *operator in curved spacetimes*, *JHEP* **02** (2020) 094, [arXiv:1903.07561].

[11] T. D. Brennan, C. Ferko, E. Martinec, and S. Sethi, *Defining the $T\overline{T}$ Deformation on* AdS_2, arXiv:2005.00431.

[12] A. Adams, N. Arkani-Hamed, S. Dubovsky, A. Nicolis, and R. Rattazzi, *Causality, analyticity and an IR obstruction to UV completion*, *JHEP* **10** (2006) 014, [hep-th/0602178].

[13] S. Caron-Huot and V. Van Duong, *Extremal Effective Field Theories*, *JHEP* **05** (2021) 280, [arXiv:2011.02957].

[14] S. Caron-Huot, D. Mazac, L. Rastelli, and D. Simmons-Duffin, *Sharp boundaries for the swampland*, *JHEP* **07** (2021) 110, [arXiv:2102.08951].

[15] S. Caron-Huot, D. Mazac, L. Rastelli, and D. Simmons-Duffin, *AdS bulk locality from sharp CFT bounds*, *JHEP* **11** (2021) 164, [arXiv:2106.10274].

[16] D. Carmi and S. Caron-Huot, *A Conformal Dispersion Relation: Correlations from Absorption*, *JHEP* **09** (2020) 009, [arXiv:1910.12123].

[17] D. Mazáč, L. Rastelli, and X. Zhou, *A basis of analytic functionals for CFTs in general dimension*, *JHEP* **08** (2021) 140, [arXiv:1910.12855].

[18] S. Caron-Huot, D. Mazac, L. Rastelli, and D. Simmons-Duffin, *Dispersive CFT Sum Rules*, *JHEP* **05** (2021) 243, [arXiv:2008.04931].

[19] P. H. Ginsparg, *APPLIED CONFORMAL FIELD THEORY*, in *Les Houches Summer School in Theoretical Physics: Fields, Strings, Critical Phenomena*, 9, 1988. hep-th/9108028.

[20] P. Di Francesco, P. Mathieu, and D. Senechal, *Conformal Field Theory*. Graduate Texts in Contemporary Physics. Springer-Verlag, New York, 1997.

[21] G. Mussardo, *Statistical field theory: an introduction to exactly solved models in statistical physics*. Oxford Univ. Press, New York, NY, 2010.

[22] A. Recknagel and V. Schomerus, *Boundary Conformal Field Theory and the Worldsheet Approach to D-Branes*. Cambridge Monographs on Mathematical Physics. Cambridge University Press, 11, 2013.

[23] J. L. Cardy, *Conformal Invariance and Surface Critical Behavior*, *Nucl. Phys. B* **240** (1984) 514–532.

[24] J. L. Cardy, *Boundary Conditions, Fusion Rules and the Verlinde Formula*, *Nucl. Phys. B* **324** (1989) 581–596.

[25] J. L. Cardy, *Boundary conformal field theory*, `hep-th/0411189`.

[26] E. Lauria, M. Milam, and B. C. van Rees, *Perturbative RG flows in AdS: an étude*, `arXiv:2309.10031`.

[27] D. M. McAvity and H. Osborn, *Energy momentum tensor in conformal field theories near a boundary*, *Nucl. Phys.* **B406** (1993) 655–680, [`hep-th/9302068`].

[28] D. McAvity and H. Osborn, *Conformal field theories near a boundary in general dimensions*, *Nucl. Phys. B* **455** (1995) 522–576, [`cond-mat/9505127`].

[29] P. Liendo, L. Rastelli, and B. C. van Rees, *The Bootstrap Program for Boundary CFT_d*, *JHEP* **07** (2013) 113, [`arXiv:1210.4258`].

[30] J. L. Cardy, *Effect of Boundary Conditions on the Operator Content of Two-Dimensional Conformally Invariant Theories*, *Nucl. Phys. B* **275** (1986) 200–218.

[31] A. Cappelli, C. Itzykson, and J. B. Zuber, *Modular Invariant Partition Functions in Two-Dimensions*, *Nucl. Phys. B* **280** (1987) 445–465.

[32] P. Ruelle and O. Verhoeven, *Discrete symmetries of unitary minimal conformal theories*, *Nucl. Phys. B* **535** (1998) 650–680, [`hep-th/9803129`].

[33] J. L. Cardy and D. C. Lewellen, *Bulk and boundary operators in conformal field theory*, *Phys. Lett. B* **259** (1991) 274–278.

[34] D. C. Lewellen, *Sewing constraints for conformal field theories on surfaces with boundaries*, *Nucl. Phys. B* **372** (1992) 654–682.

[35] M. Hogervorst, M. Meineri, J. Penedones, and K. S. Vaziri, *Hamiltonian truncation in Anti-de Sitter spacetime*, *JHEP* **08** (2021) 063, [`arXiv:2104.10689`].

[36] S. Fredenhagen, M. R. Gaberdiel, and C. A. Keller, *Bulk induced boundary perturbations*, *J. Phys. A* **40** (2007) F17, [`hep-th/0609034`].

[37] M. R. Gaberdiel, A. Konechny, and C. Schmidt-Colinet, *Conformal perturbation theory beyond the leading order*, *J. Phys. A* **42** (2009) 105402, [`arXiv:0811.3149`].

[38] S. Fredenhagen, M. R. Gaberdiel, and C. Schmidt-Colinet, *Bulk flows in Virasoro minimal models with boundaries*, *J. Phys. A* **42** (2009), no. 49 495403, [`arXiv:0907.2560`].

[39] I. Heemskerk, J. Penedones, J. Polchinski, and J. Sully, *Holography from Conformal Field Theory*, *JHEP* **10** (2009) 079, [arXiv:0907.0151].

[40] A. L. Fitzpatrick, E. Katz, D. Poland, and D. Simmons-Duffin, *Effective Conformal Theory and the Flat-Space Limit of AdS*, *JHEP* **07** (2011) 023, [arXiv:1007.2412].

[41] I. Runkel, *Boundary structure constants for the A series Virasoro minimal models*, *Nucl. Phys. B* **549** (1999) 563–578, [hep-th/9811178].

[42] D. Mazac and M. F. Paulos, *The analytic functional bootstrap. Part II. Natural bases for the crossing equation*, *JHEP* **02** (2019) 163, [arXiv:1811.10646].

[43] D. Mazac, *Analytic bounds and emergence of AdS_2 physics from the conformal bootstrap*, *JHEP* **04** (2017) 146, [arXiv:1611.10060].

[44] D. Mazac and M. F. Paulos, *The analytic functional bootstrap. Part I: 1D CFTs and 2D S-matrices*, *JHEP* **02** (2019) 162, [arXiv:1803.10233].

[45] K. Ghosh, A. Kaviraj, and M. F. Paulos, *Polyakov blocks for the 1D CFT mixed correlator bootstrap*, arXiv:2307.01257.

[46] L. Córdova, Y. He, and M. F. Paulos, *From conformal correlators to analytic S-matrices: CFT_1/QFT_2*, *JHEP* **08** (2022) 186, [arXiv:2203.10840].

[47] S. M. Chester, W. Landry, J. Liu, D. Poland, D. Simmons-Duffin, N. Su, and A. Vichi, *Carving out OPE space and precise $O(2)$ model critical exponents*, *JHEP* **06** (2020) 142, [arXiv:1912.03324].

[48] W. Knop and D. Mazac, *Dispersive sum rules in AdS_2*, *JHEP* **10** (2022) 038, [arXiv:2203.11170].

[49] J. Penedones, J. A. Silva, and A. Zhiboedov, *Nonperturbative Mellin Amplitudes: Existence, Properties, Applications*, *JHEP* **08** (2020) 031, [arXiv:1912.11100].

[50] J. Maldacena, S. H. Shenker, and D. Stanford, *A bound on chaos*, *JHEP* **08** (2016) 106, [arXiv:1503.01409].

[51] T. Hartman, S. Jain, and S. Kundu, *Causality Constraints in Conformal Field Theory*, *JHEP* **05** (2016) 099, [arXiv:1509.00014].

[52] F. A. Smirnov, *Reductions of the sine-Gordon model as a perturbation of minimal models of conformal field theory*, *Nucl. Phys. B* **337** (1990) 156–180.

[53] T. Eguchi and S.-K. Yang, *Deformations of Conformal Field Theories and Soliton Equations*, *Phys. Lett. B* **224** (1989) 373–378.

[54] A. B. Zamolodchikov, *Integrable field theory from conformal field theory*, *Adv. Stud. Pure Math.* **19** (1989) 641–674.

[55] H. Chen, A. L. Fitzpatrick, and D. Karateev, *Bootstrapping 2d ϕ^4 theory with Hamiltonian truncation data*, *JHEP* **02** (2022) 146, [arXiv:2107.10286].

[56] M. F. Paulos, J. Penedones, J. Toledo, B. C. van Rees, and P. Vieira, *The S-matrix bootstrap. Part I: QFT in AdS*, *JHEP* **11** (2017) 133, [arXiv:1607.06109].

[57] P. Fonseca and A. Zamolodchikov, *Ising field theory in a magnetic field: Analytic properties of the free energy*, hep-th/0112167.

[58] N. Levine and M. F. Paulos, *Bootstrapping bulk locality. Part I: Sum rules for AdS form factors*, arXiv:2305.07078.

[59] M. Meineri, J. Penedones, and T. Spirig, *Renormalization group flows in AdS and the bootstrap program*, arXiv:2305.11209.

[60] D. Karateev, S. Kuhn, and J. a. Penedones, *Bootstrapping Massive Quantum Field Theories*, *JHEP* **07** (2020) 035, [arXiv:1912.08940].

[61] M. Correia, J. Penedones, and A. Vuignier, *Injecting the UV into the Bootstrap: Ising Field Theory*, arXiv:2212.03917.

[62] I. Runkel, *Structure constants for the D series Virasoro minimal models*, *Nucl. Phys. B* **579** (2000) 561–589, [hep-th/9908046].

[63] V. S. Dotsenko and V. A. Fateev, *Conformal Algebra and Multipoint Correlation Functions in Two-Dimensional Statistical Models*, *Nucl. Phys. B* **240** (1984) 312.

[64] V. S. Dotsenko and V. A. Fateev, *Four Point Correlation Functions and the Operator Algebra in the Two-Dimensional Conformal Invariant Theories with the Central Charge c < 1*, *Nucl. Phys. B* **251** (1985) 691–734.

[65] V. S. Dotsenko and V. A. Fateev, *Operator Algebra of Two-Dimensional Conformal Theories with Central Charge C <= 1*, *Phys. Lett. B* **154** (1985) 291–295.

[66] I. Esterlis, A. L. Fitzpatrick, and D. Ramirez, *Closure of the Operator Product Expansion in the Non-Unitary Bootstrap*, *JHEP* **11** (2016) 030, [arXiv:1606.07458].

[67] F. A. Dolan and H. Osborn, *Conformal Partial Waves: Further Mathematical Results*, arXiv:1108.6194.

[68] D. Gaiotto, D. Mazac, and M. F. Paulos, *Bootstrapping the 3d Ising twist defect*, *JHEP* **03** (2014) 100, [arXiv:1310.5078].

[69] A. Homrich, J. a. Penedones, J. Toledo, B. C. van Rees, and P. Vieira, *The S-matrix Bootstrap IV: Multiple Amplitudes*, *JHEP* **11** (2019) 076, [arXiv:1905.06905].

[70] E. Lauria, P. Liendo, B. C. Van Rees, and X. Zhao, *Line and surface defects for the free scalar field*, *JHEP* **01** (2021) 060, [arXiv:2005.02413].

[71] C. P. Herzog and A. Shrestha, *Conformal surface defects in Maxwell theory are trivial*, *JHEP* **08** (2022) 282, [arXiv:2202.09180].

[72] C. Behan, L. Di Pietro, E. Lauria, and B. C. Van Rees, *Bootstrapping boundary-localized interactions*, *JHEP* **12** (2020) 182, [arXiv:2009.03336].

[73] C. Behan, L. Di Pietro, E. Lauria, and B. C. van Rees, *Bootstrapping boundary-localized interactions II. Minimal models at the boundary*, *JHEP* **03** (2022) 146, [arXiv:2111.04747].

[74] T. Nishioka, Y. Okuyama, and S. Shimamori, *Comments on epsilon expansion of the O(N) model with boundary*, *JHEP* **03** (2023) 051, [arXiv:2212.04078].

[75] T. Nishioka, Y. Okuyama, and S. Shimamori, *The epsilon expansion of the O(N) model with line defect from conformal field theory*, *JHEP* **03** (2023) 203, [arXiv:2212.04076].

[76] A. B. Zamolodchikov, *Thermodynamic Bethe Ansatz in Relativistic Models. Scaling Three State Potts and Lee-yang Models*, *Nucl. Phys. B* **342** (1990) 695–720.

[77] A. B. Zamolodchikov, *Irreversibility of the Flux of the Renormalization Group in a 2D Field Theory*, *JETP Lett.* **43** (1986) 730–732.

[78] M. F. Paulos, J. Penedones, J. Toledo, B. C. van Rees, and P. Vieira, *The S-matrix bootstrap II: two dimensional amplitudes*, *JHEP* **11** (2017) 143, [arXiv:1607.06110].